THE HONG KONG
POLYTECHNIC UNIVERSITY
香港理工大學
Pao Yue-kong Library
包玉剛圖書館

Copyright Undertaking

This thesis is protected by copyright, with all rights reserved.

By reading and using the thesis, the reader understands and agrees to the following terms:

1. The reader will abide by the rules and legal ordinances governing copyright regarding the use of the thesis.
2. The reader will use the thesis for the purpose of research or private study only and not for distribution or further reproduction or any other purpose.
3. The reader agrees to indemnify and hold the University harmless from and against any loss, damage, cost, liability or expenses arising from copyright infringement or unauthorized usage.

IMPORTANT

If you have reasons to believe that any materials in this thesis are deemed not suitable to be distributed in this form, or a copyright owner having difficulty with the material being included in our database, please contact lbsys@polyu.edu.hk providing details. The Library will look into your claim and consider taking remedial action upon receipt of the written requests.

Pao Yue-kong Library, The Hong Kong Polytechnic University, Hung Hom, Kowloon, Hong Kong

http://www.lib.polyu.edu.hk

SYSTEMIC HYPERTENSION LEADS TO DECLINED RETINAL FUNCTIONS VIA NEUROINFLAMMATION-RELATED PATHWAYS

CUI YINGKUN

PhD

The Hong Kong Polytechnic University

2026

The Hong Kong Polytechnic University

School of Optometry

Systemic Hypertension Leads to Declined Retinal Functions via Neuroinflammation-related Pathways

Cui Yingkun

A thesis submitted in partial fulfillment of the

requirements for the degree of Doctor of Philosophy

August 2024

CERTIFICATE OF ORIGINALITY

I hereby declare that this thesis is my own work and that, to the best of my knowledge and belief, it reproduces no material previously published or written, nor material that has been accepted for the award of any other degree or diploma except where due acknowledgment has been made in the text.

_____ **(Signed)**

_____Cui Yingkun_____(Name of student)

Abstract

Systemic hypertension (HT) is a leading cause of premature death globally. Glaucoma, a common eye disease, is the major cause of irreversible blindness worldwide. Despite their prevalence, the relationship between HT and glaucoma risk remains elusive. The interaction between blood pressure (BP) and intraocular pressure (IOP), a major glaucoma risk factor, is not fully understood. This study investigated the effects of chronic HT on IOP, retinal function, and structure across different HT stages, employing transcriptomic analysis to explore molecular retinal changes. We also studied the impact of endothelin-2 (EDN2) knockout and endothelin receptor antagonists on IOP and retinal function.

Using spontaneously hypertensive rats (SHR) and normotensive Wistar-Kyoto rats (WKY) as models, we measured BP, IOP, retinal function, structure, and vessel lumen areas at 4, 8, and 12 months, both cross-sectionally and longitudinally. SHR exhibited consistently higher BP but surprisingly lower IOP than WKY. Retinal functional responses were similar at 4 months but significantly reduced in SHR at 8 and 12 months compared to WKY. SHR displayed thinner total retinal and inner plexiform layers from 4 months onward. Both retinal arteries and veins had markedly narrower lumens in SHR at all time points, suggesting reduced retinal blood flow.

Transcriptomic analysis of SHR retinas at 8 months revealed upregulation of inflammatory pathways, including leukocyte migration, chemokine signaling, complement and coagulation cascades, and cytokine-receptor interactions. By 12 months, neuroinflammation-related pathways such as Toll-like receptor and NF-κB signaling were also upregulated. SHR showed fewer retinal ganglion cells at 8 and 12 months and enlarged, more numerous microglia at 12 months. Elevated EDN2 expression was found in 8-month SHR retinas at both mRNA and protein levels. These findings strongly suggest that retinal degeneration in SHR is primarily driven by mechanisms independent of IOP and increased neuroinflammation.

To confirm the involvement of the endothelin system, adeno-associated virus-mediated EDN2 knockout and intravitreal injections of endothelin receptor antagonists (Bq123 for EDNRA and Bq788 for EDNRB) were performed. EDN2 knockout enhanced retinal function in SHR without influencing IOP and suppressed inflammatory pathways. Similarly, Bq123 lowered IOP in WKY but not SHR, but improved SHR retinal function and downregulated retinal mRNA of IL-1α, endothelin-1, and EDNRA. Bq788 showed no significant effects. These results indicate the involvement of EDN2 and EDNRA in HT-induced retinal degeneration, and targeting these pathways may alleviate retinal damage.

In summary, we demonstrate that chronic HT contributes to retinal degeneration primarily through impaired blood flow and inflammation rather than elevated IOP, with endothelin signaling playing a significant role. Our results provide new insights into therapeutic strategies for treating HT-related retinal diseases.

Publications and Presentations from the Thesis

Publications

Cui, Y. K., L. Pan, T. Lam, C. Y. Wen and C. W. Do (2022). Mechanistic links between systemic hypertension and open angle glaucoma. Clin Exp Optom **105**(4): 362-371.

Shafiq, M., M. Rafique, Y. Cui, L. Pan, C. W. Do and E. A. Ho (2023). An insight on ophthalmic drug delivery systems: Focus on polymeric biomaterials-based carriers. J Control Release **362**: 446-467.

Presentations

Cui, Y., L. Pan, C. Wen and C. W. Do (2022). Systemic hypertension is associated with declined retinal functions via intraocular pressure (IOP)-independent mechanism. Invest Ophthalmol Vis Sci **63**(7): 1297 – F0112.

Cui, Y., L. Pan, L. Zhang, M. Wu, C. Wen and C. W. Do (2024). Chronic systemic hypertension induces functional retinal deterioration via neuroinflammation. The International Conference of Vision and Eye Research (iCover), Hong Kong.

Cui, Y., L. Pan, L. Zhang, M. Wu, C. Wen and C. W. Do (2024). Systemic hypertension leads to declined retinal functions via neuroinflammation related pathways. Invest Ophthalmol Vis Sci **65**(7): 6763-6763.

Li, H., Y. Cui, M. M. Wu, E. Ho, K. H. Wong and C. W. Do (2025). Biomimetic nano-platform for enhanced drug delivery in retinal diseases. Invest Ophthalmol Vis Sci 66(8): 2348-2348.

Pan, L., Y. Cui, F. Xu, Z. Han, M. Yang, T. C. Lam, K. S. Cho, D. Chen and C. W. Do (2023). Baicalein alleviates retinal ischemia-induced neuroinflammation by regulating

intracellular calcium homeostasis. Invest Ophthalmol Vis Sci **64**(8): 2003-2003.

Acknowledgments

I sincerely thank my supervisors, Dr. Chi-wai Do and Dr. Chunyi Wen, for their patient support, teaching, and guidance. I feel very honored to be their student. I would like to appreciate the help from Dr. Feng Pan, Dr. Samantha Shan, Dr. Thomas Lam, and all my team members in the past few years. I'm very grateful to Dr. Li Pan, who has taught me most of the techniques used in my study. I would like to thank the animals used in my study for their valuable sacrifice. Lastly, I would like to thank my parents and grandparents, who have always encouraged me to continue my studies.

Sincerely,

Cui Yingkun

Table of Contents

List of Figures

	WKY rats
Figure 8F	Cross-sectional measurements of the RNFL thicknesses in 4-, 8-, and 12-month-old SHR and WKY
Figure 8G	Cross-sectional measurements of the IPL thicknesses in 4-, 8-, and 12-month-old SHR and WKY
Figure 8H	Cross-sectional measurements of the total retinal thicknesses in 4-, 8-, and 12-month-old SHR and WKY
Figure 9A	Fundus view of the circular scan for inner lumen area of retinal arteries and veins measurements
Figure 9B	Schematic diagram indicating the measured arterial (red circle) and venous (blue circle) regions
Figure 9C	Representative images of inner lumen area of retinal arteries and veins from 4-, 8-, and 12-month-old SHR and WKY
Figure 9D	Cross-sectional measurements of inner lumen area of retinal arteries in 4-, 8-, and 12-month-old SHR and WKY
Figure 9E	Cross-sectional measurements of inner lumen area of retinal veins in 4-, 8-, and 12-month-old SHR and WKY
Figure 10A	Representative images of arterial blood velocities acquired from a 12-month-old SHR
Figure 10B	Representative images of arterial blood velocities acquired from a 12-month-old WKY
Figure 10D	Cross-sectional measurements of mean arterial blood velocity in 4-, 8-, and 12-month-old SHR and WKY
Figure 10E	Cross-sectional measurements of peak arterial blood velocity in 4-, 8-, and 12-month-old SHR and WKY
Figure 11A	Experimental design
Figure 11B	Longitudinal measurements of SBP in SHR and WKY
Figure 11C	Longitudinal measurements of DBP in SHR and WKY
Figure 11D	Longitudinal measurements of IOP in SHR and WKY

Figure 11E	Longitudinal measurements of pSTR in SHR and WKY
Figure 11F	Longitudinal measurements of a-wave in SHR and WKY
Figure 11G	Longitudinal measurements of b-wave in SHR and WKY
Figure 11H	Longitudinal measurements of RNFL thicknesses in SHR and WKY
Figure 11I	Longitudinal measurements of IPL thicknesses in SHR and WKY
Figure 11J	The longitudinal measurements of total retina thicknesses in SHR and WKY
Figure 11K	Longitudinal measurements of inner lumen area of retinal arteries in SHR and WKY
Figure 11L	Longitudinal measurements of inner lumen area of retinal veins in SHR and WKY
Figure 11M	The longitudinal measurements of peak blood velocity of the central retinal artery in SHR and WKY
Figure 11N	The longitudinal measurements of mean blood velocity of the central retinal artery in SHR and WKY
Figure 12	The positive feedback loop involving AngII, NO, and the endothelin system in the pathogenesis of HT
Figure 13A	qPCR results of retina samples from 8-month-old SHR and WKY
Figure 13B	Volcano plot of differentially expressed targets
Figure 13C	Expression levels of EDN2 in SHR and WKY
Figure 13D	Heatmap of selected target genes
Figure 13E	Upregulated KEGG pathways in 8-month-old SHR compared to WKY
Figure 13F	Downregulated KEGG pathways in 8-month-old SHR compared to WKY
Figure 14A	qPCR results of retina samples from 12-month-old SHR and WKY
Figure 14B	Volcano plot of differentially expressed targets
Figure 14C	Expression levels of EDN2 in SHR and WKY
Figure 14D	Heatmap of selected target genes

Figure 14E	Upregulated KEGG pathways in 12-month-old SHR compared to WKY
Figure 14F	Downregulated KEGG pathways in 12-month-old SHR compared to WKY
Figure 15A	Experimental workflow of the mounting and staining process
Figure 15B	Representative images from the 8- and 12-month-old SHR and WKY retinas
Figure 15C	Retinal ganglion cell counts
Figure 15D	Microglial cell counts
Figure 15E	Microglial soma size measurements
Figure 16A	Representative images captured from cryosectioned retinal slides of 8-month-old SHR and WKY
Figure 16B	Quantification of EDN2 fluorescence intensities
Figure 16C	EDN2 weight percentage determined by ELISA
Figure 16D	GFAP weight percentage determined by ELISA
Figure 17A	The correlation between EDN2 and C2 in the human retina with mild AMD
Figure 17B	The correlation between EDN2 and C3 in the human retina with mild AMD
Figure 17C	The correlation between EDN2 and C1R in the human retina with mild AMD
Figure 17D	The correlation between EDN2 and C1S in the human retina with mild AMD
Figure 17E	The correlation between EDN2 and C1QA in the human retina with mild AMD
Figure 17F	The correlation between EDN2 and C1QB in the human retina with mild AMD
Figure 17G	The correlation between EDN2 and C1QC in the human retina with mild AMD

Figure 17H	The correlation between EDN2 and C4A in the human retina with mild AMD
Figure 17I	The correlation between EDN2 and C4B in the human retina with mild AMD
Figure 17J	The correlation between EDN2 and C5AR2 in the human retina with mild AMD
Figure 17K	The correlation between EDN2 and GFAP in the human retina with mild AMD
Figure 17G	The correlation between EDN2 and CD68 in the human retina with mild AMD
Figure 17H	The correlation between EDN2 and TGFB1 in the human retina with mild AMD
Figure 17N	The correlation between EDN2 and IL6 in the human retina with mild AMD
Figure 17O	The correlation between EDN2 and age in the human retina with mild AMD
Figure 17P	A heatmap of the aforementioned targets, with subjects categorized by different age groups
Figure 18A	Molecular structure of Bq123 sodium salt
Figure 18B	Molecular structure of Bq788 sodium salt
Figure 19A	Experimental protocol for AAV treatment and measurements
Figure 19B	Pre- and post-treatment measurements of SBP in SHR and WKY
Figure 19C	Pre- and post-treatment measurements of DBP in SHR and WKY
Figure 19D	Pre- and post-treatment measurements of IOP in SHR and WKY
Figure 19E	Pre- and post-treatment measurements of pSTR in SHR and WKY
Figure 19F	Pre- and post-treatment measurements of a-wave in SHR and WKY
Figure 19G	Pre- and post-treatment measurements of b-wave in SHR and WKY
Figure 20A	Pre- and post-treatment measurements of total retinal area in SHR and WKY

Figure 20B	Representative images of pre- and post-treatment lumen areas of retinal arteries and veins from SHR and WKY
Figure 20C	Pre- and post-treatment measurements of lumen areas of retinal arteries in SHR and WKY
Figure 20D	Pre- and post-treatment measurements of lumen areas of retinal veins in SHR and WKY
Figure 21A	qPCR results of SHR injected with either EDN2 KO AAV or control AAV
Figure 21B	Volcano plots showing downregulated targets in SHR treated with EDN2 KO AAV
Figure 21C	EDN2 expression examined by RNA sequencing in SHR treated with EDN2 KO AAV and control AAV
Figure 21D	Heatmap of the targets of interest
Figure 21E	Upregulated KEGG pathways in SHR injected with EDN2 KO AAV compared to those injected with control AAV
Figure 21F	Downregulated KEGG pathways in SHR injected with EDN2 KO AAV compared to those injected with control AAV
Figure 22A	qPCR results showing WKY injected with EDN2 KO AAV compared to WKY injected with control AAV
Figure 22B	Volcano plots illustrating differentially expressed targets in WKY injected with EDN2 KO AAV versus control AAV
Figure 22C	EDN2 expressions analyzed by RNA sequencing in WKY injected with EDN2 KO AAV and control AAV
Figure 22D	Heatmap of the targets of interest
Figure 22E	Upregulated KEGG pathways in WKY injected with EDN2 KO AAV compared to control AAV.
Figure 22F	Downregulated KEGG pathways in WKY injected with EDN2 KO AAV compared to control AAV.
Figure 23A	Representative images from post-treatment SHR and WKY retinas

Figure 23B	Retinal ganglion cell counts from post-treatment SHR retinas
Figure 23C	Retinal ganglion cell counts from post-treatment WKY retinas
Figure 23D	Microglial cell counts from post-treatment SHR retinas
Figure 23E	Microglial cell counts from post-treatment WKY retinas
Figure 23F	Microglial soma size measurements from post-treatment SHR retinas
Figure 23G	Microglial soma size measurements from post-treatment WKY retinas
Figure 24A	Representative images of SHR and WKY injected with EDN2 KO AAV or control AAV
Figure 24B	Quantification of EDN2 fluorescence intensities
Figure 24C	EDN2 protein levels measured by ELISA
Figure 24D	GFAP protein levels measured by ELISA
Figure 25A	Experimental design for treatment with Bq123 and Bq788 in SHR and WKY
Figure 25B	IOP of SHR and WKY following the injections of Bq123, Bq788, or PBS
Figure 25C	pSTR of SHR and WKY following the injections of Bq123, Bq788, or PBS
Figure 25D	a-wave of SHR and WKY following the injections of Bq123, Bq788, or PBS
Figure 25E	b-wave of SHR and WKY following the injections of Bq123, Bq788, or PBS
Figure 25F	qPCR results for SHR injected with Bq123 compared to SHR injected with PBS
Figure 25G	qPCR results for SHR injected with Bq788 compared to SHR injected with PBS
Figure 25H	qPCR results for WKY injected with Bq123 compared to WKY injected with PBS
Figure 25I	qPCR results for WKY injected with Bq788 compared to WKY

	injected with PBS
Figure 26	A schematic diagram summarizing the major findings

List of Abbreviations

36B4	Acidic ribosomal phosphoprotein P0
8-OHdG	8-Hydroxy-2'-deoxyguanosine
AACG	Acute angle-closure glaucoma
AAV	Adeno-associated virus
ACC	American College of Cardiology
ACE1	Angiotensin Converting Enzyme 1
ACE2	Angiotensin Converting Enzyme 2
AH	Aqueous humor
AIF1	Ionized calcium-binding adapter molecule 1
AMD	Age-related macular degeneration
AngII	Angiotensin II
AT1	Angiotensin type I receptor
AT2	Angiotensin type II receptor
ATP	Adenosine triphosphate
BDNF	Brain-derived neurotrophic factor
BP	Blood Pressure
BRB	Blood-retinal barrier
BSA	Bovine serum albumin
C1Q	Complement component 1q
C1QA	Complement C1q A Chain
C1QB	Complement C1q B Chain
C1QC	Complement C1q C Chain
C1R	Complement component 1r
C1S	Complement component 1s
C2	Complement 2
C3	Complement 3
C4A	Complement component 4A

C4B	Complement component 4B
C5AR2	Complement component 5A receptor 2
C7	Complement 7
C9	Complement 9
CCL2	C-C motif chemokine ligand 2
CD68	Cluster of differentiation 68
CO	Cardiac output
COX2	Cyclooxygenase 2
CYBB	Cytochrome B-245 beta chain
DAMPs	Damage-associated molecular patterns
DBP	Diastolic blood pressure
Disc 1	Disrupted in schizophrenia
ECM	Extracellular matrix
EDN1	Endothelin-1
EDN2	Endothelin-2
EDN3	Endothelin-3
EDNRA	Endothelin type A receptor
EDNRB	Endothelin type B receptor
ELISA	Enzyme-linked immunosorbent assay
ERG	Electroretinography
FRAP	Ferric-reducing activity of plasma
GCL	Ganglion cell layer
GFAP	Glial fibrillary acid protein
HT	Hypertension
IgG	Immunoglobulin G
IL-10	Interleukin-10
IL-1α	Interleukin 1α
IL-1β	Interleukin 1β
IL-6	Interleukin 6

INL	Inner nuclear layer
IOP	Intraocular pressure
IR	Ischemia/reperfusion
JNC 7	The Seventh Report of the United States Joint National Committee on Prevention, Detection, Evaluation, and Treatment of High Blood Pressure
JNK	Jun NH2-terminal kinase
KEGG	Kyoto Encyclopedia of Genes and Genomes
KO	Knockout
L-NAME	NG-nitro-L-arginine methyl ester
L-NMMA	NG-monomethyl-L-arginine
MAP	Mean arterial pressure
MIGS	Minimally invasive glaucoma surgery
MRI	Magnetic resonance imaging
mTOR	Mechanistic target of the rapamycin
MYD88	Myeloid differentiation primary response 88
NADPH	Nicotinamide adenosine dinucleotide phosphate
NAM	Nicotinamide
NF-κB	Nuclear factor kappa-light-chain-enhancer of activated B
NO	Nitric Oxide
NOS	Nitric oxide synthase
NOS2	Nitric Oxide Synthase 2
NOS3	Nitric Oxide Synthase 3
NPE	Non-pigmented ciliary epithelium
NTG	Normal tension glaucoma
OAG	Open-angle glaucoma
OCT	Optical coherence tomography
OHT	Ocular hypertension
ONL	Outer nuclear layer

OPL	Outer plexiform layer
OPP	Ocular perfusion pressure
P2X7	P2X purinoceptor 7
p38 MARK	p38 mitogen-activated protein kinases
PACG	Primary angle-closure glaucoma
PAMPs	Pathogen-associated molecular patterns
PBS	Phosphate-buffered saline
PE	Pigmented ciliary epithelium
POAG	Primary open-angle glaucoma
pSTR	Positive scotopic threshold response
qPCR	Quantitative polymerase chain reaction
RAAS	Renin-Angiotensin-Aldosterone System
RGC	Retinal ganglion cell
RNFL	Retinal nerve fiber layer
ROCK	Rho-associated protein kinases
ROS	Reactive oxygen species
RPE	Retinal pigmented epithelium
RSNA	Renal sympathetic nerve activity
SBP	Systolic blood pressure
SHR	Spontaneously hypertensive rats
TGFB1	Transforming growth factor β1
TLR	Toll-like receptors
TM	Trabecular meshwork
TNF-α	Tumor necrosis factor-α
TPR	Total peripheral vascular resistance
TRAK1/2	Trafficking kinesin protein 1 or 2
TRPV1	Transient receptor potential vanilloid 1
TUNEL	Terminal deoxynucleotidyl transferase dUTP nick end labeling
VEGF	Vascular endothelial growth factor

VEP	Visual evoked potential
WKY	Wistar Kyoto rats
WT	Wild type

Chapter 1. Introduction to the Pathogenesis of Glaucoma

1. Ocular anatomy and physiology

1.1. Anatomy of the Eyeball

The human eyeball can generally be divided into three layers: the outer supporting layer, the middle uveal layer, and the inner retinal layer. The outer layer includes the cornea and sclera, while the middle layer consists of the iris, ciliary body, and choroid. The lens is attached to the ciliary body by the zonular fibers. Inside the eyeball, there are three chambers: the anterior chamber, the posterior chamber, and the vitreous chamber. The anterior chamber is the space between the cornea and the anterior surface of the iris. The posterior chamber lies between the posterior surface of the iris and the anterior surface of the crystalline lens. The vitreous chamber is located between the posterior surface of the lens and the retina. To receive visual signals, light rays must pass sequentially through the cornea, anterior chamber, pupil, lens, and vitreous body before reaching the retina. In the retina, light is converted into visual signals that are transmitted to the brain via the optic nerve (Kels, Grzybowski et al. 2015). Figure 1 illustrates the anatomy of the eyeball. This study focuses on the impact of blood pressure (BP) on intraocular pressure (IOP) and the retina. Therefore, the fluid dynamics and retinal structures will be emphasized in this chapter.

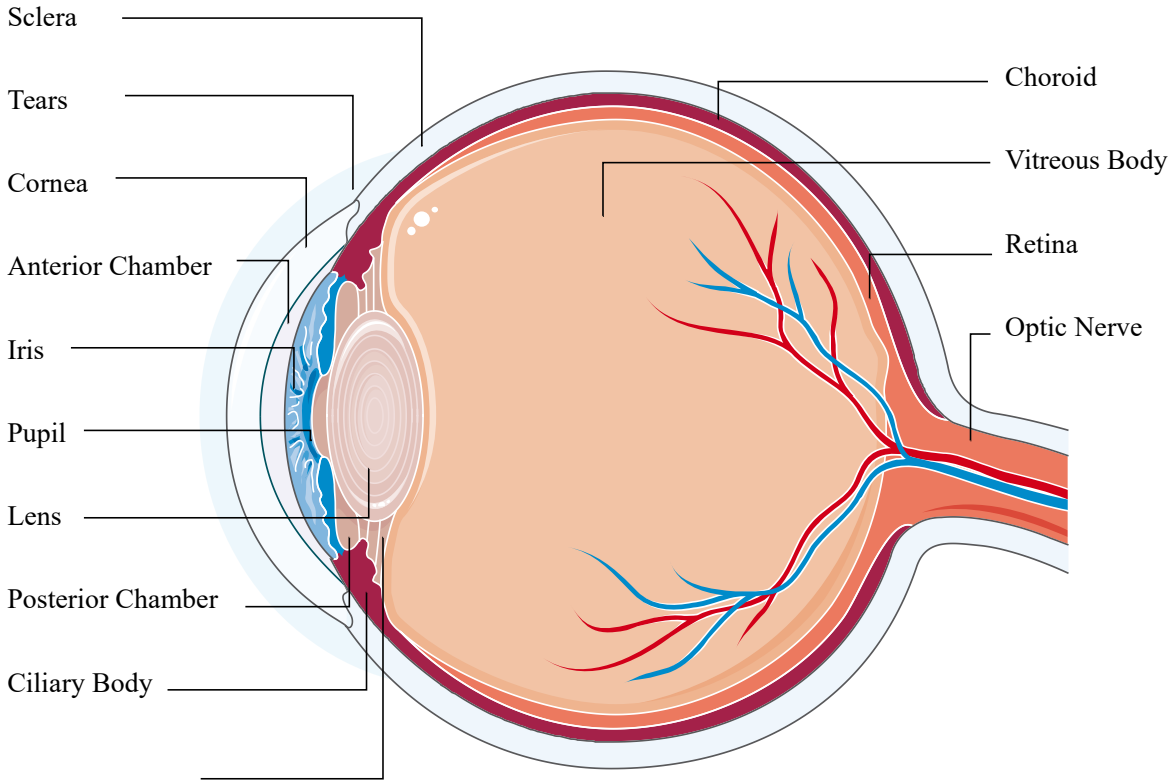

Figure 1. Anatomy of the eyeball.

1.2. IOP and Aqueous Flow Dynamics

IOP refers to the fluid pressure inside the eye (Duke-Elder 1926). In healthy individuals, normal IOP typically ranges from 11 to 21 mmHg (Kelly and Farrell 2018). Under normal conditions, IOP is mainly regulated by the continuous production (inflow) and drainage (outflow) of aqueous humor (AH) (Duke-Elder 1926). AH is a clear fluid located in the anterior chamber that supplies nutrients to avascular structures such as the cornea, lens, and trabecular meshwork (TM) (Freddo, Civan et al. 2021). The AH dynamics generally involve secretion by the ciliary body processes, flow from the posterior chamber to the anterior chamber, and drainage via either the trabecular outflow pathway or the uveoscleral outflow pathway (Choplin and Traverso 2014). The formation of AH occurs in three steps: 1) ultrafiltration allows fluid to pass from the ciliary capillaries into the ciliary stroma; 2) ions are actively transported from the stroma across the bilayered ciliary epithelium into the posterior chamber, and 3) water movement follows, driven by the resulting osmotic gradient (Choplin and Traverso 2014). Ion pumps, including paired Na^+/H^+ and Cl^-/HCO_3^- antiporters, as well as the $Na^+/K^+/2Cl^-$ symporter, are located on the pigmented ciliary epithelium (PE) cells and mediate ion transport from the ciliary stroma into these cells. Na^+ and Cl^- ions then move through intercellular gap junctions to the non-pigmented ciliary epithelium (NPE) cells. Finally, ions are transported into the posterior chamber via Na^+/K^+/ATPases, Cl^- channels, K^+ channels, and the $Na^+/K^+/2Cl^-$ symporter on NPE cells. Water follows osmotic pressure gradients and exits the NPE cells into the posterior chamber through aquaporin channels (Li, Shan et al. 2023). Figure 2 illustrates the pathway of ion movement during AH secretion from the ciliary stroma to the posterior chamber. The outflow of AH occurs via two main pathways: the trabecular outflow pathway and the uveoscleral outflow pathway (Choplin and Traverso 2014). In the trabecular pathway, the AH passes through the TM, Schlemm's canal, collector channels, and episcleral veins to enter the systemic circulation. The TM consists of three layers: the inner uveal meshwork, the middle corneoscleral meshwork, and the outer juxtacanalicular meshwork. Resistance to fluid drainage increases progressively from the inner to the outer meshwork layer. In the

uveoscleral outflow pathway, AH flows into the supraciliary space, then through spaces between ciliary muscle bundles, and eventually exits through the sclera (Choplin and Traverso 2014). These pathways are illustrated in Figure 3.

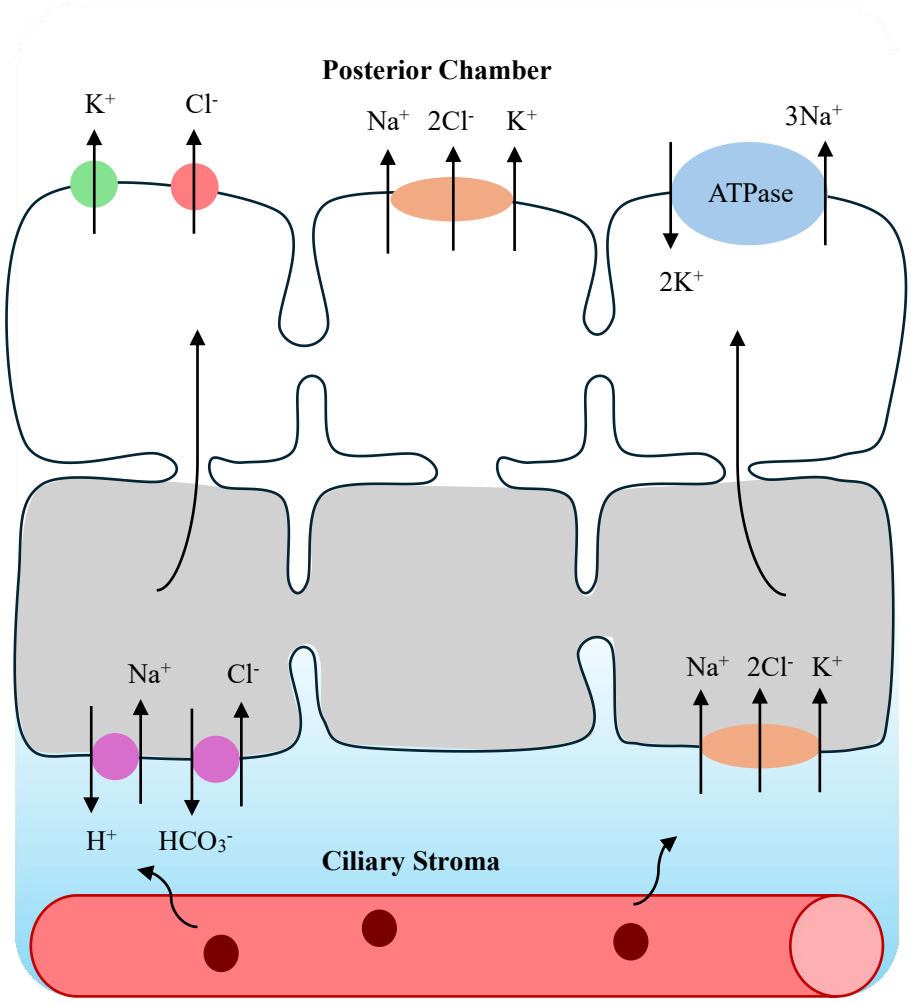

Figure 2. The routes of active ion transport during aqueous humor secretion.

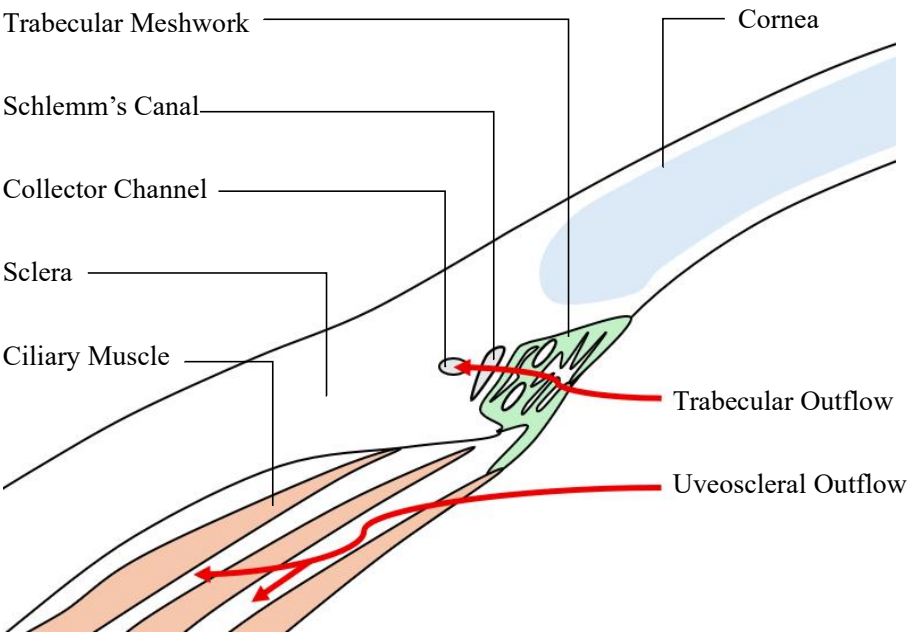

Figure 3. The routes of aqueous humor outflow.

1.3. Structures of the Retina

The structures of the human retina are illustrated in Figure 4. The retina is composed of retinal pigmented epithelium (RPE) cells, photoreceptors, bipolar cells, retinal ganglion cells (RGCs), horizontal cells, amacrine cells, and glial cells, including astrocytes, Müller cells, and microglia. The RPE lines the outermost layer, which plays a vital role in nourishing the photoreceptors. Photoreceptors can be classified into rods and cones responsible for scotopic and photopic vision, respectively. The soma of photoreceptors form the outer nuclear layer (ONL). These photoreceptors transduce visual signals to intermediate cells in the inner nuclear layer (INL), including bipolar, horizontal, and amacrine cells. The intermediate cells then transfer the signals to the RGCs. The soma of RGCs form the ganglion cell layer (GCL), and their axons constitute the retinal nerve fiber layer (RNFL). RGC axons pass through the lamina cribrosa and form the optic nerve, which transfers visual signals to the brain (Gensheimer, Veerman et al. 2025). Müller glia span radially across the retina, and their foot processes form the inner and outer limiting membranes (Wang, Cioffi et al. 2002). Astrocytes are primarily located in the RNFL, and microglia normally reside in the inner retinal layers, including the GCL to INL. Under pathological conditions, Müller cells and astrocytes may undergo gliosis, and microglia can become activated and migrate to other layers (Telegina, Kozhevnikova et al. 2018). The retina's blood supply originates from two sources: the central retinal artery and the choriocapillaris. The inner retinal layers, from the RNFL to the outer plexiform layer (OPL), are supplied by the central retinal artery, whereas the photoreceptors and RPE layers receive blood from the choriocapillaris (Sun and Smith 2018).

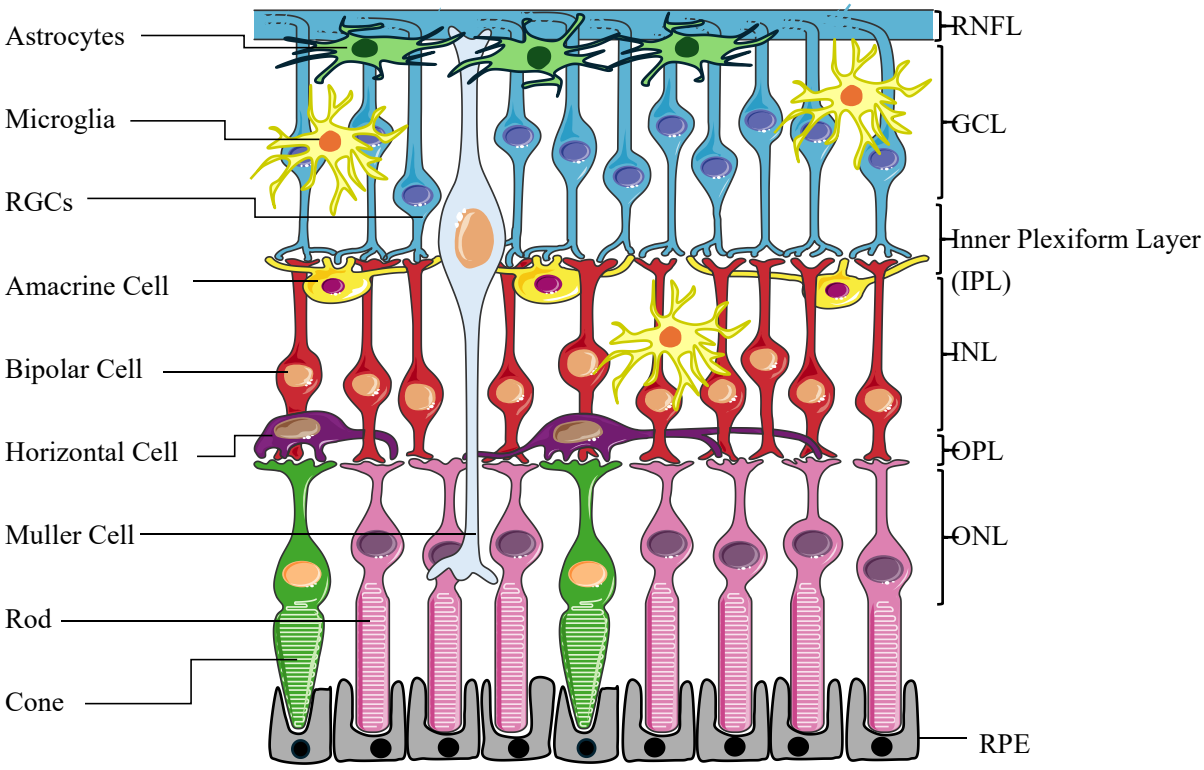

Figure 4. Structures of the human retina.

2. Prevalence, Type, and Treatments of Glaucoma

Glaucoma refers to a group of ocular conditions characterized by the loss of RGCs, leading to characteristic visual field defects and damage to the optic nerve (Costa, Arcieri et al. 2009). It is the leading cause of irreversible blindness worldwide (Dandona and Dandona 2006). As the disease progresses, the optic disc exhibits thinning of the neural rim, pallor, and progressive cupping (Agarwal, Gupta et al. 2009). It is estimated that over 76 million people suffered from glaucoma globally in 2020 (Tham, Li et al. 2014). Key risk factors for glaucoma include aging, genetic predisposition, and elevated IOP. Aging significantly elevates glaucoma risk through multiple mechanisms (Kapetanakis, Chan et al. 2016, Zhang, Huang et al. 2024). First, aging increases aqueous outflow resistance as extracellular materials accumulate in the trabecular meshwork, narrowing outflow pathways (Miyazaki, Segawa et al. 1987). Second, it impairs energy supply to RGCs, which have high metabolic demands and thus vulnerable; humans lose approximately 4,000 RGC axons annually (Jonas, Schmidt et al. 1992, Calkins 2013). Aged RGCs also showed delayed recovery from acute IOP elevation compared to younger ones (Lee, Zhao et al. 2022). Third, age-related declines in ocular blood flow increase glaucoma susceptibility (Kuroda, Uji et al. 2016). Current clinical treatments focus primarily on lowering IOP (Tribble, Hui et al. 2023). Glaucoma is generally classified into primary open-angle glaucoma (POAG), normal tension glaucoma (NTG), primary angle-closure glaucoma (PACG), and acute angle-closure glaucoma (AACG) based on different etiologies (Gerstenblith and Rabinowitz 2012). The most prevalent type is POAG, characterized by elevated IOP with a wide-open and clear anterior chamber angle (Stone, Fingert et al. 1997). NTG similarly features an open and clear anterior chamber angle along with progressive optic neuropathy, but it is characterized by IOP levels comparable to those of healthy individuals. Due to the similarities between POAG and NTG, they are often grouped as open-angle glaucoma (OAG). In contrast, PACG is characterized by peripheral anterior synechiae and chronic IOP elevation. AACG results from acute obstruction of the anterior chamber angle, leading to a sudden increase in IOP

(Gerstenblith and Rabinowitz 2012). In some cases, an identifiable pathological cause may induce elevated IOP, termed secondary glaucoma, such as traumatic glaucoma (Blanton 1964, Iannucci, Manni et al. 2023).

Current treatments for glaucoma include eye drops, surgical interventions, and laser therapy. Topical eye drops are commonly considered the first-line treatment for glaucoma (Gazzard, Konstantakopoulou et al. 2019). Commonly used topical eye drops include prostaglandin analogs, β-blockers, α -agonists, carbonic anhydrase inhibitors, Rho-associated protein kinases (ROCK) inhibitors, and muscarinic receptor agonists (Lusthaus and Goldberg 2019, Pagano, Lee et al. 2023). However, these medications have undesirable side effects that may lead to non-compliance. Prostaglandin analogs can cause increased periocular pigmentation; β-blockers may lead to bradyarrhythmia and hypotension; α-agonists can induce drowsiness and dry mouth; carbonic anhydrase inhibitors may cause anorexia and renal issues; ROCK inhibitors may lead to conjunctiva hyperemia and corneal verticillate, and muscarinic receptor agonists can cause miosis-induced blurred vision or even retinal tear or detachment (Lusthaus and Goldberg 2019, Haga, Waller et al. 2022, Jethva, Bhagat et al. 2022). Laser trabeculoplasty may cause fewer side effects, but its effectiveness often declines over time (Weinand and Althen 2006, Shi and Jia 2012). If these treatments become ineffective, due to drug resistance or poor compliance, surgical intervention may be indicated to lower IOP (Garg and Gazzard 2020). Minimally invasive glaucoma surgery (MIGS) employs microscopic equipment and small incisions to reduce IOP with less invasiveness than traditional procedures. However, MIGS carries risks such as stent malpositioning and obstruction, limiting its applicability in some patients (Dhingra and Bhartiya 2020). Trabeculectomy surgery is regarded as the gold standard for glaucoma surgery, reducing IOP by creating a fistula between the anterior chamber and subconjunctival space, providing an alternate pathway for AH to exit the eye (Razeghinejad, Fudemberg et al. 2012). If trabeculectomy does not achieve the desired target IOP, other options, such as tube

shunt, may be explored (Singh and Gedde 2011). Although surgical interventions can result in a more significant IOP reduction, various risks, including scarring and postoperative infection, are increased (Stein, Ruiz et al. 2008).

The pathophysiology of glaucoma remains unclear. Although lowering IOP is currently the only effective treatment, many patients continue to experience vision loss due to disease progression, even after their IOP is well controlled (Chauhan and Drance 1992). The pathogenesis of glaucoma is commonly explained by two main theories: the mechanical theory and the vascular theory (Flammer 1994, Yamamoto and Kitazawa 1998, Ahmad 2024). According to the mechanical theory, elevated IOP exerts pressure on ocular structures, subsequently damaging the axons and RGCs (Nemesure, Honkanen et al. 2007, Fernandez-Albarral, Ramirez et al. 2024). Several mechanisms have been proposed to explain how this compression leads to axonal damage, including direct apoptosis of RGCs, blockage of axonal transport, mitochondrial dysfunction, and neuroinflammation. In contrast, the vascular theory posits that RGC damage results from ischemia due to insufficient blood supply to the optic nerve. These theories are likely interconnected, as neither mechanism alone fully accounts for the variability observed in glaucomatous damage (Flammer and Orgul 1998, Dengler-Crish, Smith et al. 2014, Soto and Howell 2014, Levkovitch-Verbin 2015, Jassim, Inman et al. 2021, Cui, Pan et al. 2022).

3. The Mechanical Theory

3.1. Apoptosis of RGCs

Elevated IOP may induce RGC death through multiple mechanisms, including mechanical injury, alterations in anterograde and retrograde axonal transport, changes in the retinal extracellular matrix (ECM), and direct or indirect pressure-induced apoptosis (Guo, Moss et al. 2005, Dengler-Crish, Smith et al. 2014). Both clinical and animal studies suggest that increased IOP causes RGC death primarily through apoptosis, a programmed form of cell death characterized by enzymatic digestion of DNA (Garcia-Valenzuela, Shareef et al. 1995, Kerrigan, Zack et al. 1997). For example, retinal sections from patients with POAG exhibited more apoptotic RGCs detected by Terminal deoxynucleotidyl transferase dUTP nick end labeling (TUNEL) staining compared to healthy controls (Kerrigan, Zack et al. 1997). This indicates that high IOP triggers RGC death not only by passive mechanical compression but also programmed cell death (Garcia-Valenzuela, Shareef et al. 1995). The exact pathways through which elevated IOP causes RGC apoptosis are not fully understood. Recent research shows that membrane-bound receptors such as TRPV1 and P2X7 mediate hydrostatic pressure-induced RGC apoptosis (Sappington, Sidorova et al. 2009, Hu, Lu et al. 2010, Dong, Hu et al. 2018). These channels elevate intracellular Ca^{2+} levels in RGCs under elevated pressure, promoting apoptosis, while antagonists targeting TRPV1 or P2X7 effectively prevent this in rat RGCs (Sappington, Sidorova et al. 2009, Hu, Lu et al. 2010). In addition, P2X7 activation triggers microglial responses that contribute to RGC death (Dong, Hu et al. 2018). These studies support the notion that hydrostatic pressure directly and independently induces RGC apoptosis.

The mechanisms underlying hydrostatic pressure-induced neuronal apoptosis may include disrupted transmembrane ion fluxes and altered neuronal electrophysiological activity (Agar, Yip et al. 2000, Sappington, Sidorova et al. 2009). In addition, other retinal cells, especially glial cells, also contribute to RGCs' apoptosis in vivo.

Coculture experiments of RGCs with glial cells showed that elevated hydrostatic pressure increases glial secretion of tumor necrosis factor-α (TNF-α) and nitric oxide synthase (NOS). Blocking glia-secreted TNF-α or NOS reduced RGC apoptosis by approximately 50%, indicating that glial cells exacerbate pressure-induced RGC death (Tezel and Wax 2000). Thus, elevated IOP causes RGC apoptosis via both direct neuronal injury and indirect glial-mediated mechanisms. Alterations in the retinal ECM may represent another pathway through which increased IOP induces RGC apoptosis. For example, decreased laminin deposition in the retina correlates with IOP elevation and may contribute to RGC loss (Guo, Moss et al. 2005). Moreover, caspases, a family of cysteine proteases crucial for neuronal apoptosis, are also believed to mediate RGC apoptosis (Kermer, Klocker et al. 1998). Impaired axonal transport caused by elevated IOP may lead to RGC apoptosis by disrupting neurotrophic support. High IOP can impair retrograde transport of neurotrophins such as brain-derived neurotrophic factor (BDNF) from RGC axon terminals back to the soma (Quigley, Nickells et al. 1995). In rat models of elevated IOP, the neurotrophic receptor tyrosine kinase B accumulates in the optic nerve. The retrograde transport of BDNF from the superior colliculus to the retina is reduced (Pease, McKinnon et al. 2000). Consequently, neurotrophin deprivation may also lead to RGC apoptosis in POAG.

3.2. Axonal Transport Blockage

The proper physiological function of RGC relies on the efficient axonal trafficking of molecules (Dengler-Crish, Smith et al. 2014). Transport from the cell body to the axon terminal is known as anterograde transport, while transport from the axon terminal back to the cell body is called retrograde transport. Since the axon is essential for neuronal communication with other cells, it has a substantial metabolic demand. Proteins and energy required by the axon are produced in the cell body and delivered via active anterograde transport (Sheng and Cai 2012, Yu, Cringle et al. 2013, Dengler-Crish, Smith et al. 2014). On the other hand, survival factors such as

BDNF are transported from the superior colliculus back to the soma of RGCs (Pease, McKinnon et al. 2000). Retrograde transport is also responsible for bringing aging proteins and organelles back to the cell body for degradation (Maday, Twelvetrees et al. 2014). The molecular motors mediating anterograde and retrograde transport belong to the kinesin and dynein families, respectively (Cai and Sheng 2009, Dengler-Crish, Smith et al. 2014, Maday, Twelvetrees et al. 2014).

In animal models of ocular hypertension (OHT), RGCs exhibit deficits in both anterograde and retrograde transport following IOP elevation (Anderson and Hendrickson 1974, Dengler-Crish, Smith et al. 2014, Maddineni, Kasetti et al. 2020). In particular, reductions in anterograde transport precede impairments in retrograde transport (Dengler-Crish, Smith et al. 2014). The loss of axonal transport induced by high IOP may result from mechanical compression at the optic nerve head and ischemic damage (Anderson and Hendrickson 1974, Dengler-Crish, Smith et al. 2014). In OHT, dyes used as markers for anterograde transport fail to reach distal regions of the optic nerve (Maddineni, Kasetti et al. 2020). At moderate levels of OHT, RGCs may sustain normal protein synthesis. However, once hypertension surpasses a critical threshold, RGCs' function deteriorates and protein synthesis ceases (Anderson and Hendrickson 1974). Disruption of anterograde transport impairs mitochondrial activities along the axon, leading to decreased energy supply for the neuron (Quintero, Shiga et al. 2022). Elevated IOP has been shown to compromise the metabolism of RGCs by impairing Disrupted in schizophrenia (Disc1), a key protein involved in mitochondrial trafficking. Disc1 interacts with the Miro1 and trafficking kinesin protein 1/2 (TRAK1/2) complex, which connects mitochondria to kinesin motors along microtubules for transport (Quintero, Shiga et al. 2022). Expression of the Disc1 gene is reduced in RGCs in OHT eyes, and restoring Disc1 levels via adeno-associated virus (AAV) vectors improves retinal and oculomotor function (Quintero, Shiga et al. 2022). Thus, OHT impairs retinal functions by disrupting regular mitochondrial anterograde transport. Importantly, these changes in

anterograde transport occur before detectable structural loss of RGCs (Maddineni, Kasetti et al. 2020, Quintero, Shiga et al. 2022). Restoring anterograde transport could provide novel therapeutic targets for glaucoma. In addition to Disc1, CD82, a membrane glycoprotein, has been proposed to exert neuroprotective effects by restoring anterograde transport through activating the mechanistic target of rapamycin (mTOR) signaling pathway (Ye, Huang et al. 2021).

Retrograde transport is impaired at a later stage compared to anterograde transport (Calkins 2012, Dengler-Crish, Smith et al. 2014). One possible explanation is that dynein motors have more adenosine triphosphate (ATP) hydrolyzing sites and can take larger steps than kinesin motors, making retrograde transport more resilient (Calkins 2012). Retrograde transport is crucial for RGCs' function and survival because essential neurotrophins, including BDNF, are transported from the superior colliculus back to the RGCs' soma (Quigley, Nickells et al. 1995, Pease, McKinnon et al. 2000). Deprivation of retrograde BDNF transport leads to RGC degeneration (Johnson, Bull et al. 2011, Lambert, Carlson et al. 2017). In ischemia/reperfusion (IR) injury models, both anterograde and retrograde transport are impaired. Intraocular supplementation of BDNF preserves levels of kinesin and dynein in the retina and restores both types of axonal transport (Du, Wang et al. 2020). This restoration of transport also rescues visual functions (Du, Wang et al. 2020). Therefore, strategies to preserve retinal BDNF may represent promising new directions for glaucoma treatment. For example, oral administration of HE3286, a synthetic sterol derivative, restores anterograde transport and retinal BDNF in OHT models, indicating its potential neuroprotective role in glaucoma (Lambert, Carlson et al. 2017).

3.3. Mitochondria Changes and Oxidative Stress

IOP-dependent mitochondrial alterations and increased oxidative stress represent important mechanisms contributing to RGCs' apoptosis (Ju, Liu et al. 2007, Williams, Harder et al. 2017, Chen, Kang et al. 2020, Mirzaei, Gupta et al. 2020, Tribble,

Otmani et al. 2021). Mitochondrial dysfunction leads to higher reactive oxygen species (ROS) production, establishing a close link between oxidative stress and mitochondrial impairment. The oxidative stress arising from mitochondrial dysfunction causes cellular damage (Chen, Kang et al. 2020). Clinical studies have demonstrated a positive correlation between both systemic and local oxidative stress levels and the risk of POAG (Lee, Sheck et al. 2012, Tanito, Kaidzu et al. 2015, Van Bergen, Crowston et al. 2015). For example, lymphoblasts from POAG patients showed reduced oxidative phosphorylation complex I-driven ATP synthesis (Lee, Sheck et al. 2012, Van Bergen, Crowston et al. 2015). Besides, complete mitochondrial genome sequencing of POAG patients reveals mutations likely to inhibit complex I activity (Banerjee, Banerjee et al. 2013, Sundaresan, Simpson et al. 2015). Nicotinamide (NAM), or vitamin B3, is also reduced in the plasma of POAG patients (Kouassi Nzoughet, Chao de la Barca et al. 2019). Collectively, these findings suggest that mitochondrial dysfunction, increased oxidative stress, and complex I defects play significant roles in POAG pathogenesis. Experimental models support these clinical observations. Rat retinas subjected to OHT demonstrate elevated ROS levels and decreased mitochondrial membrane potential, indicative of mitochondrial dysfunction (Chen, Kang et al. 2020). OHT alters the expression of proteins critical for mitochondrial biogenesis and dynamics, including Mitofusin-2, Optic atrophy 1, and Dynamin-related protein 1, which regulate mitochondrial fusion and fission processes (Ju, Kim et al. 2008, Chen, Kang et al. 2020, Zeng, You et al. 2023). Proteomic analyses of retinal tissue in animal glaucoma models show reduced abundance of mitochondrial ATP synthase and increased oxidative stress markers (Mirzaei, Gupta et al. 2020). RNA sequencing of RGCs from DBA/2J mice reveals that metabolic dysfunction emerges early in disease progression, with functional impairments preceding neurodegeneration (Williams, Harder et al. 2017). Morphologically, increased mitochondrial fission and cristae depletion are observed in RGC axons of DBA/2J mice (Ju, Kim et al. 2008). Elevated IOP may directly induce these mitochondrial changes. In cultured RGCs, increased hydrostatic pressure

triggers mitochondrial fission, abnormal cristae depletion, reduced cellular ATP levels, and excessive ROS generation (Ju, Liu et al. 2007, Chen, Kang et al. 2020). Given the well-established relationship between IOP elevation and retinal mitochondrial dysfunction, antioxidants have emerged as promising therapeutic agents for glaucoma. Resveratrol, a natural polyphenolic compound, has been shown to mitigate mitochondrial alterations induced by OHT, thereby protecting RGCs (Chen, Kang et al. 2020). NAM supplementation rescues RGCs without affecting IOP in DBA/2J mice (Williams, Harder et al. 2017, Williams, Harder et al. 2017). NAM prevents OHT-induced metabolic disturbances and preserves mitochondrial morphology in the retina (Tribble, Otmani et al. 2021).

3.4. Neuroinflammation

Increased immune responses have been implicated in glaucomatous neurodegeneration. Three types of resident glial cells, namely astrocytes, Müller cells, and microglia, are localized within the retina and optic nerve. These cells mediate local inflammatory responses and become activated in response to glaucoma-related insults. Upon activation, microglia redistribute throughout the retina and optic nerve, producing cytokines that may induce cytotoxic neuronal injury (Adornetto, Russo et al. 2019). The activation of astrocytes, Müller cells, and microglia has been observed following IOP elevation (Zhang, Wang et al. 2009, Wang, Liu et al. 2017). For example, increased glial fibrillary acid protein (GFAP) expression appears in the end-feet and processes of Müller cells after acute IOP elevation (Zhang, Wang et al. 2009). Microglial activation occurs in both acute and chronic IOP elevations (Bosco, Steele et al. 2011, Howell, Macalinao et al. 2011, Yang, Luo et al. 2011, Wang, Liu et al. 2017, Wang, Song et al. 2020). Immunoglobulin G (IgG) autoantibody accumulation has been detected in the RGC layer and co-localizes with activated microglial cells in glaucomatous donor eyes. Concomitantly, increased levels of TNF- α , interleukin 6 (IL-6), and interleukin 1-β (IL-1β) have been found in glaucomatous retinas compared to healthy retinas (Gramlich, Beck et al. 2013).

Several key molecules play critical roles in neuroinflammation during glaucomatous degeneration, including Toll-like receptors (TLR), nuclear factor kappa-light-chain-enhancer of activated B cells (NF-κB), and complement proteins. A positive feedback loop exists between activated microglia and astrocytes, as microglia upregulate interleukin 1-α (IL-1α) and TNF-α expression, further stimulating astrocyte activation (Liddelow, Guttenplan et al. 2017). Neurotoxic reactive astrocytes, in turn, release cytokines and chemokines, including C-C motif chemokine ligand 2 (CCL2) and IL-6, which re-activate microglia, perpetuating inflammation (Liddelow, Guttenplan et al. 2017). Glia activation can be triggered by various exogenous or endogenous stimuli, including damage-associated molecular patterns (DAMPs) and pathogen-associated molecular patterns (PAMPs) (Vernazza, Tirendi et al. 2020, Mahaling, Low et al. 2022). Oxidative stress mediates neuroinflammation in glaucoma progression by increasing the generation of advanced glycation end products. The binding of advanced glycation end products to their receptors on glial cells activates these cells to secrete neurotoxic cytokines (Adornetto, Russo et al. 2019). It has been demonstrated that tempol, a multifunctional antioxidant, effectively reduces TNF-α expression in the retina and optic nerve of OHT mouse models. Similarly, mice deficient in superoxide dismutase-1, a key antioxidant enzyme, exhibit increased neuroinflammation and more severe neuronal loss after IOP elevation (Yang, Hondur et al. 2016).

Upregulation of TLRs has been identified in glaucomatous human retinas. Proteomic analyses show significantly higher expression of TLR2, TLR4, and TLR7 in glaucomatous donors (Luo, Yang et al. 2010). It has been suggested that microglia predominantly express TLR2 and TLR4, while astrocytes may express TLR3. Heat shock proteins and oxidative stress likely stimulate TLR overexpression, and many heat shock proteins are also upregulated in the glaucomatous human retina (Luo, Yang et al. 2010). Activated TLRs mediate downstream signaling cascades, including p38 MAPK, JNK signaling, and NF-κB pathways, leading to secondary immune cell

activation and overproduction of cytokines such as TNF-α (Luo, Yang et al. 2010). Elevated expressions of TNF-α, inducible NOS, and p38 MAPK have also been observed in a rat model of acute IOP elevation (Wang, Liu et al. 2017). Consequently, at least in part, retinal damage in glaucoma may be mediated by TLR-induced cytokine expression. NF-κB, a transcription factor complex downstream of TLR signaling, is upregulated in glaucomatous retina and promotes cytokine production by microglia (Yang, Luo et al. 2011, Wang, Song et al. 2020). Inhibition of NF-κB reduces the expression of TLR4, IL-6, and TNF-α in activated microglia (Wang, Song et al. 2020).

Complement activation is among the earliest changes in glaucoma, preceding detectable axonal loss caused by elevated IOP. Suppressing complement activities protects against IOP-induced retinal injury in mouse models (Howell, Macalinao et al. 2011, Williams, Tribble et al. 2016). Complement C1q A chain (C1QA), a key effector in the complement cascade, is expressed by activated microglia following IOP elevation. Mice with mutated C1QA exhibit greater preservation of RGCs under elevated IOP conditions, indicating that complement inhibition may protect against glaucomatous degeneration (Howell, Macalinao et al. 2011).

Following glial activation, cytokine expression increases, including TNF-α and IL-6 (Wang, Song et al. 2020). Elevated TNF-α binds to TNF-α receptor 1 (TNFR1) in RGCs, inducing apoptosis via caspase-8 activation (Oliveira, Vasconcellos et al. 2014). Histological studies have shown increased TNF-α expression in retinal glial cells and overexpression of TNFR1 specifically in glaucomatous RGCs, suggesting RGC sensitivity to TNF-α-mediated cytotoxicity (Tezel, Li et al. 2001). In the rat OHT model, AH IL-6 level rises with IOP elevation and negatively correlates with the number of RGCs (Song, Song et al. 2018). The role of IL-6 in RGCs' survival remains controversial. IL-6 KO mice display similar IOP elevations but show protection of RGC structure and vision following eight weeks of elevated IOP

(Echevarria, Formichella et al. 2017). Similarly, IL-6 deficiency protects RGCs after optic nerve crush in mice (Fisher, Mizrahi et al. 2001). On the contrary, studies indicate that IL-6 may exert anti-apoptotic effects, as RGCs' survival decreases in rat eyes when glial IL-6 is depleted (Sappington, Chan et al. 2006).

4. The Vascular Theory

4.1. Evidence Supporting the Vascular Theory

Although IOP remains the primary recognized risk factor for glaucoma, many patients experience disease progression even with well-controlled IOP, suggesting the involvement of additional pathogenic factors other than mechanical pressure (Chauhan and Drance 1992). The vascular theory suggests that glaucomatous damage arises from inadequate blood flow, or perfusion, to ocular tissues (Bonomi, Marchini et al. 2000). Recent studies reinforce the significance of vascular health in glaucoma. Epidemiological and clinical evidence link glaucoma risk, particularly in NTG, with systemic vascular dysregulation, including conditions such as migraine and Raynaud's phenomenon, which reduce blood flow and may contribute to vasospasm (Wang, Mitchell et al. 1997, Bednarczyk, Remler et al. 1998, Cursiefen, Wisse et al. 2000). NTG patients exhibit delayed restoration of normal blood flow after temperature changes and elevated levels of endothelin-1 (EDN1), a potent vasoconstrictor implicated in disease progression (O'Brien and Butt 1999, Resch, Garhofer et al. 2009). Magnetic resonance imaging (MRI) studies reveal NTG-associated cerebral small vessel ischemia, infarcts, and corpus callosum atrophy, underscoring potential systemic circulatory contributions to glaucoma risk (Ong, Farinelli et al. 1995). Additional evidence demonstrates a positive relationship between reduced ocular perfusion and glaucoma risk (Chung, Harris et al. 1999, Grunwald, Piltz et al. 1999, Mitchell, Leung et al. 2005, Amerasinghe, Aung et al. 2008). Generalized narrowing of retinal arteries has been observed in glaucomatous retinas, and this arterial narrowing is significantly associated with glaucomatous optic nerve damage (Mitchell, Leung et al. 2005). Importantly, thinning of retinal vessels may not be directly related to IOP, suggesting that the association between vessel thinning and glaucoma risk is independent of IOP (Amerasinghe, Aung et al. 2008). The peripheral retina of NTG patients shows reduced blood flow as measured by laser Doppler flowmetry (Chung, Harris et al. 1999). Furthermore, blood flow in the optic nerve head is decreased in

glaucomatous eyes (Ong, Farinelli et al. 1995, Stroman, Stewart et al. 1995, Chung, Harris et al. 1999, Grunwald, Piltz et al. 1999, Mitchell, Leung et al. 2005, Amerasinghe, Aung et al. 2008, Resch, Garhofer et al. 2009).

4.2. The Theory of OPP

The amount of blood supplied to the eye primarily depends on perfusion pressure, defined as the difference between arterial and venous pressure. Generally, higher perfusion pressure corresponds to increased blood flow and a lower risk of ischemia. While the pressure outside the vein is negligible in most tissues, in the eye, IOP elevates venous pressure in the retinal and choroidal circulations to levels approximately equal to IOP (Costa, Harris et al. 2014). Therefore, arterial pressure must be sufficiently high to overcome this venous pressure and maintain normal blood flow. Because IOP compresses ocular vessels, it can impede circulation. In a healthy eye, venous blood flows smoothly through the retinal and choroidal vessels, with venous pressure just before exiting the eye slightly exceeding IOP (Duke-Elder 1926). Hence, ocular perfusion pressure (OPP) is defined as the difference between arterial pressure and IOP within the retina and choroid, representing the arteriovenous pressure gradient in the eye (Civan, Benos et al. 2008). According to Ohm's law, blood flow is proportional to the arteriovenous pressure gradient divided by vascular resistance. Thus, higher OPP is believed to increase ocular blood flow and reduce the risk of ischemia or glaucoma development (Van Keer, Breda et al. 2016). Since OPP depends on both arterial pressure and IOP, blood pressure (BP) is considered a key factor influencing ocular blood flow, retinal health, and glaucoma risk (Costa, Harris et al. 2014).

4.3. Low BP or OPP Increases the Risk of Glaucoma

OPP influences retinal blood flow, and thus low OPP or low BP may increase the risk of glaucoma (Goldberg, Hollows et al. 1981, Richler, Werner et al. 1982, Pillunat,

Stodtmeister et al. 1989, Kaiser, Flammer et al. 1993, Sommer and Tielsch 1996, Leske, Wu et al. 2002, Zheng, Wong et al. 2010, Okumura, Yuki et al. 2012, Tham, Lim et al. 2018, Lee, Yang et al. 2020). Low OPP has been linked to a higher risk of OAG (Zheng, Wong et al. 2010, Kim, Oh et al. 2020). It has been suggested that HT may not have a direct connection to OAG risk; however, low diastolic OPP is positively associated with glaucoma (Sommer and Tielsch 1996). Later, Tham et al. (2018) proposed that low systolic OPP is related to POAG, whereas diastolic OPP is not (Tham, Lim et al. 2018). Zheng et al. (2010) reported that low DBP, mean OPP, and diastolic OPP all represent risk factors for glaucoma (Zheng, Wong et al. 2010).

Some studies have shown that NTG patients may have lower systolic OPP compared to individuals without glaucoma (Pillunat, Stodtmeister et al. 1989), while other research indicates that higher baseline OPP reduces the chance of developing glaucoma over four years (Leske, Wu et al. 2002). It remains unclear whether IOP or BP is the primary factor linking OPP to glaucoma risk. Ramdas et al. (2011) observed a negative association between OPP and OAG risk, but this connection weakened after adjusting for IOP, suggesting that IOP may predominantly influence OAG risk (Ramdas, Wolfs et al. 2011). In contrast, Tham et al. (2018) reported a negative association between systolic OPP and POAG risk after adjusting for IOP (Tham, Lim et al. 2018). Zheng et al. (2010) also proposed that low mean OPP and diastolic OPP are risk factors for OAG following IOP adjustment (Zheng, Wong et al. 2010). Therefore, high IOP combined with low BP exacerbates the damage caused by low OPP (Zheng, Wong et al. 2010, Tham, Lim et al. 2018). Several studies have demonstrated that low DBP is also a risk factor for glaucoma progression (Richler, Werner et al. 1982, Okumura, Yuki et al. 2012). POAG patients with well-controlled IOP but ongoing progression show lower diurnal and nocturnal SBP than those with less progression (Kaiser, Flammer et al. 1993). Lower DBP in the ophthalmic artery has been observed in NTG patients compared to those with OHT but no progression (Goldberg, Hollows et al. 1981). In NTG patients, low SBP is associated with a higher

risk of RNFL defect progression, and low DBP is associated with an increased risk of macular GCL-IPL thinning (Lee, Yang et al. 2020). Among non-glaucomatous individuals, the cup-to-disc ratio is larger in those with DBP below 90 mmHg due to antihypertensive treatment compared to those with higher or untreated normal DBP (Topouzis, Coleman et al. 2006). Therefore, low OPP, whether caused by high IOP or low BP, may be associated with an increased risk of glaucoma due to insufficient ocular perfusion (Goldberg, Hollows et al. 1981, Topouzis, Coleman et al. 2006, Zheng, Wong et al. 2010, Ramdas, Wolfs et al. 2011, Tham, Lim et al. 2018, Lee, Yang et al. 2020, Cui, Pan et al. 2022).

4.4. Large Nocturnal BP or OPP Dip Increases the Risk of Glaucoma

The nocturnal BP dip refers to the difference between nighttime and daytime BP. The positive correlation between the magnitude of the nocturnal dip and glaucoma risk supports the vascular theory, as the nocturnal dip also indicates a form of low OPP. Over-dippers, who experience a nocturnal BP dip greater than 20%, have been shown to have a higher risk of optic disc hemorrhage compared to those with smaller dips (Kim, Park et al. 2017). Larger nocturnal BP dips are observed in glaucoma patients compared to normal subjects, with the magnitude being greater in NTG patients than in POAG patients (Meyer, Brandi-Dohrn et al. 1996, Muzyka, Nizankowska et al. 1997). NTG patients with larger nocturnal DBP dips and longer dip durations are more likely to exhibit parapapillary choroidal microvasculature dropout, an indicator of impaired optic nerve head perfusion that positively correlates with the severity of visual field defects (Shin, Jo et al. 2021). Glaucoma patients with disease progression show larger nocturnal BP dips than those with stable visual fields (Graham, Drance et al. 1995, Graham and Drance 1999). Compared to healthy controls, DBP fluctuation, the difference between the highest and lowest values over 24 hours, is higher in POAG patients (Costa, Jimenez-Roman et al. 2010). In NTG patients, Charlson et al. (2014) found that the longer the duration during which nocturnal mean arterial pressure (MAP) is 10 mmHg lower than the diurnal MAP, the greater the likelihood of

disease progression (Charlson, de Moraes et al. 2014). For untreated NTG patients, mean OPP fluctuations significantly correlate with the severity of visual field loss, although mean OPP itself does not correspond with the level of visual field defects (Choi, Kim et al. 2021). Fluctuations in circadian mean OPP and MAP are significantly associated with RNFL thickness in NTG patients (Choi, Kim et al. 2007). Patients with NTG who experience greater mean OPP fluctuations are more likely to have disease progression (Sung, Lee et al. 2009). Overall, the mean OPP fluctuation is considered a consistent clinical risk factor for NTG severity and a predictor of disease progression (Choi, Kim et al. 2007, Sung, Lee et al. 2009).

In addition to evidence showing that a greater nocturnal dip is linked to an increased risk of OAG, BP or OPP variability, defined as the standard deviation of multiple measurements in the same individual, has also been identified as a predictor for OAG. In a prospective study, POAG patients with higher visit-to-visit SBP standard deviation tend to have an increased risk of disease progression (Lee, Jung et al. 2017). Kashiwagi (2001) noted that the nocturnal dip is smaller in progressing NTG patients compared to non-progressing patients, but nocturnal BP deviation is larger in the progressing group. This suggests that nocturnal dip alone is not as strong a predictor for NTG progression as nocturnal BP variability (Kashiwagi, Hosaka et al. 2001). It is also observed that increased mean OPP variability is associated with a higher likelihood of visual field defect progression. Increased diurnal mean OPP variability significantly predicts visual field deterioration (Lee, Choi et al. 2015). NTG patients with worse visual field defects tend to exhibit a greater nocturnal BP dip and circadian SBP variability (Jin, Seo et al. 2017).

Chapter 2. Systemic Hypertension Induces Retinal Degeneration Through Intraocular Pressure-Independent Mechanisms

1. Introduction

1.1. The Prevalence and Pathogenesis of Primary HT

Hypertension (HT) is a prevalent and life-threatening disease. HT is the leading cause of cardiovascular disease and premature death worldwide (Mills, Stefanescu et al. 2020). From 1990 to 2015, over half of the deaths attributable to ischemic heart disease, hemorrhagic stroke, and ischemic stroke were linked to HT (Forouzanfar, Liu et al. 2017). During this period, deaths associated with SBP above 140 mmHg accounted for 14.0% of all deaths (Forouzanfar, Liu et al. 2017). It is estimated that more than 1.5 billion people worldwide will suffer from HT by 2025 (Perkovic, Huxley et al. 2007). In 2010, only half of the HT patients were aware of their condition, about one-third received treatment, and fewer than 15% achieved BP control globally (Mills, Bundy et al. 2016). In the United States, it was predicted that over 45% of adults aged 20 and older, approximately 120 million people, had HT between 2017 and 2020. Nonetheless, 38% of HT individuals in the US were unaware of their condition (Tsao, Aday et al. 2023). In China and India, the number of HT patients is expected to exceed 500 million by 2025 (Perkovic, Huxley et al. 2007). The Seventh Report of the United States Joint National Committee on Prevention, Detection, Evaluation, and Treatment of High Blood Pressure (JNC 7) provides the commonly used definition of HT, as listed in Table 1 (Chobanian, Bakris et al. 2003, Hall, Granger et al. 2012). However, the 2017 Guideline for High Blood Pressure in Adults from the American College of Cardiology (ACC) offers a different, stricter definition (Table 1) (Whelton, Carey et al. 2018). The ACC classification designates SBP between 120-139 mmHg or DBP between 80-89 mmHg as HT (Whelton, Carey et al. 2018). This modification was made because the risk of cardiovascular disease increases even at these lower BP ranges (Whelton, Carey et al. 2018).

Organization	Classification	Definition (Unit: mmHg)
JNC 7	Normal BP	SBP < 120, and DBP < 80
	Prehypertension	120 ≤ SBP ≤ 139, and 81 ≤ DBP ≤ 89
	Stage 1 HT	140 ≤ SBP ≤ 159, or 90 ≤ DBP ≤ 99
	Stage 2 HT	SBP ≥ 160, or DBP ≥ 100
ACC	Normal BP	SBP < 120, and DBP < 80
	Elevated BP	120 ≤ SBP ≤ 129, and DBP < 80
	Stage 1 HT	130 ≤ SBP ≤ 139, or 80 ≤ DBP ≤ 89
	Stage 2 HT	SBP ≥ 140, or DBP ≥ 90

Table 1. The classifications of HT based on JNC 7 and ACC.

In the short term, BP is determined by cardiac output (CO) and total peripheral vascular resistance (TPR), as represented by the formula Mean Arterial Pressure (MAP) = CO x TPR (Hall, Omoto et al. 2024). Cardiac output refers to the total volume of blood circulated. However, this formula may not accurately reflect more complex, long-term conditions such as chronic HT (Hall, Granger et al. 2012). During the progression of chronic HT, increased BP can induce gradual structural changes in the vessels, including rarefaction and hypertrophy. These adaptations help maintain normal blood flow despite elevated BP, thereby ensuring that blood flow meets metabolic demands. If treated early, vascular hypertrophy may gradually regress, allowing restoration of some vascular function. However, in chronic and severe HT patients, BP reduction must be treated cautiously because significant vascular injury has already occurred, and abrupt BP lowering might lead to hypoperfusion.

Several factors contribute to the pathogenesis of HT, including abnormal activation of the sympathetic nervous system, dysregulation of vasoactive hormones, and vascular endothelial dysfunction (Hall, Granger et al. 2012, Hall, Omoto et al. 2024). Changes

in sympathetic innervation and hormone secretion can alter CO, while endothelial dysfunction increases TPR. The renal system directly regulates BP. When BP drops too low, the renal system increases sodium and water retention to restore it. However, elevated renal perfusion pressure enhances urination, lowering BP. (Hall, Guyton et al. 1986). Sympathetic nerves and vasoactive hormones modulate BP by influencing renal function (Hall, Granger et al. 2012).

Sympathetic nerve activity affects renal activity and BP through renal sympathetic nerve activity (RSNA). In patients with drug-resistant HT, renal sympathetic nerve ablation effectively lowers BP (Azizi, Sapoval et al. 2015, Townsend, Mahfoud et al. 2017, Kandzari, Bohm et al. 2018), indicating that abnormal RSNA is at least partly involved in HT pathogenesis. Sympathetic activity is modulated by peripheral baroreceptors or chemoreceptors (Hall, Granger et al. 2012). Baroreceptors detect BP changes, modulating it via autonomic reflexes affecting the heart and blood vessels. Chemoreceptors respond to oxygen and carbon dioxide levels, thereby influencing BP (Hall, Granger et al. 2012). For drug-resistant HT, chronic carotid baroreceptor stimulation reduces BP, heart rate variability, and heart rate turbulence onset (Wustmann, Kucera et al. 2009). This likely occurs through sympathetic inhibition and parasympathetic activation (Wustmann, Kucera et al. 2009). Adjusting the baroreflex presents a novel HT treatment regime (Wustmann, Kucera et al. 2009). The carotid body acts as a peripheral chemoreceptor sensing ambient pH and partial pressures of oxygen and carbon dioxide (Iturriaga, Alcayaga et al. 2021). Overactive carotid body sensitivity has been observed in animal models of primary HT (Tan, Lu et al. 2010). Carotid body activity can be suppressed by breathing 100% oxygen; HT patients undergoing hyperoxia show transient reductions in SBP, DBP, and total TPR, effects not seen in healthy controls (Sinski, Lewandowski et al. 2014). Therefore, carotid body overactivation might contribute to abnormal sympathetic innervation and HT.

The Renin-Angiotensin-Aldosterone System (RAAS) is central to BP regulation (Hall, Omoto et al. 2024). It consists of two main pathways: the Angiotensin Converting Enzyme 1 (ACE1)-Angiotensin II (AngII)-Angiotensin type I receptor (AT1) (ACE1-AngII-AT1) axis and the Angiotensin Converting Enzyme 2 (ACE2)-Angiotensin (1-7)-Mas receptor (ACE2-Angiotensin(1-7)-Mas) axis (Holappa, Vapaatalo et al. 2017). Renin cleaves Angiotensinogen to produce Angiotensin I, a weak vasoconstrictor. ACE1 then converts Angiotensin I into AngII, which binds to AT1 receptors to promote aldosterone secretion, vasoconstriction, and BP elevation. Conversely, the ACE2 pathway generates Angiotensin (1-7), which activates Mas receptors to induce vasodilation, antiproliferation, and antifibrosis (Holappa, Vapaatalo et al. 2017). The ACE1-AngII-AT1 axis regulates kidney function by promoting sodium and water retention (Hall, Omoto et al. 2024). AngII stimulates aldosterone secretion by the adrenal gland and increases sodium and water reabsorption in renal tubules and arterioles, increasing BP (Hall, Omoto et al. 2024). AngII-induced chronic HT primarily occurs through AT1 receptors in the kidney, as supported by studies using systemic AT1 KO mice (Crowley, Gurley et al. 2006). Wild-type (WT) mice develop HT and cardiac remodeling following AngII infusion, whereas AT1 KO mice do not. This was further supported by the transplantation experiments. WT kidneys transplanted into AT1 KO mice restore the hypertensive response, while AT1 KO kidneys in WT mice significantly attenuate it. While other organs like the brain, heart, and vasculature may contribute, their roles are less significant compared to the kidney (Crowley, Gurley et al. 2006, Hall, Omoto et al. 2024). Aldosterone acts on mineralocorticoid receptors in renal distal tubules and collecting tubules, enhancing sodium reabsorption, especially during low sodium intake. Thus, AngII raises BP either directly or via aldosterone stimulation (Hall, Omoto et al. 2024).

Vascular endothelial dysfunction is another key HT risk factor. It involves impaired regulation of vasodilation and vasoconstriction by endothelial cells, caused by

damage or imbalance of vasodilators and vasoconstrictors. Overactivated endothelin system, Nitric Oxide (NO) deficiency, increased oxidative stress, and heightened vascular inflammation are the contributing factors (Hall, Omoto et al. 2024). The specific causes of vascular endothelial dysfunction will be discussed later.

1.2. Ocular Disorders Related to HT

As HT progresses, structural alterations in blood vessels can gradually lead to pathological ocular conditions such as hypertensive retinopathy and hypertensive choroidopathy (Chopra, Sharma et al. 2014). In the early stage of hypertensive retinopathy, retinal arteries narrow and arteriovenous nicking occurs. As the condition worsens, disruption of the blood-retinal barrier leads to retinal hemorrhages, cotton-wool spots, and hard exudates. At the advanced stage, it causes optic disc swelling (Chua, Cheung et al. 2020). The exact mechanism underlying hypertensive papilledema is unclear but may involve ischemia from constricted posterior ciliary arteries, increased intracranial pressure, or hypertensive encephalopathy (Chatterjee, Chattopadhyay et al. 2002). The choroidal circulation, similar to the retinal circulation, may also be compromised in HT (Bourke, Patel et al. 2004). Obstruction in choroidal arteries and choriocapillaris can cause degeneration of the overlying RPE. Characteristic signs of hypertensive choroidopathy include Elschnig spots and Siegrist streaks, representing pigmentary changes secondary to ischemia (Bourke, Patel et al. 2004). Furthermore, leakage from the choroidal circulation may result in subretinal fluid accumulation and potential retinal detachment (Bourke, Patel et al. 2004).

HT is also associated with ocular disorders such as diabetic retinopathy, age-related macular degeneration (AMD), and cataract (Srivastava and Rema 2005). The prevalence of HT is substantially higher in diabetic patients compared to the general population (Srivastava and Rema 2005). HT may exacerbate diabetic retinopathy by altering retinal hemodynamics and increasing ocular vascular endothelial growth factor (VEGF) levels (Srivastava and Rema 2005). Patients with neovascular AMD

are more likely to have DBP higher than 95 mmHg compared to those without AMD, potentially related to atherosclerotic changes caused by HT (Hyman, Schachat et al. 2000). HT is also considered a risk factor for cataract (Mylona, Dermenoudi et al. 2019). It has been hypothesized that elevated IOP in HT patients enhances the pressure gradient across the lens, accelerating glucose accumulation and cataract formation (Mylona, Dermenoudi et al. 2019). The link between HT and IOP will be discussed in the following sections.

1.3. The Relationship Between HT and the Risk of Glaucoma

To what extent HT influences glaucomatous neurodegeneration remains uncertain. Various studies have demonstrated a positive correlation between HT and OAG. The Blue Mountains Eye Study revealed that without IOP adjustment, each 10 mmHg increase in SBP corresponded to a 10% higher OAG prevalence. Similarly, a 10 mmHg increase in SBP, DBP, or MAP was linked to a 20-30% increase in OHT prevalence (Mitchell, Lee et al. 2004). A meta-analysis also showed that patients with HT have about a 1.2-fold higher risk of developing OAG than healthy individuals, with a stronger association for POAG than NTG (Bae, Lee et al. 2014). This aligns with other studies showing a positive link between HT and POAG (Bonomi, Marchini et al. 2000, Orzalesi, Rossetti et al. 2007). However, the relationship between HT and NTG is more controversial. For example, some reports suggest no correlation (Dielemans, Vingerling et al. 1995), while others indicate that NTG patients exhibit higher nocturnal DBP and MAP (Plange, Kaup et al. 2006) and are more prone to develop HT (Wierzbowska, Wierzbowski et al. 2012). It is estimated that approximately 8% of HT patients may develop glaucoma, with NTG being the most common type (Gangwani, Chan et al. 2013).

Despite the evidence of a positive correlation between HT and OAG, some studies suggest that HT might be protective. Leske et al. reported that HT reduced the risk of OAG by up to 50% over a 4-year follow-up (Leske, Wu et al. 2002). Another study

found that OAG patients with SBP > 160 mmHg had better visual acuity and visual fields than those with SBP < 120 mmHg, with low SBP patients more likely to be visually impaired (Peräsalo and Raitta 1990). One explanation is that many HT patients in Leske et al.'s study were on antihypertensive medication and may have maintained better vascular health, preserving microvascular function and arterial wall integrity (Leske, Wu et al. 2002, Harazny, Ritt et al. 2007). Thus, for patients under 60, HT might increase ocular blood flow and safeguard the eye (Tielsch, Katz et al. 1995). In contrast, elderly OAG patients often suffer from ocular ischemia and impaired ocular blood flow regulation, so elevated BP may be needed to maintain perfusion (Peräsalo and Raitta 1990). The complex relationship among BP, antihypertensive treatment, ocular perfusion, and glaucoma risk will be discussed later.

1.4. The Relationship Between BP and IOP

It is suggested that POAG has a stronger association with HT than NTG (Bae, Lee et al. 2014). This raises the possibility that HT may increase POAG risk by increasing IOP. HT patients are more likely to have higher IOP compared to normotensive subjects. The prevalence of OHT is approximately 8.1% in treated HT patients and 8.2% in untreated HT, compared to 4.2% in normal controls (Mitchell, Lee et al. 2004). A longitudinal study found that over 9 years, IOP increased by an average of 0.22 mmHg in normotensive subjects but 0.49 mmHg in HT subjects (Wu, Nemesure et al. 2006). Other studies also document positive correlations between BP and IOP (Bonomi, Marchini et al. 2000, Chen and Lai 2005, Xu, Wang et al. 2007). A meta-analysis showed that each 10 mmHg increase in SBP corresponds to a 0.26 mmHg increase in IOP, and each 10 mmHg increase in DBP corresponds to a 0.34 mmHg increase in IOP (Zhao, Cho et al. 2014). Although statistically significant, these IOP elevations are generally not considered clinically significant.

Several hypotheses may account for the relationship between BP and IOP. First, common regulation by the sympathetic nervous innervation, which, when

overactivated, induces HT and IOP elevation (Wyss 1993, Luo, Li et al. 2020). Sympathetic stimulation can increase outflow resistance by reducing the cross-sectional area of Schlemm's canal in rats (Luo, Li et al. 2020). Second, HT may increase perfusion pressure in ciliary arteries, enhancing AH formation, although this remains plausible as a reduction of AH production was only observed when the ciliary blood flow decreased by > 25% (Bulpitt, Hodes et al. 1975). Normally, AH production remains relatively stable when the ciliary blood flow increases (Kiel, Hollingsworth et al. 2011). Third, RAAS influences both HT and glaucoma (Holappa, Vapaatalo et al. 2017). Systemic RAAS inhibitors like losartan and captopril reduce IOP in POAG patients, suggesting systemic RAAS modulates ocular RAAS and IOP (Costagliola, Di Benedetto et al. 1995, Costagliola, Verolino et al. 2000). AngII and ACE1 have been detected in the retina, ciliary body, and AH (Holappa, Vapaatalo et al. 2017), possibly affecting IOP via transforming growth factor β1 (TGFB1) (Cui, Pan et al. 2022). AngII stimulates TGFB1 gene expression (Gibbons, Pratt et al. 1992), and TGFB1 increases AH outflow resistance by promoting extracellular matrix deposition in the trabecular meshwork (Lightman, Rechthand et al. 1987, Gibbons, Pratt et al. 1992, Fleenor, Shepard et al. 2006, Cui, Pan et al. 2022).

1.5. The Influence of HT on the Retinal Structures

Despite known retinal vascular changes in hypertensive retinopathy, such as arterial narrowing (Ikram, Witteman et al. 2006), the broader impact of HT on retinal structure and function remains incompletely understood (Ikram, Witteman et al. 2006). HT has been linked to reduced retinal capillary density (Chua, Chin et al. 2019) and thinning of the macula and peripapillary RNFL (Xu, Zhou et al. 2013, Kong, Kwun et al. 2015, Sahin, Sahin et al. 2015, Akay, Gundogan et al. 2016, Lim, Lee et al. 2019). Animal models, such as Spontaneous hypertensive rats (SHR), display ocular degenerations including decreased vascular density, irregular and tortuous vessels, and loss of RGCs and photoreceptors (Sabbatini, Strocchi et al. 2001, Dong, Gustafson et al. 2019, Leskova, Warar et al. 2020, Li, Wang et al. 2020). Functional

retinal changes related to HT have been assessed in only one study by Sicard et al., which reported reduced electroretinogram (ERG) b-wave amplitudes in SHR compared to normotensive Wistar Kyoto rats (WKY) (Dong, Gustafson et al. 2019). These models provide insight into HT-induced retinal alterations, although further research is needed to elucidate detailed mechanisms.

2. Objectives

As mentioned above, glaucoma is the leading cause of irreversible blindness worldwide. However, the correlation between HT and the risk of glaucoma remains controversial, as studies have reported both positive and negative associations. In addition, IOP is recognized as a significant risk factor for glaucoma. Despite this, the influence of BP on IOP has not yet been well documented. In this study, the IOP profile of the chronic hypertensive and normotensive rats will be examined, and the relationship between BP and IOP will be investigated.

Previous research has identified characteristic features of hypertensive retinopathy and choroidopathy. Nevertheless, many questions remain unanswered regarding how HT affects the eye. Although some studies suggest that HT may lead to retinal degeneration, the extent to which HT affects the different retinal cell types is poorly understood. It is also unknown whether the various stages of chronic HT differentially affect the retina. Retinal structural changes induced by chronic HT have not been thoroughly explored, and there is little literature on how chronic HT may influence retinal functions. This study will assess the effects of HT on retinal structure and functional responses in both hypertensive and normotensive rats throughout the progression of HT.

While it is generally agreed that HT causes narrowing and stiffening of blood vessels, hemodynamic changes at different stages of HT remain inadequately documented. This study will investigate the retinal hemodynamics at various stages of HT by measuring the inner lumen area of retinal arteries and veins near the optic nerve and the blood velocities of the central retinal artery at different stages of HT.

Taken together, the primary objectives of this study are:

- To investigate the relationship between BP and IOP at different stages of HT;
- To evaluate the effects of HT on retinal structure and functional responses at different stages of HT; and

- To investigate the impact of HT on retinal hemodynamics throughout the progression of HT.

3. Methods

3.1. Animals

As mentioned earlier, SHR and WKY have been used as animal models for HT and normotensive controls, respectively. The development of the SHR model was first described by Okamoto and Aoki in 1963 (Okamoto and Aoki 1963) to mimic primary HT in humans (Okamoto and Aoki 1963). The model was established by selecting one WKY with persistently high SBP (150-175 mmHg) and one female rat with slightly higher SBP (130-140 mmHg) relative to their peers as parental animals. Through selective breeding of WKY with SBP over 150 mmHg, the mean SBP in the 6^{th} filial generation exceeded 170 mmHg. Because this selective breeding involved no treatment to induce HT, the SHR model closely resembles primary HT in humans (Okamoto and Aoki 1963, Yamori 2013). Following the establishment of SHR, Okamoto et al. further selectively inbred SHR exhibiting stroke to develop a subtype termed stroke-prone SHR (Okamoto 1974). Due to the frequent occurrence of stroke and cerebral hemorrhage in this strain, the stroke-prone SHR has become a valuable model for studying vascular diseases caused by HT (Yamori 2013).

In our study, we aimed to investigate the influence of HT on the retina, including the hemodynamic changes. Therefore, we used stroke-prone SHR as the animal model and WKY as normotensive controls. Throughout this study, the term SHR specifically refers to the stroke-prone SHR. Both SHR and WKY animals were housed in a temperature-controlled room with a 12-hour light/dark cycle and had free access to food and water. The light intensity in the animal housing room was approximately 300 lux. All experimental procedures and animal handling complied with the ARVO Statement for the Use of Animals in Ophthalmic and Vision Research and were approved by the Animal Ethics Sub-committee at The Hong Kong Polytechnic University. The BP, IOP, functional retinal responses, retinal structure, and hemodynamic parameters were measured at 4, 8, and 12 months of age in both SHR and WKY groups. This study comprised two parts: a cross-sectional study involving

all available animals at each targeted age, and a longitudinal study in which a cohort of SHR and WKY was followed from 4 months to 12 months of age.

3.2. Measurement of BP

The SBP and DBP of SHR and WKY were measured using the BP-2000 Blood Pressure Analysis System (Visitech Systems). This system consists of a measurement platform, a control unit, and a computer, as shown in Figure 5A. A red-light source is positioned beneath the rat's tail being measured, and the amount of light transmitted through the tail is recorded in real-time. The amount of scattered red light is proportional to the degree of the vessel dilation. Variations in the light transmitted through the tail were monitored and displayed on the computer screen. During each measurement, a tail cuff gradually increases compressive pressure. As the cuff pressure increases, the degree of the vessel dilation decreases, causing the signal to weaken. When the signal amplitude begins to decline, it corresponds to the DBP, while the pressure at which the signal amplitude disappears corresponds to the SBP. Measurements were conducted between 2 pm and 5 pm. Prior to data collection, the animals were trained to adapt to the system over three days. For each time point, 20 consecutive measurements were taken, and the average values were used to determine the final DBP and SBP readings

3.3. Measurement of IOP

The IOP was measured using the Tonolab rebound tonometer (Icare, Finland) between 1 pm and 3 pm, as shown in Figure 6A. Six readings were averaged for each measurement. The sequence of measurements was randomized between the SHR and WKY groups. All measurements and training for BP and IOP were conducted while the animals were awake. To ensure the reliability of the IOP and BP data, all procedures were performed gently to minimize any discomfort to the animals.

3.4. Measurements of Functional Retinal Responses

Functional retinal responses of SHR and WKY were recorded using a full-field ERG (Ganzfeld, Q450; RETI Animal, Roland Consult, Germany). The animals were dark-adapted for at least 6 hours prior to data acquisition. Before the measurements, the animals were fully anesthetized with a ketamine-xylazine mixture and their pupils dilated using 0.5% tropicamide (Mydrin-P, Santen Pharmaceutical, Japan). The exact dosage of anesthetic drugs was 66.67 mg/kg of Ketamine plus 6.67 mg/kg of Xylazine. Gold ring active electrodes were placed gently on the corneal surface after applying one drop of lubricating gel to the eye. Reference electrodes were inserted into the lateral canthi, and the ground electrode was inserted into the base of the tail, as shown in Figure 7A. The response from RGCs was represented by the positive scotopic threshold response (pSTR) (Fortune, Bui et al. 2004), recorded at the stimulation intensity of -4.8 log cd s/m^2. The response from photoreceptors was represented by the a-wave (Nixon, Bui et al. 2001), while the b-wave has been estimated to reflect the responses from bipolar cells and Muller cells (Bhatt, Hunt et al. 2023). The amplitudes of a and b-waves were measured under single-flash stimulation with an intensity of 1.3 log cd s/m^2. All recordings were conducted under a bandpass filter of 0.1–1000 Hz.

3.5. Measurements of Retinal Thickness using OCT

The retinal morphologies were imaged using an Optical Coherence Tomography (OCT) system (Envisu-R2210, Bioptigen, Leica Microsystems, IL, USA) (Figure 8A). During the measurements, the animals were fully anesthetized with a ketamine-xylazine mixture, and their pupils were dilated with 0.5% tropicamide (Mydrin-P, Santen Pharmaceutical, Japan). A single lubricant eye drop (Systane, Alcon Laboratories) was applied to moisten the eye and enhance the optical quality of the corneal surface. Retinal thickness was measured radially from the center of the optic nerve at a radius of 1 mm. Measurements included the thicknesses of the total retina, RNFL, and IPL (Figure 8D). For each OCT scan, one hundred images were

obtained, of which eight images were selected for data analysis: the 1st, 13th, 26th, 38th, 51st, 63rd, 76th, and 88th images, as illustrated in Figure 8B. If the images overlapped with inner retinal vasculature, making accurate RNFL thickness measurements difficult due to vascular interference, adjacent images were used instead. Thickness measurements were performed manually using ImageJ in a masked manner. During the analysis, the optic nerve head area was excluded, specifically the central area with a radius of 0.5 mm, as illustrated in Figure 8C. Figure 8B displays the images analyzed, with red lines indicating the selected areas. The unshaded area in Figure 8C represents the measured area for each individual image.

3.6. Measurements of the Inner Lumen Area of Retinal Arteries and Veins

Similarly, the inner lumen area of retinal arteries and veins was estimated using the Doppler mode of the OCT system (Envisu-R2210, Bioptigen, Leica Microsystems, IL, USA) (Zhao, Nguyen et al. 2018, Lakshmanan, Wong et al. 2023). The inner lumen area of the arteries and veins supplying the inner retina near the optic disc was recorded using a circle scan with 50 replicates. The circle scan was centered on the optic nerve head with a radius of 0.25 mm, as illustrated in Figure 9A. The blue circle in Figure 9A represents the scan area. A representative image is shown in Figure 9B, where the portion of the inner retina (circled by red) represents the arterial blood flow, and the portion of the inner retina (circled by blue) represents the venous blood flow (Lakshmanan, Wong et al. 2023). The results were analyzed manually using ImageJ. Fifty images were obtained for each Doppler OCT scan, and 10 images were selected for data analysis: the 6th, 11th, 16th, 21st, 26th, 31st, 36th, 41st, and 46th images.

3.7. Measurement of Blood Velocities of the Central Retinal Artery

The blood velocities of the central retinal artery were measured using a Doppler 3D imaging system (FUJIFILM VisualSonics VevoLAZR Multimodality Imaging Platform). The animals were anesthetized with isoflurane throughout the experiment to ensure rapid anesthesia and recovery. Before the procedure, a generous layer of

ultrasound gel was applied and smoothed onto the transducer face, and ultrasound gel was also applied to the rat's eye. Care was taken to avoid hair near the eye to prevent interference with the probe surface. Any air bubbles within the ultrasound gel were removed before performing ultrasound imaging. During the experiment, the Doppler 3D mode was activated, and both the probe and the rat were positioned to allow visualization of ocular structures, including the cornea, iris, and arterial and venous blood supply to the retina. As shown in Figure 10A-B, the red area represents the arterial signal, while the blue area represents the venous signal. After locating the central retinal artery, the detector was positioned to obtain the highest blood velocities. Both peak and mean velocities were measured. Each captured image comprised twelve cycles and three readings, as illustrated in Figure 10A-B. The reading for each image was calculated as the mean of all three measurements. Three images were captured for each eye, and the highest velocity value among them was recorded as the final measurement.

4. Results

4.1. Cross-sectional Studies

4.1.1. BP

The SBP and DBP were measured in SHR and WKY at 4, 8, and 12 months. SHR exhibited significantly higher SBP than WKY at all measured time points, as illustrated in Figure 5B. For the DBP, SHR values were significantly higher than in WKY only at 12 months (Figure 5C). Both the SBP and DBP in SHR increased over time, whereas in WKY, neither the SBP nor the DBP changed significantly. The SBP difference in SBF was significant at 4 months and increased with age. At 4 months, the mean SBP difference between SHR and WKY exceeded 30 mmHg. Specifically, the SBP in SHR was higher than in WKY by 29%, 35%, and 58% at 4, 8, and 12 months, respectively. The DBP in SHR was higher than in WKY by 90% at 12 months.

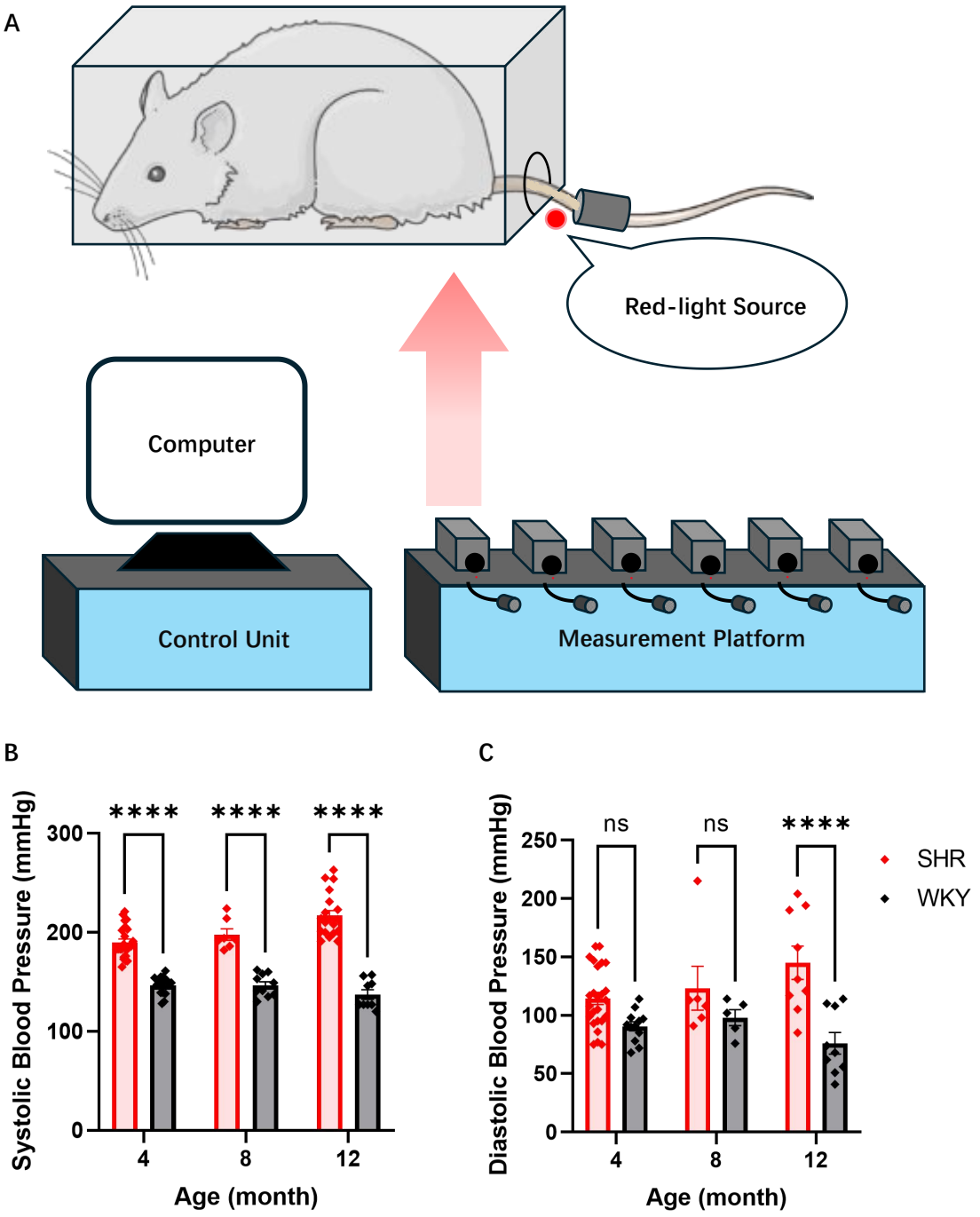

Figure 5. A. Illustration of the Blood Pressure Analysis System used to measure BP in a rat (rat image sourced from Servier Medical Art); **B-C.** Cross-sectional measurements of SBP and DBP in SHR and WKY. Data are presented as Mean ± SEM. **** $P < 0.0001$ (Two-way ANOVA with Bonferroni's multiple comparisons test).

4.1.2. IOP

The IOP was measured at 4, 8, and 12 months in both SHR and WKY. While SHR exhibited significantly higher BP than age-matched WKY, their IOP was significantly lower (Figure 6B). IOP remained consistent over time in both groups. However, the difference in mean IOP between SHR and WKY was less than 1.2 mmHg at all measured time points. The mean IOP in SHR was 9.1, 9.5, 9.4, and 9.5 mmHg at 4, 8, 12, and 15 months, respectively, compared to 10.2, 10.3, 10.5, and 10.3 mmHg in WKY at the corresponding ages. Although the IOP difference between SHR and WKY was statistically significant, it is unlikely to have a substantial impact on ocular physiology and may not be clinically significant.

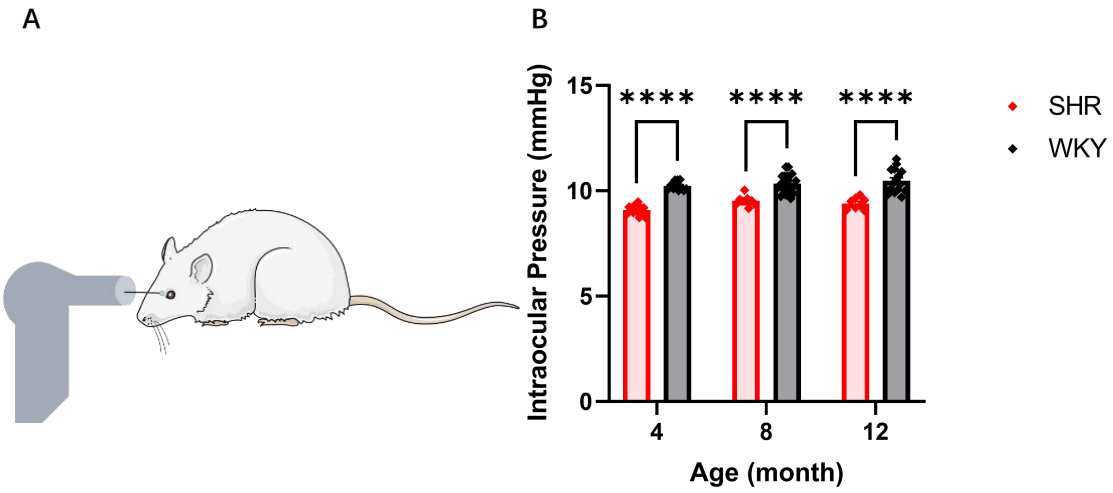

Figure 6. A. Illustration of IOP measurement using a rebound tonometer; **B.** Cross-sectional measurements of IOP in SHR and WKY. Data are presented as Mean ± SEM. ** $P < 0.01$; **** $P < 0.0001$ (Two-way ANOVA with Bonferroni's multiple comparisons test).

4.1.3. Functional Retinal Responses

The functional retinal responses of 4, 8, and 12-month-old SHR and WKY are summarized in Figures 7F-H. A decline in retinal responses was observed with aging in both groups. However, retinal function decreased earlier in SHR than in WKY. At 4 months, ERG amplitudes showed no significant difference between SHR and WKY. By 8 and 12 months, SHR exhibited a significant reduction in ERG amplitudes of pSTR, a-wave, and b-wave. At 8 months, these responses were reduced by 29%, 12%, and 11%, respectively, in SHR compared to WKY. At 12 months, reductions increased to 32%, 28%, and 19%, respectively.

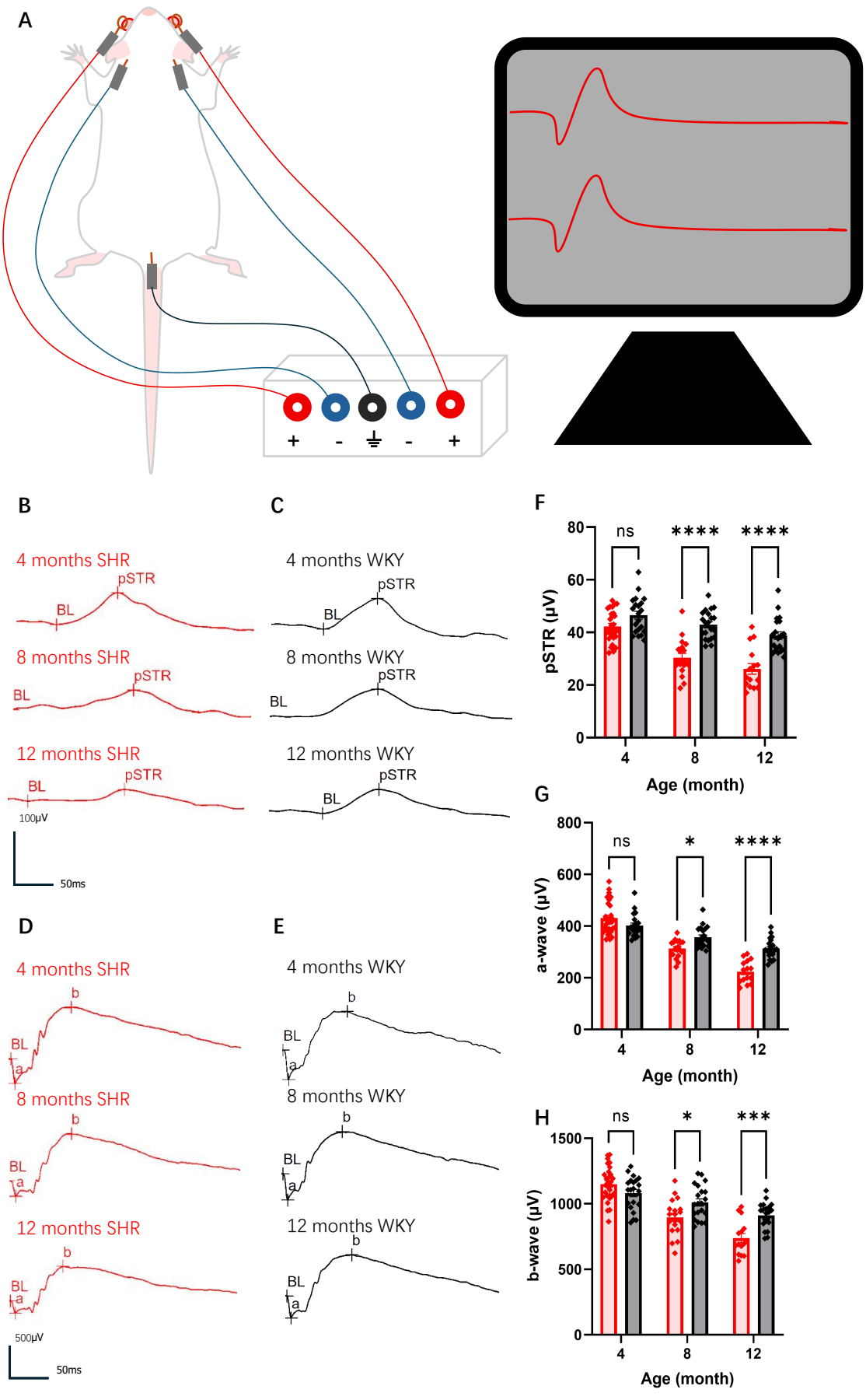
A
+ - - +
B
4 months SHR
pSTR
BL
8 months SHR
pSTR
BL
12 months SHR
BL
pSTR
100μV
50ms
C
4 months WKY
pSTR
BL
8 months WKY
pSTR
BL
12 months WKY
pSTR
BL
D
4 months SHR
b
BL
a
8 months SHR
b
BL
a
12 months SHR
b
BL
a
500μV
50ms
E
4 months WKY
b
BL
a
8 months WKY
b
BL
a
12 months WKY
b
BL
a
F
ns
****
****
pSTR (μV)
80
60
40
20
0
4
8
12
Age (month)
G
ns
*
****
a-wave (μV)
800
600
400
200
0
4
8
12
Age (month)
H
ns
*
***
b-wave (μV)
1500
1000
500
0
4
8
12
Age (month)

Figure 7. A. Illustration of the full-field ERG setup; **B.** pSTR waveforms from 4, 8, and 12-month-old SHR; **C.** pSTR waveforms from 4-, 8-, and 12-month-old WKY; **D.** a and b-waveforms from 4-, 8-, and 12-month-old SHR; **E.** a and b-waveforms from 4, 8, and 12-month-old WKY; **F-H.** Cross-sectional measurements of pSTR, a-wave, and b-wave amplitudes in 4, 8, and 12-month-old SHR and WKY. Data are presented as Mean ± SEM. * $P < 0.05$; *** $P < 0.001$; **** $P < 0.0001$ (Two-way ANOVA with Bonferroni's multiple comparisons test).

4.1.4. The Retinal Thicknesses

The OCT results showed retinal thickness measurements in SHR and WKY at 4, 8, and 12 months (Figure 8F-H). For the RNFL, there were no significant differences between SHR and WKY at any time point. The thickness of IPL decreased with age in both groups. However, SHR exhibited significantly thinner IPL at all measured time points. Specifically, IPL thickness was reduced by 7.9%, 5.8%, and 6.7% in SHR compared to WKY at 4, 8, and 12 months, respectively. Total retinal thickness decreased with age in both SHR and WKY, with SHR showing thinner retinas at all time points. Specifically, retinal thickness was reduced by 4.0%, 4.0%, and 5.76% in SHR compared to WKY at 4, 8, and 12 months, respectively.

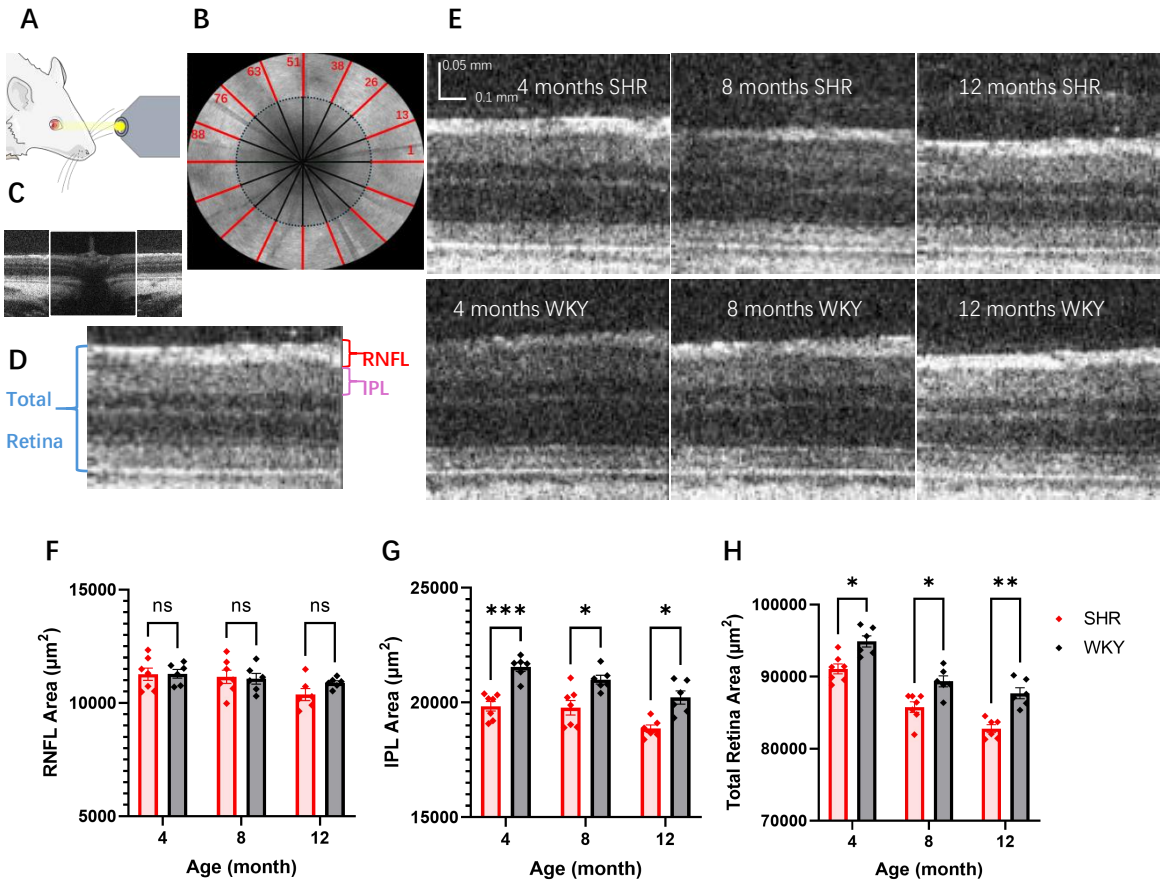

Figure 8. A. Illustration of the OCT settings; **B.** Example of analyzed images selected from 100 captures; **C.** Illustration of the area excluded from analysis (the shaded central region); **D.** Identification of the RNFL, IPL, and total retina layers; **E.** Representative OCT images from 4-, 8-, and 12-month-old SHR and WKY; **F-H.** Cross-sectional measurements of the RNFL, IPL, and total retina thicknesses in 4-, 8-, and 12-month-old SHR and WKY. Data are presented as Mean ± SEM. * P <0.05; ** P < 0.01; *** P < 0.001 (Two-way ANOVA with Bonferroni's multiple comparisons test).

4.1.5. The Inner Lumen Area of Retinal Arteries and Veins

The inner lumen area of retinal arteries and veins in SHR was consistently lower than in WKY at all measured time points, as shown in Figure 9D-E. At 4, 8, and 12 months, the inner lumen area of retinal arteries in SHR was reduced by 61%, 64%, and 73%, respectively, compared to WKY. For the inner lumen area of retinal arteries, it decreased with age in both SHR and WKY. For the inner lumen area of retinal veins, SHR also exhibited smaller areas than age-matched WKY at all time points. Specifically, inner lumen area of retinal veins in SHR was 61%, 68%, and 56% lower than in WKY at 4, 8, and 12 months, respectively. In both groups, the inner lumen area of retinal veins did not change significantly with age. These results indicate that vascular remodeling in the retinas of SHR is more severe than in WKY at 4 months of age. In retinal arteries, the degree of remodeling in SHR progressively increases with age compared to WKY. For retinal veins, remodeling remains consistently higher in SHR than in WKY, although the extent does not change over time.

4.1.6. Blood Velocities of the Central Retinal Artery

The mean blood velocity of the central retinal artery was comparable between SHR and WKY at 4 and 8 months, as shown in Figure 10D-E. At 12 months, the mean blood velocity was 21% higher in SHR. No significant difference in peak blood velocity was detected between SHR and WKY at 4 and 8 months. At 12 months, SHR exhibited a significantly elevated peak blood velocity, 15% higher than that of WKY. The slight increase in blood velocity may represent a compensatory response to enhance blood flow.

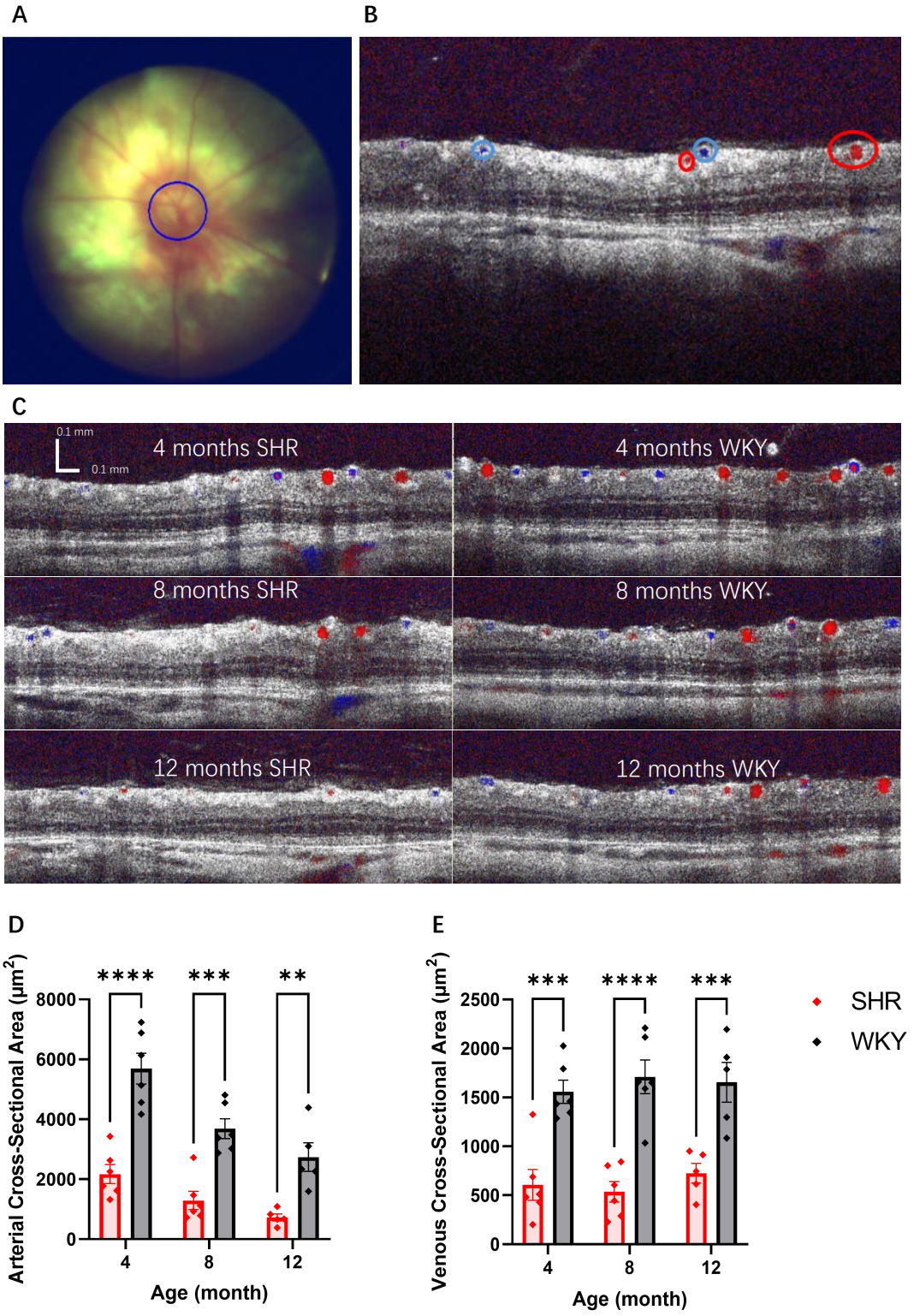

Figure 9. A. Fundus view of the circular scan for inner lumen area of retinal arteries and veins measurements; **B**. Schematic diagram indicating the measured arterial (red circle) and venous (blue circle) regions; **C.** Representative images of inner lumen area of retinal arteries and veins from 4-, 8-, and 12-month-old SHR and WKY; **D-E.** Cross-sectional measurements of inner lumen area of retinal arteries and veins in 4-,

8-, and 12-month-old SHR and WKY. Data are presented as Mean ± SEM. ** P < 0.01; *** P < 0.001; **** P < 0.0001 (Two-way ANOVA with Bonferroni's multiple comparisons test).

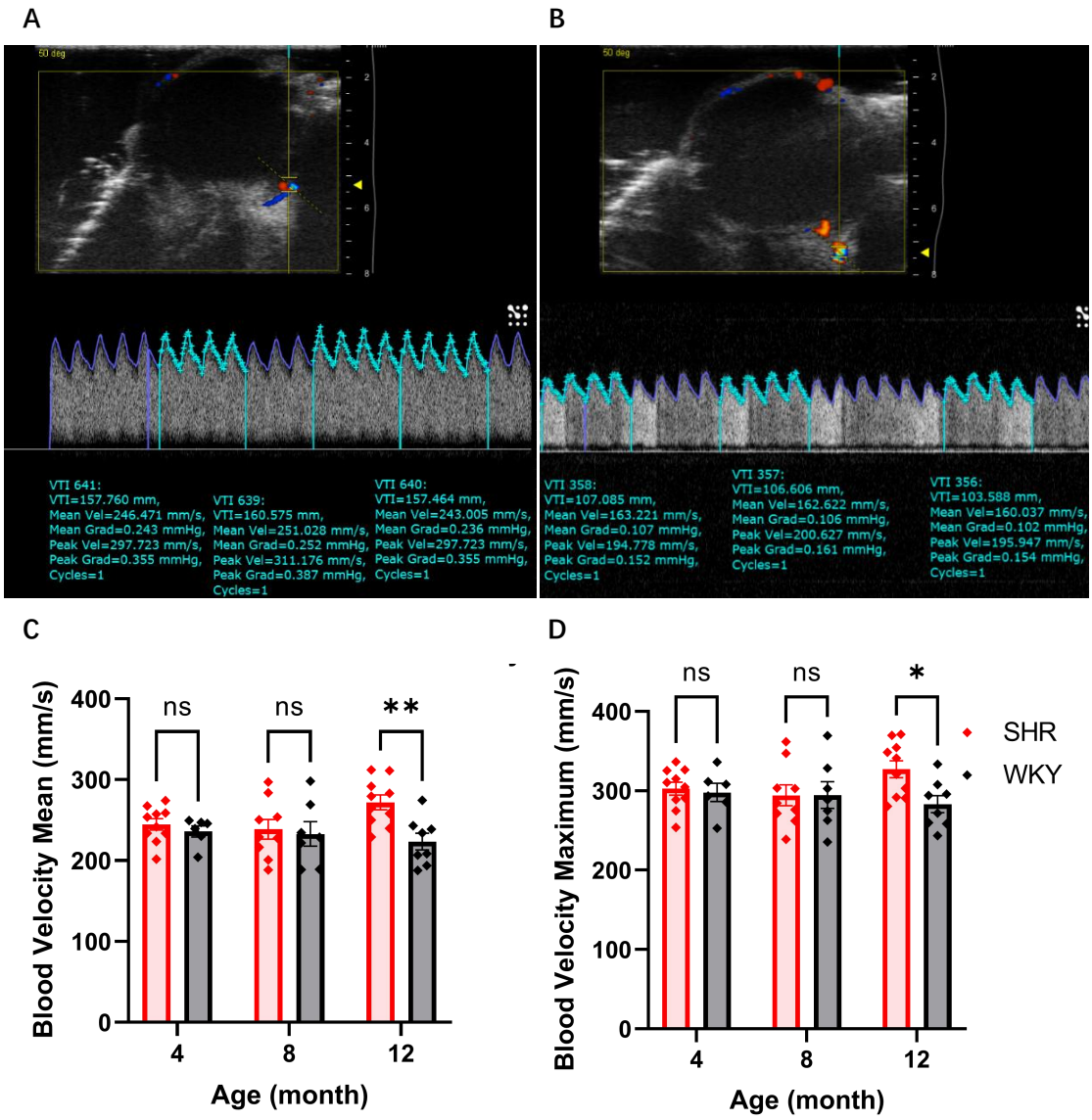

Figure 10. A-B. Representative images of arterial blood velocities acquired from a (A) 12-month-old SHR and a (B) 12-month-old WKY; **D-E.** Cross-sectional measurements of mean and peak arterial blood velocities in 4-, 8-, and 12-month-old SHR and WKY. Data are presented as Mean ± SEM. * $P < 0.05$; ** $P < 0.01$ (Two-way ANOVA with Bonferroni's multiple comparisons test).

4.2. Longitudinal Studies

For the longitudinal studies, groups of SHR and WKY were monitored continuously from 4 to 12 months. The BP, IOP, functional retinal response, retinal thickness, inner lumen area of retinal arteries and veins, and blood velocities of the central retinal artery are summarized in Figure 11. Consistent with the results obtained from the cross-sectional studies, SBP was significantly higher in SHR than in age-matched WKY (Figure 411). The DBP was also significantly higher in SHR at 12 months (Figure 11C). The SBP in SHR exceeded that in WKY by 26%, 47%, and 47% at 4, 8, and 12 months, respectively (Figure 11B). For DBP, SHR was higher than WKY by 57% at 12 months (Figure 11C). Both SBP and DBP in SHR increased over time, while in WKY, these measures did not change significantly. Similarly, IOP in WKY was significantly higher than in SHR at all measured time points, although the difference in mean IOP between SHR and WKY was less than 1.4 mmHg across all time points (Figure 11D). In addition, the amplitudes of pSTR, a-wave, and b-wave decreased over time in both SHR and WKY. The pSTR and a-wave amplitudes in SHR were significantly reduced compared to WKY at 8 and 12 months, while the b-wave amplitude was significantly reduced in SHR at 12 months. At 8 months, SHR showed a 27% reduction in pSTR amplitude and a 19% reduction in a-wave amplitude. At 12 months, the amplitudes of pSTR, a-wave, and b-wave in SHR were reduced by 40%, 29%, and 23%, respectively (Figure 11E-G). Retinal thickness measurements are shown in Figure 11H-J. All measured layers demonstrated a significant decline with age in both SHR and WKY. No significant difference in RNFL thickness was detected between SHR and WKY at any time point (Figure 11H). SHR showed significantly thinner IPL at all measured time points. IPL thickness was reduced by 6.6%, 8.9%, and 8.1% in SHR compared to WKY at 4, 8, and 12 months, respectively (Figure 11I). Total retinal thickness was consistently thinner in SHR at all time points, reduced by 4.6%, 6.1%, and 7.3% at 4, 8, and 12 months, respectively (Figure 11J). Inner lumen area of retinal arteries and veins was consistently lower in SHR than in WKY at all time points. At 4, 8, and 12 months, the inner lumen area of retinal arteries in SHR was reduced by 72%, 62%, and 77%, respectively, compared

to WKY. The inner lumen area of retinal arteries and decreased with age in both groups (Figure 11K). The inner lumen area of retinal veins decreased with age in SHR but remained stable in WKY. In addition, the inner lumen area of retinal veins in SHR is also lower than that of age-matched WKY at all time points (Figure 11L). The inner lumen area of retinal veins in SHR was lower than in age-matched WKY at all time points, with reductions of 70%, 69%, and 63% at 4, 8, and 12 months, respectively. There were no significant differences in blood velocities of the central retinal artery between SHR and WKY at all time points. In both groups, blood velocities increased over time, with SHR showing a more substantial rise than WKY (Figure 11M-N). Similar to the cross-sectional study, we expect that retinal blood flow is significantly reduced in SHR due to smaller lumen areas, despite blood velocity being relatively similar to that of WKY. Overall, the results of the longitudinal studies showed good agreement with those obtained from the cross-sectional studies.

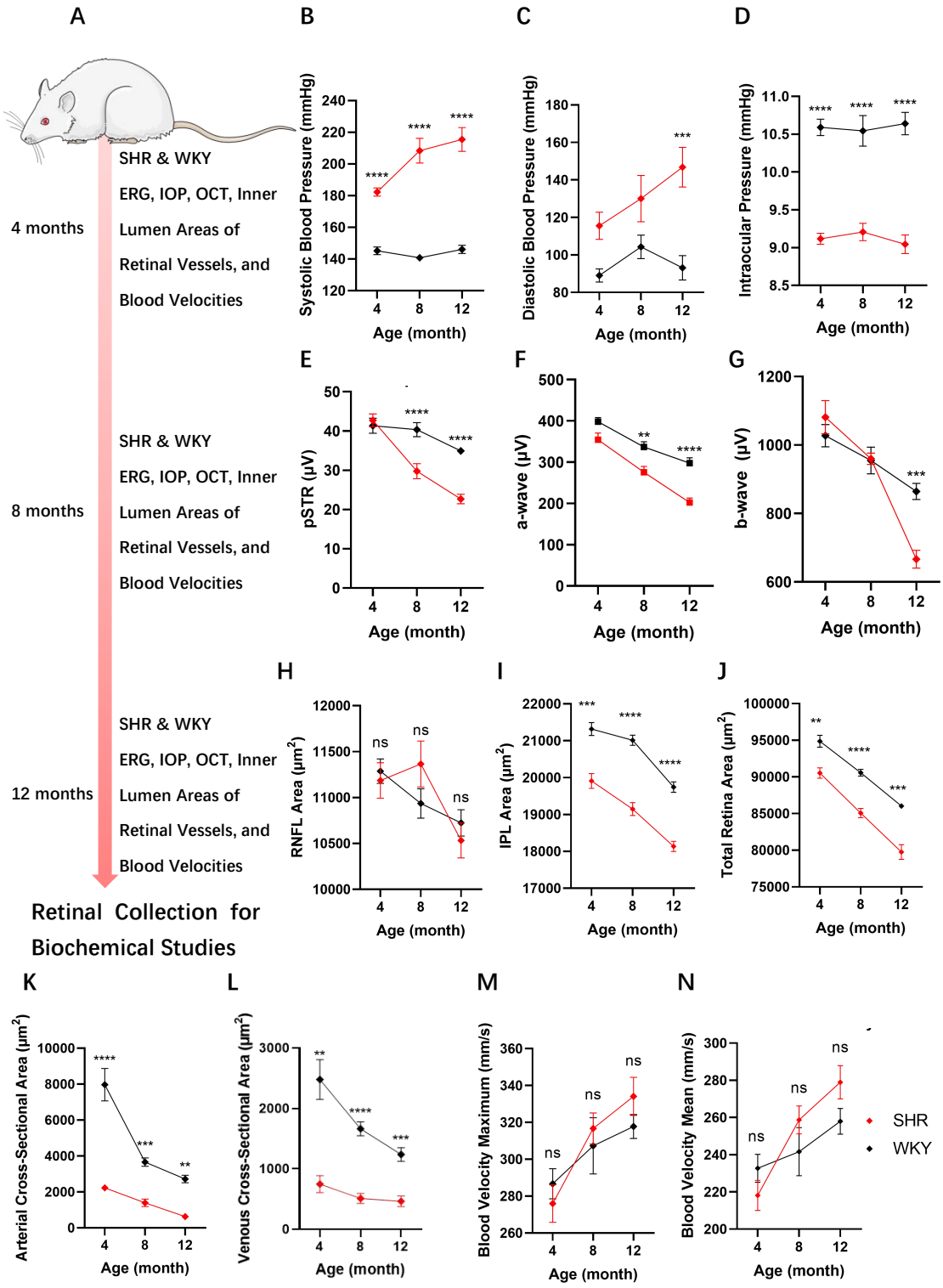

Figure 11. A. Experimental design; **B-D**. Longitudinal measurements of BP and IOP in SHR and WKY; **E-G.** Functional retinal response measurements in SHR and WKY; **H-J.** Retinal thickness measurements in SHR and WKY; **K-L.** Longitudinal measurements of inner lumen area of retinal arteries and veins in SHR and WKY; **M-N** Blood velocity measurements of the central retinal artery in SHR and WKY.

Data are presented as Mean ± SEM. * P < 0.05; ** P < 0.01; *** P < 0.001; **** P < 0.0001 (Two-way ANOVA with Bonferroni's multiple comparisons test).

5. Discussion

In this study, we investigated the influence of chronic primary HT on IOP, functional retinal responses, retinal structures, and retinal hemodynamics using both hypertensive and normotensive animal models. We conducted cross-sectional and longitudinal measurements for both SHR and WKY at different stages of HT. The results of the longitudinal studies were in good agreement with those from the cross-sectional studies. Although previous studies have examined the structural and functional differences between SHR and WKY, our study is the first to investigate these changes in both groups longitudinally. We observed accelerated structural and functional decline in SHR. Our findings showed that SHR consistently exhibited higher SBP but lower IOP than WKY at all measured time points. At an early stage of HT (4 months), the functional retinal responses in SHR were comparable to those of WKY. However, as the animals aged, the functional retinal responses in SHR declined relative to WKY. At 8 and 12 months, the pSTR, a-wave, and b-wave amplitudes in SHR were significantly reduced compared to WKY. The IPL and total retinal thickness in SHR were thinner than those in WKY as early as 4 months, and these differences persisted at older ages. The inner lumen area of retinal arteries and veins was consistently lower in SHR compared to age-matched WKY, while peak and mean blood velocities were comparable between SHR and WKY except at 12 months, whereby SHR was observed to have higher blood velocities. Our results align with a previous study where a positive correlation was observed between peak blood velocity in the common carotid artery and BP in humans (Perret and Sloop 2000). It is anticipated that increased arterial stiffness accompanying HT contributes to elevated blood velocity. Increased aortic stiffness leads to decreased diastolic blood flow, and the elevated blood velocity helps sustain diastolic blood flow. Therefore, the rise in blood velocity serves as a compensatory mechanism to maintain adequate blood flow (Perret and Sloop 2000). In our study, the inner lumen area of retinal arteries and veins in SHR was reduced by over 50% at all time points. Although peak blood velocity in SHR increased by approximately 20% compared to WKY at 12 months, the compensatory velocity increase was insufficient to offset the reduction in inner

lumen area. We suggest that SHR likely exhibits reduced overall retinal blood flow compared to WKY.

Our results revealed that SHR exhibits higher BP but, interestingly, lower IOP than WKY. Previous studies have shown conflicting results regarding the IOP difference between SHR and WKY (Vaajanen, Mervaala et al. 2008). One study indicated that IOP in SHR was higher than in WKY (Vaajanen, Mervaala et al. 2008), reporting mean IOP of 18.7 mmHg and 16 mmHg at 5 weeks, and 22.5 mmHg versus 20.2 mmHg at 15 weeks, respectively (Vaajanen, Mervaala et al. 2008). Conversely, a study by Funk et al. reported that at 8-9 months, mean IOP in SHR ranged from 7 mmHg to 7.5 mmHg, whereas WKY ranged from 15 mmHg to 16.5 mmHg (Funk, Rohen et al. 1985). Our results align with those of Funk et al., suggesting that lower IOP is seen in SHR. The reason for the discrepancy between BP and IOP in SHR is not entirely clear. One possibility is that SHR develops vascular rarefaction and hyalinization in the ciliary body connective tissue, which may reduce AH formation (Funk and Rohen 1985). Despite this, the observed IOP difference between SHR and WKY is subtle and may not be clinically significant, making it unlikely to mediate significant changes in the retina and optic nerve.

Limited evidence has documented retinal functional changes during the HT progression. To the best of our knowledge, this is the first study to longitudinally monitor functional retinal changes in SHR and WKY at different hypertensive stages. We observed reduced amplitudes of pSTR, a-wave, and b-wave in 8-month SHR compared to WKY, and these declines persisted through at least 12 months. These findings suggested that in SHR, functional responses of RGCs, photoreceptors, bipolar cells, and Muller cells are compromised, potentially leading to neurodegeneration. A previous study reported reduced b-wave amplitude by 20-30% in 11-week SHR compared to WKY (Sicard, Acar et al. 2007). In contrast, we detected significant differences starting at 8 months. Our results indicate that at 4

months, hypertensive-induced vascular changes may not yet be severe enough to cause significant functional impairment.

Previous studies have reported deterioration of retinal structures in SHR, including a reduced population of RGCs and degeneration of photoreceptors (Sabbatini, Strocchi et al. 2001, Li, Wang et al. 2020), as reflected by degeneration of the GCL at 6 months, and ONL degeneration at 10 weeks in SHR, respectively (Sabbatini, Strocchi et al. 2001, Li, Wang et al. 2020). In contrast, we observed thinning of the IPL in SHR as early as 4 months, which may indicate that synapses between RGCs and intermediate cells degenerate faster than other retinal components in SHR. In addition, total retinal thickness was reduced in SHR as early as 4 months, suggesting that structural changes precede functional degeneration.

We observed reduced functional retinal responses in SHR at 8 and 12 months. Interestingly, the IOP was consistently lower in SHR, indicating that the reduction in functional retinal responses in SHR is likely due to mechanisms other than mechanical compression. Furthermore, the inner lumen area of retinal arteries and veins was significantly smaller in SHR (>60% reduction) than in age-matched WKY. Conversely, the mean blood velocity in the central retinal artery of 12-month SHR was only slightly higher than in WKY. We propose that a decline in retinal function in SHR is due to impaired ocular perfusion. First, vessels in HT develop a higher wall-to-lumen ratio, which impedes ocular blood flow. An animal study comparing rats experiencing acute BP elevation with rats having chronic BP elevation for 4 weeks demonstrated that the latter exhibited an increased aortic wall-to-lumen ratio and decreased ocular blood flow, despite similar BP levels in both groups (He, Vingrys et al. 2014). In addition, a negative correlation between the aortic wall-to-lumen ratio and retinal peak vasodilation was observed in rats (van Koeverden, He et al. 2018). Furthermore, it was demonstrated that rats with chronic HT for 12 weeks showed reduced vasodilatory capacity in retinal vessels when BP decreased,

compared to normotensive controls. Our findings agree that prolonged HT causes vascular changes and reduces retinal perfusion. As mentioned above, insufficient blood supply to ocular structures is believed to play a key role in glaucoma. In our study, we observed reduced pSTR in SHR at 8 and 12 months compared to WKY, supporting that diminished inner retinal blood flow may contribute to deteriorated RGC function in SHR. In addition, reduced blood flow is only one aspect contributing to HT-related retinal degeneration. The following chapters will explore additional mechanistic links between HT and reduced functional retinal responses from a biochemical aspect.

Chapter 3. Neuroinflammation Mediates Hypertension-Induced Retinal Degeneration

1. Introduction

1.1. Overview of the Biochemical Aspect of the Pathogenesis of HT

Close correlations have been shown among AngII, systemic inflammation, and systemic oxidative stress. AngII affects immune cell differentiation and cytokine production by binding to AT1. Cytokines produced by AngII, such as TNF-α, can stimulate ACE production (Tanase, Gosav et al. 2019). Inflammation elevates oxidative stress. During inflammation, immune cells like neutrophils and macrophages produce ROS, including superoxide and hydrogen peroxide, through the nicotinamide adenine dinucleotide phosphate (NADPH) oxidase pathway. Chronic inflammation may lead to the overproduction of ROS. Oxidative stress causes vascular dysfunction by reacting with superoxide and reducing the bioavailability of NO (Dinh, Drummond et al. 2014). In addition, ROS promotes the secretion of cytokines such as IL-6, which can further stimulate NADPH production. AngII facilitates immune cells in generating ROS through NADPH oxidase. Increased activity of NADPH oxidase and serum superoxide can stimulate collagen production, worsening vascular dysfunction (Patel, Cardneau et al. 2006). As a result, elevated AngII levels, systemic inflammation, and oxidative stress trigger a positive feedback loop, leading to vascular dysfunction. This process plays a key role in the pathophysiology of HT. In the following sections, the effects of inflammation, oxidative stress, and other molecular factors involved in vascular dysfunction, including NO and endothelins, will be discussed.

1.2. The Role of Inflammatory Cytokines in HT

It has been suggested that inflammation plays a pivotal role in the pathogenesis of HT. BP elevation caused by AngII infusion is reduced in mice lacking T and B cells. In contrast, adoptive transfer of T cells restores the AngII infusion-induced HT (Guzik,

Hoch et al. 2007). C-reactive protein, a biomarker of inflammation, is elevated in the plasma of hypertensive patients (Bautista, Vera et al. 2005). Increased plasma levels of TNF-α and IL-6 have been identified as independent risk factors for HT (Bautista, Vera et al. 2005). Patients with HT are also more prone to elevated plasma IL-10 and IL-1β levels (Barbaro, Fontana et al. 2015). In addition, plasma IL-1β, IL-6, and TNF-α positively correlate with arterial stiffness (Mahmud and Feely 2005, Barbaro, Fontana et al. 2015).

It has been proposed that plasma cytokines might contribute to HT development by worsening vascular damage. Human endothelial cells incubated with serum from hypertensive patients exhibited a higher rate of apoptosis compared to those from normotensive subjects (Barbaro, de Araújo et al. 2015). It was revealed that infliximab, a TNF-α-neutralizing antibody, reduced apoptosis in cultured human endothelial cells, highlighting the potential role of TNF-α in triggering endothelial dysfunction by promoting apoptosis (Barbaro, de Araújo et al. 2015). In addition to mediating vascular endothelial apoptosis, cytokines may contribute to HT development by affecting vascular relaxation processes. Studies in rats have shown that TNF-α reduces endothelium-dependent, NO-mediated vascular relaxation (Giardina, Green et al. 2002). Serum infusion of TNF-α in pregnant rats elevates BP, which may be mediated through the vascular endothelin system. In pregnant rats, pretreatment with ABT-627, an endothelin type A receptor (EDNRA) antagonist, prevents TNF-α-induced BP elevation, while ABT-627 treatment does not affect BP in untreated pregnant rats (LaMarca, Cockrell et al. 2005). Apart from altering blood vessel structure and function, TNF-α has been shown to stimulate the sympathetic nervous system. Intravenous TNF-α administration activates neurons in the paraventricular nucleus of the hypothalamus and in the rostral ventrolateral medulla, leading to increased sympathetic nerve activity and BP (Zhang, Wei et al. 2003). It is also observed that IL-6 may mediate BP elevation caused by AngII. Acute AngII infusion raises BP and plasma IL-6 levels in C57/BL6 mice. In IL-6 KO mice, the BP

increase induced by AngII is less pronounced compared to control C59BL6 mice (Lee, Sturgis et al. 2006). It is likely that IL-6 promotes collagen synthesis in the arterial wall and stimulates fibrinogen production, which can lead to reduced cardiac contractility and increased left ventricular fibrosis and hypertrophy (Tanase, Gosav et al. 2019). Other inflammatory cytokines, such as cyclooxygenase 2 (COX2), cluster of differentiation 68 (CD68), and CCL2, are also associated with HT (Widlansky, Price et al. 2003, Matsuda, Umemoto et al. 2015, Hopps, Lo Presti et al. 2017, Zhao, Wang et al. 2018). Treatment with celecoxib, a selective COX2 inhibitor, markedly improves brachial arterial vasodilation in hypertensive patients, suggesting its crucial role in endothelial dysfunction (Widlansky, Price et al. 2003). CD68 has been proposed to mediate vascular macrophage infiltration and remodeling during AngII infusion, contributing to vascular damage in HT (Zhao, Wang et al. 2018). It promotes overexpression of IL-1β and IL-6 in vascular tissues during AngII infusion. Moreover, the cytoplasmic transcription factor NF-κB, which activates inflammatory responses and ROS production, can be activated by CD68. Moreover, AngII infusion has been shown to increase CCL2 expression via activated TLR4 in heart tissue (Matsuda, Umemoto et al. 2015).

1.3. Increased Systemic Oxidative Stress in HT

Evidence suggests that increased oxidative stress plays a crucial role in the pathophysiology of HT. AngII drives ROS production via NADPH oxidase (Patel, Cardneau et al. 2006), and the superoxide generated by NADPH oxidase in blood vessels can inactivate NO, leading to impaired vasodilation. In addition, superoxide and hydrogen peroxide produced by NADPH oxidase may contribute to fibroblast growth responses and hypertrophy of vascular smooth muscle cells (Griendling, Sorescu et al. 2000, Zalba, San Jose et al. 2001). It has been shown that 8-Hydroxy-2'-deoxyguanosine (8-OHdG), a biomarker of oxidative DNA damage and systemic oxidative stress, is elevated in the urine of hypertensive patients with left ventricular hypertrophy. Moreover, there is a significant correlation between urine

8-OHdG levels and the left ventricular mass index in these patients. Urinary 8-OHdG also positively correlates with plasma TNF-α and IL-6 levels, indicating a strong association between systemic inflammation and oxidative stress in hypertensive patients (Rosello-Lleti, de Burgos et al. 2012). Furthermore, a study found that levels of reduced glutathione, a key antioxidant protein involved in reducing organic peroxides, and the ferric-reducing ability of plasma (FRAP), a measure of total antioxidant capacity, are lower in the plasma of hypertensive patients compared to healthy controls. FRAP levels negatively correlate with DBP (Kashyap, Yadav et al. 2005). In experimental animal models, increased superoxide levels have been observed in the arterioles and venules of SHR (Suzuki, Swei et al. 1995). Rats with glutathione depletion exhibit significantly higher BP, accompanied by a notable decrease in urinary nitrate-plus-nitrite, a stable metabolite of NO. Administration of vitamin E and vitamin C reduces BP elevation and restores urinary NO metabolite levels in glutathione-depleted rats, but not in control rats (Vaziri, Wang et al. 2000).

1.4. The Roles of the Endothelin System in HT

EDN1, a 21-amino acid peptide, is a potent vasoconstrictor secreted by vascular endothelial cells, exerting its effects on the underlying smooth muscle (Nakas-Icindic, Zaciragic et al. 2004). An early study has shown that plasma EDN1 concentrations are elevated in patients diagnosed with essential HT (Shichiri, Hirata et al. 1990). Two distinct endothelin receptor subtypes have been characterized: endothelin receptor type A (EDNRA) and type B (EDNRB). It is widely accepted that EDNRA mediates vasoconstriction, whereas EDNRB promotes vasodilation by increasing NO production. Some research suggests that EDN1 overexpression in the endothelium may lead to arterial hypertrophy and endothelial dysfunction independent of BP elevation (Schiffrin 2005). Investigations have demonstrated that EDN1 activates NADPH oxidase in human endothelial cells (Duerrschmidt, Wippich et al. 2000). Furthermore, EDN1 induces superoxide anion production in rat carotid arteries in a dose-dependent manner. This effect can be blocked by ABT-627, a selective EDNRA

antagonist. These findings support the hypothesis that EDN1 contributes to endothelial dysfunction by promoting ROS-mediated inactivation of NO (Li, Fink et al. 2003). Moreover, administration of EDN1 infusion markedly elevates BP in rats, a phenomenon that can be completely inhibited by Tempol, a superoxide anion scavenger (Sedeek, Llinas et al. 2003). On the other hand, ROS has been demonstrated to upregulate EDN1 synthesis, indicating a positive feedback loop whereby EDN1 overexpression mediates vascular remodeling, NO depletion, and endothelial impairment via increased ROS generation (Kahler, Mendel et al. 2000). EDN1 is also believed to play a key role in HT caused by AngII infusion. Studies in rats have demonstrated that AngII administration increases EDN1 levels in mesenteric arteries. The administration of LU135252, an EDNRA antagonist, abolishes these vascular changes and partially attenuates the AngII-induced BP elevation. It is likely that AngII induces vascular alterations by increasing EDN1 production via EDNRA (Moreau, d'Uscio et al. 1997). In addition, EDNRA antagonists have been found to reduce BP in patients with chronic renal failure (Goddard, Johnston et al. 2004), indicating that EDNRA mediates BP elevation.

In addition to EDN1, there are two other isoforms of endothelin: endothelin-2 (EDN2) and endothelin-3 (EDN3). EDN2 has a similar affinity for both EDNRA and EDNRB receptors, mimicking the action of EDN1 (Ling, Maguire et al. 2013). However, EDN1 is the most abundant isoform in the cardiovascular system, while EDN2 is primarily produced in the intestine and kidney (Nakas-Icindic, Zaciragic et al. 2004). EDN3 is mainly localized to neurons and glia (Giaid, Gibson et al. 1991) and exhibits much higher affinity for EDNRB than EDNRA, differing from EDN1 and EDN2 (Kurihara, Kurihara et al. 2001). Mice lacking EDN3 display a deficiency of ganglion neurons and develop aganglionic megacolon (Kurihara, Kurihara et al. 2001). EDN2 may contribute to HT and increase myocardial fibrosis (Sharma, Hingorani et al. 1999, Liefeldt, Rylski et al. 2010). Limited research exists on the precise effects of EDN3 on BP.

1.5. The Role of NO in HT

NO is a key vasodilator produced by vascular endothelial cells. It has been shown that NO inactivation plays a role in the pathogenesis of HT. Elevated ROS levels in HT scavenge NO, thereby reducing its bioavailability. The decreased availability of NO leads to endothelial dysfunction and impaired vasodilation, which in turn exacerbates HT. Studies have shown that patients with essential HT exhibit lower total NO production compared to healthy individuals (Forte, Copland et al. 1997). Oral administration of NG-nitro-L-arginine methyl ester (L-NAME), an NO synthase inhibitor, raises BP in rats. Treatment with losartan, an angiotensin receptor blocker, partially attenuates the hypertensive response induced by L-NAME (Ribeiro, Antunes et al. 1992). In addition to NO deficiency, hypertensive patients display reduced vascular sensitivity to both vasodilatory and vasoconstrictive stimuli. Infusion of NG-monomethyl-L-arginine (L-NMMA), another NO synthase inhibitor, elicits a less pronounced reduction in blood flow in HT subjects compared to normotensive controls. Similarly, acetylcholine infusion results in attenuated vasodilation in HT individuals relative to healthy subjects. Notably, L-NMMA significantly blunts vasodilation in normotensive controls, but this effect is diminished in hypertensive patients (Panza, Casino et al. 1993). This decreased vascular sensitivity may be linked to NO deficiency, as L-NMMA administration increases pulse wave velocity in healthy individuals, highlighting NO’s role in modulating arterial stiffness beyond its vasodilatory effects. The diminished response could result from arterial stiffening attributable to chronic NO deficiency (Kinlay, Creager et al. 2001). An interaction among the renin-angiotensin-aldosterone system, EDN1, and the NO system has been characterized. Administration of captopril, an ACE inhibitor, reduces EDN1 levels and enhances endothelial NO production. This beneficial effect of captopril is abolished by L-NMMA, suggesting that NO mediates the inhibitory effect of captopril on EDN1. It is postulated that captopril prevents bradykinin's breakdown, stimulating NO synthesis and suppressing EDN1 expression (Momose, Fukuo et al. 1993). Figure

12 illustrates the positive feedback loop involving AngII, NO, and the endothelin system in the development of HT.

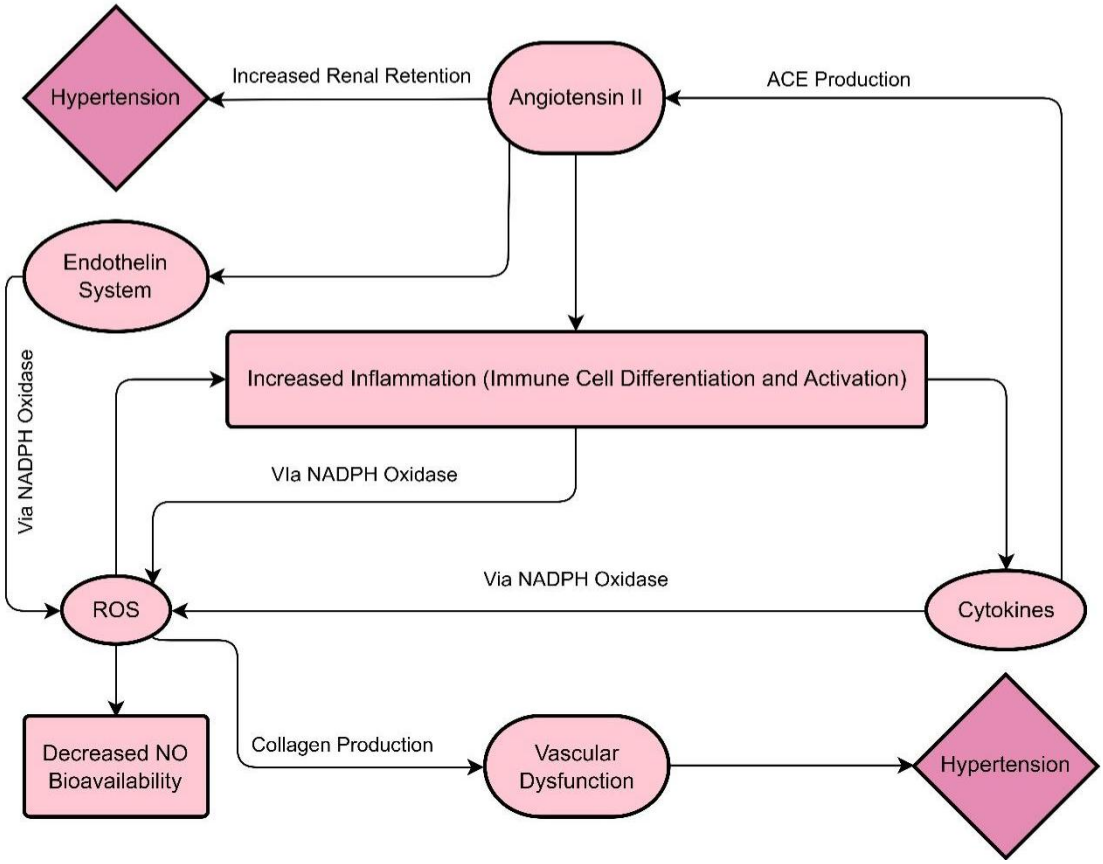

Figure 12. The positive feedback loop involving AngII, NO, and the endothelin system in the pathogenesis of HT.

2. Objectives

As described in Chapter 1, neuroinflammation and oxidative stress are pathogenic factors in glaucoma development. In addition to altered blood flow, glaucoma and HT may share pathophysiological mechanisms. Increased inflammation likely contributes to reduced retinal responses, as observed in SHR with elevated BP. While HT is known to affect the systemic biochemical environment, specific alterations in the eye caused by HT remain poorly understood.

This study aims to investigate biochemical changes in the retina induced by HT. To achieve this, we performed quantitative polymerase chain reaction (qPCR) and bulk RNA sequencing to assess gene expression in retinas of age-matched SHR and WKY. Since glial activation is a hallmark of neuroinflammation, we evaluated neuroinflammation levels by assessing microglia expression in the retinas of both SHR and WKY. In addition, retinal astrocyte activity was quantified using enzyme-linked immunosorbent assay (ELISA). We also observed decreased retinal responses in SHR compared to WKY, prompting RGC quantification in both groups.

Although EDN2 has been implicated in HT (Sharma, Hingorani et al. 1999, Liefeldt, Rylski et al. 2010), its precise functional role in HT-induced pathology remains unclear. We hypothesize that EDN2 may play a key role in HT-induced retinal degeneration. To explore this, we used immunohistochemistry and ELISA to examine EDN2 localization and abundance in the retinas of SHR and WKY.

The major objectives of this study are:

- To investigate retinal biochemical changes caused by HT using transcriptomic analyses;
- To assess neuroinflammation in SHR and WKY retinas through immunohistology methods; and
- To characterize the localization and abundance of EDN2 in SHR and WKY

retinas.

3. Methods

3.1. The qPCR and RNA Sequencing

Both 8-month and 12-month SHR and WKT were used. For retinal extraction, the eyeball was immersed in cold phosphate-buffered saline (PBS) to prevent RNA degradation. The vitreous was carefully removed from the retina. After isolation, the retina was immediately transferred to liquid nitrogen and stored at -80 °C. RNA was extracted from the retina using the Quick-RNA Miniprep Kit (Zymo Research, USA) and subsequently stored at -80 °C for subsequent qPCR or RNA sequencing analysis. RNA sequencing was performed by the Beijing Genomics Institute (BGI). Samples were shipped to the laboratory at -70 °C in an insulated container filled with dry ice. Results were analyzed using R Studio. For qPCR, cDNA was synthesized using the High-Capacity cDNA Reverse Transcription Kit (Thermo Fisher Scientific, USA). mRNA expression levels of targets related to cellular senescence, inflammation, and the endothelin system were evaluated: IL-6, TNF-α, IL-1α, IL-1β, CCL2, COX2, CD68, EDN1, EDN2, EDN3, EDNRA, and EDNRB. The housekeeping gene used was acidic ribosomal phosphoprotein P0 (36B4). Primer sequences are listed in Table 2.

Gene	Forward (5'to 3')	Reverse (5'to 3')
EDN1	CCACAGACCAAGGGAACAGA	GATGGCCTCCAACCTTCTTAG
EDN2	CTCCTGGCTTGACAAGGAATG	GCTGTCTGTCCCGCAGTGTT
EDN3	AGAAGCAGGAGACTGGAGGTC	CAGCTAAGGCTGGTGGACTT
EDNRA	ACCGTCTTCTGCTTGGTTGT	GCAACAGAGGCATGACTGAAA
EDNRB	CCTAAGGCAGTTGAGGACCTG	GCCGTTTTCAGTCTCGCA
IL-6	TCCTACCCCAACTTCCAATGCTC	TTGGATGGTCTTGGTCCTTAGCC
TNF-α	ATGGGCTCCCTCTCATCAGT	GCTTGGTGGTTTGCTACGAC
IL-1α	AAGACAAGCCTGTGTTGCTGAAGG	TCCCAGAAGAAAATGAGGTCGGTC

IL-1β	GAGGCTGACAGACCCCAAAAGAT	GCACGAGGCATTTTTGTTGTTCA
CCL2	ATCACCAGCAGCAGGTGTCCCAAA GAAGCT	AGAAGTGCTTGAGGTGGTTGTGGA AAAGAG
COX2	CTGTATCCCGCCCTGCTGGTG	ACTTGCGTTGATGGTGGCTGTCTT
CD68	TGTACCTGACCCAGGGTGGAA	GAATCCAAAGGTAAGCTGTCCGTA A
36B4	CGACCTGGAAGTCCAACTAC	ATCTGCTGCATCTGCTTG

Table 2. The sequences of the qPCR primers.

3.2. The Immunohistochemistry

To stain microglia and RGCs, the retina was carefully peeled from the eye to preserve its structural integrity. It was then fixed in 4% paraformaldehyde for 45 minutes. After fixation, the retina was transferred to Mojito Buffer (containing 1% donkey serum, 10% bovine serum albumin (BSA), 2.5% Triton, and 0.5% Tween in PBS) for 2 hours to block nonspecific binding. Following blocking, the retina was washed for 10 minutes in Washing Buffer (containing 0.1% Tween and 2.5% Triton in citrate buffer, pH=6). RGCs were stained with an anti-Brn3a antibody, and microglia were stained with an anti-Iba1 antibody. The retina was incubated with primary antibodies for 48 hours in Staining Solution (containing 1% donkey serum, 1% goat serum, 3% BSA, 0.1% Tween, and 2.5% Triton in Citrate Buffer, pH=6). The primary antibodies used were Mouse anti-Brn3a (Sigma Millipore, Cat. No. MAB1585) and Rabbit anti-Iba1 (Wako, Cat. No. 019-19741). After incubation, the retina was washed five times for 5 minutes each and then incubated with secondary antibodies: Goat anti-Rabbit IgG (H+L) Cross-Adsorbed Secondary Antibody, Alexa Fluor™ 488 (Cat. No. A-11008), and Goat anti-Mouse IgG (H+L) Cross-Adsorbed Secondary Antibody, Alexa Fluor™ 555 (Cat. No. A-21422). The retinas were counterstained with DAPI and flat-mounted under a coverslip. Slides were imaged using an upright confocal microscope at 20x magnification. For each retina, 24 images were captured. The number and soma size

of microglia were measured manually using ImageJ, and the number of RGCs was counted manually. For staining GFAP or EDN2, cryosectioning was performed instead of flat mounting to investigate their localization. The eyeball was cryosectioned, and sections within 1 mm of the optic nerve head were used for staining. Five images were captured per slide.

3.3. The ELISA

GFAP has been proposed as a key indicator of retinal astrocyte activation (Pekny and Nilsson 2005). Therefore, we measured retinal GFAP levels to evaluate astrocyte activation. The expression levels of EDN2 and GFAP in the retina were quantified using ELISA (Rat Glial Fibrillary Acidic Protein, GFAP ELISA Kit, Bioassay Technology Laboratory, Cat. No. E0538Ra; Rat Endothelin 2, ET-2 ELISA Kit, Bioassay Technology Laboratory, Cat. No. E1006Ra). Their weight percentages were calculated after determining the final concentration of EDN2 or GFAP in the samples.

4. Results

4.1. The Transcriptomic Results

4.1.1. The 8-month Transcriptomic Results

Figure 13A illustrates the qPCR results for the 8-month-old SHR and WKY. At 8 months, IL-6, EDN2, and CD68 were significantly elevated in the retina of SHR. The expression levels of EDN3 and COX2 were marginally increased in SHR compared to the WKY control group. Surprisingly, TNF-α expression was significantly suppressed in SHR. The RNA sequencing results are presented in Figure 13B-F. Differentially expressed targets in SHR, with an adjusted P value < 0.05 and a log2 fold change > 1.1 compared to WKY, are displayed using a volcano plot (Figure 13B). We observed significant overexpression of CD68 and C3 in SHR. When analyzed individually, EDN2 was also significantly elevated in SHR, as shown in Figure 13C. A detailed analysis of specific target genes is provided in Figure 13D, focusing on those involved in the pathophysiology of HT and glaucoma. These targets include cytokines related to inflammation, components of complement activation, TLRs and their downstream transducer Myeloid differentiation primary response 88 (MYD88), the endothelin system, and markers of microglial activation or phagocytosis, as well as NO synthases. Figure 13D displays a heatmap of these targeted genes. Several complement components, such as C2, C1R, C1S, C3, and C1QA, were upregulated in SHR. In addition, several TLRs, including TLR2, TLR7, and TLR8, along with MYD88, were upregulated in SHR. The inflammation marker TGFB1, associated with glaucoma, was also elevated. Two markers of microglial activation or phagocytosis, CD68 and CYBB, were upregulated in SHR. Nitric Oxide Synthase 3 (NOS3), which mediates vasodilation, was downregulated in SHR. The Kyoto Encyclopedia of Genes and Genomes (KEGG) pathways significantly up- or down-regulated (P < 0.1) are listed in Figure 13E-F. Several neuroinflammation-related pathways, including leukocyte transendothelial migration, chemokine signaling, complement and coagulation

cascades, and cytokine-cytokine receptor interaction, were upregulated in SHR. On the contrary, oxidative phosphorylation was downregulated in SHR.

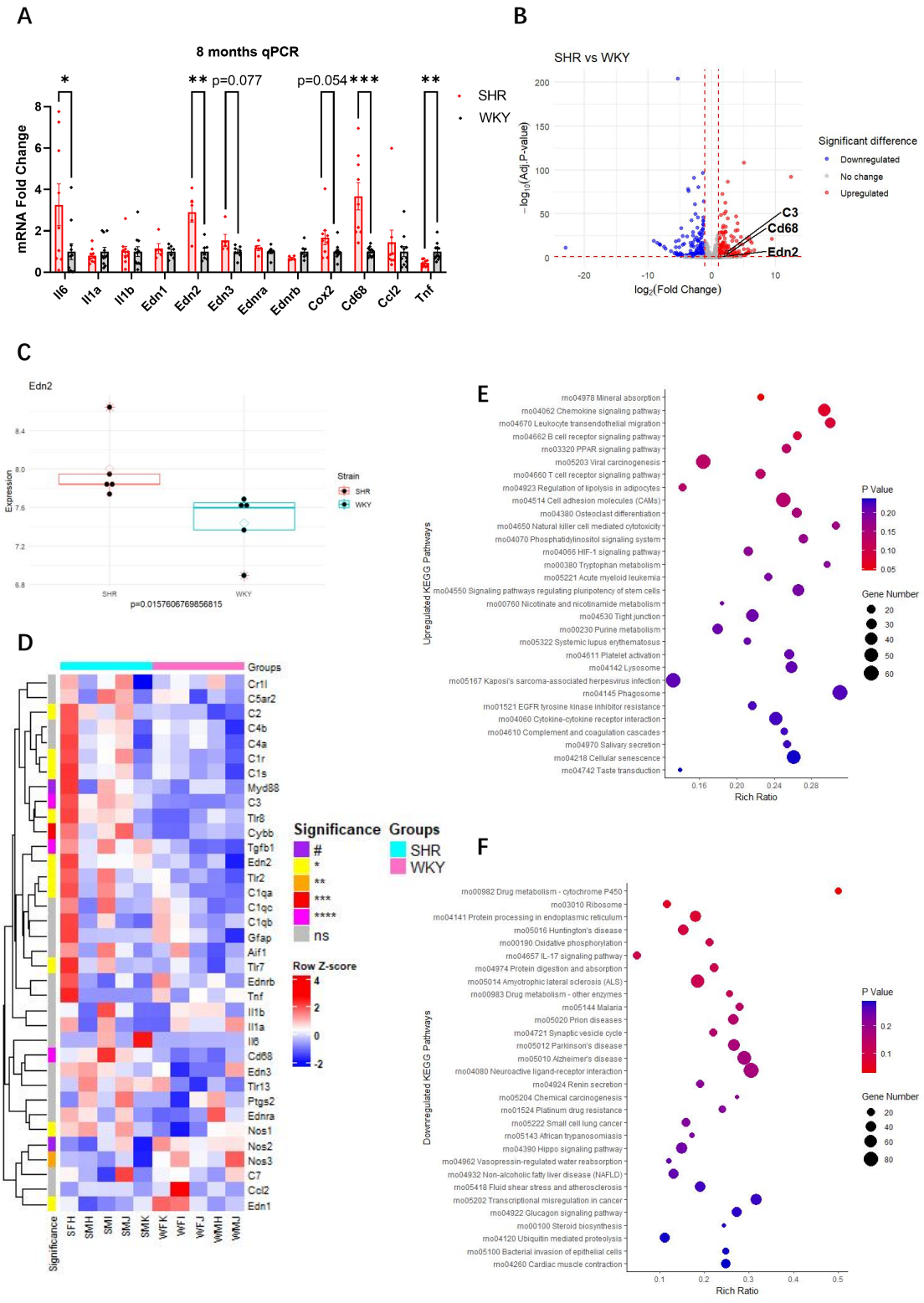

Figure 13. A. qPCR results of retina samples from 8-month-old SHR and WKY. Data are presented as Mean ± SEM (* P < 0.05, ** P < 0.01, *** P < 0.001, Student's t-test); **B.** Volcano plot of differentially expressed targets; **C.** Expression levels of EDN2 in SHR and WKY; **D.** Heatmap of selected target genes; **E-F**. Upregulated and downregulated KEGG pathways in 8-month-old SHR compared to WKY.

4.1.2. The 12-month Transcriptomic Results

As shown in Figure 14A, at 12 months, IL-1β, EDN1, EDN3, EDNRA, CD68, and CCL2 were significantly elevated, while IL-1α was marginally increased in SHR. The RNA sequencing results are presented in Figure 14B-F. Consistent with the 8-month results, CD68 and C3 were significantly upregulated in SHR (Figure 14B). EDN2 did not reach the threshold of differential expression; however, individual analysis confirmed a significant elevation in SHR ($P < 0.01$), as shown in Figure 14C. Furthermore, several genes including TGFB1, C1QA, C1R, C1S, C2, C3, CD68, TLR2, TLR7, TLR8, MyD88, and CYBB were upregulated in 12-month-old SHR. Additional upregulation was noted for EDN2, EDN3, TLR13, CR1L, C1QB, C1QC, C4A, C4B, C5AR2, C7, IL-1α, GFAP, AIF1, and CCL2. In contrast, NOS2 expression was downregulated in SHR. Figure 14E-F present the KEGG pathways exhibiting significant upregulation and downregulation, respectively. Pathways associated with neuroinflammatory processes, including cytokine-cytokine receptor interaction, leukocyte transendothelial migration, complement and coagulation cascades, chemokine signaling, and toll-like receptor signaling, were upregulated in SHR. Metabolic pathways and oxidative phosphorylation were downregulated in 12-month SHR.

Collectively, these RNA sequencing data indicate that molecular targets implicated in the pathogenesis of glaucoma, particularly those related to neuroinflammation, are significantly upregulated in SHR relative to age-matched WKY controls at both 8 and 12 months. Notably, these differences were more pronounced at 12 months, as evidenced by the increased number of significantly altered markers detected at this age.

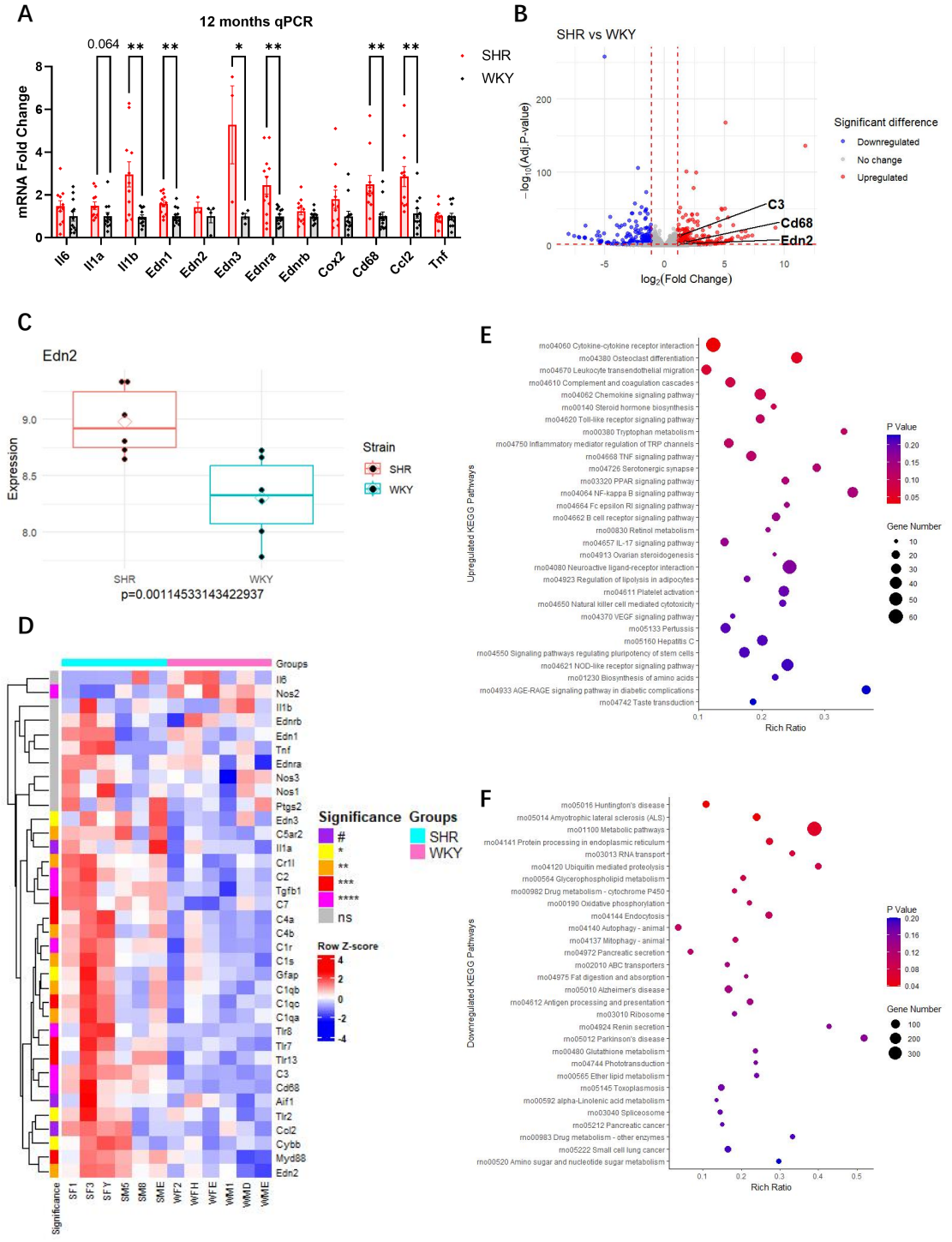

Figure 14. A. qPCR results of retinal samples from 12-month-old SHR and WKY. Data are presented as Mean ± SEM, * $P < 0.05$, ** $P < 0.01$ (Student's t-test); **B.** Volcano plot of differentially expressed targets; **C.** Expression levels of EDN2 in SHR and WKY; **D.** Heatmap of selected target genes; **E-F.** Upregulated and downregulated KEGG pathways in 12-month-old SHR compared to WKY.

4.2. The Immunohistochemistry Staining and ELISA

4.2.1. The Staining for RGCs and Microglia

The mounting staining was performed on retinas from 8- and 12-month-old SHR and WKY. The experimental workflow is illustrated in Figure 15A. Representative images from the 8- and 12-month retinas of SHR and WKY are shown in Figure 15B. The number of RGCs was significantly decreased by 12% in SHR compared to WKY at 8 months. At 12 months, the RGC count in SHR was reduced by 14% relative to WKY. Regarding microglial count, no significant difference was observed between SHR and WKY at 8 months. At 12 months, microglial numbers were significantly higher in SHR. Microglial soma size was increased in SHR as early as 8 months and remained elevated through 12 months. Specifically, at 8 months, microglial soma size in SHR was 23% larger than in WKY, and at 12 months, it was 16% larger, with both differences being significant.

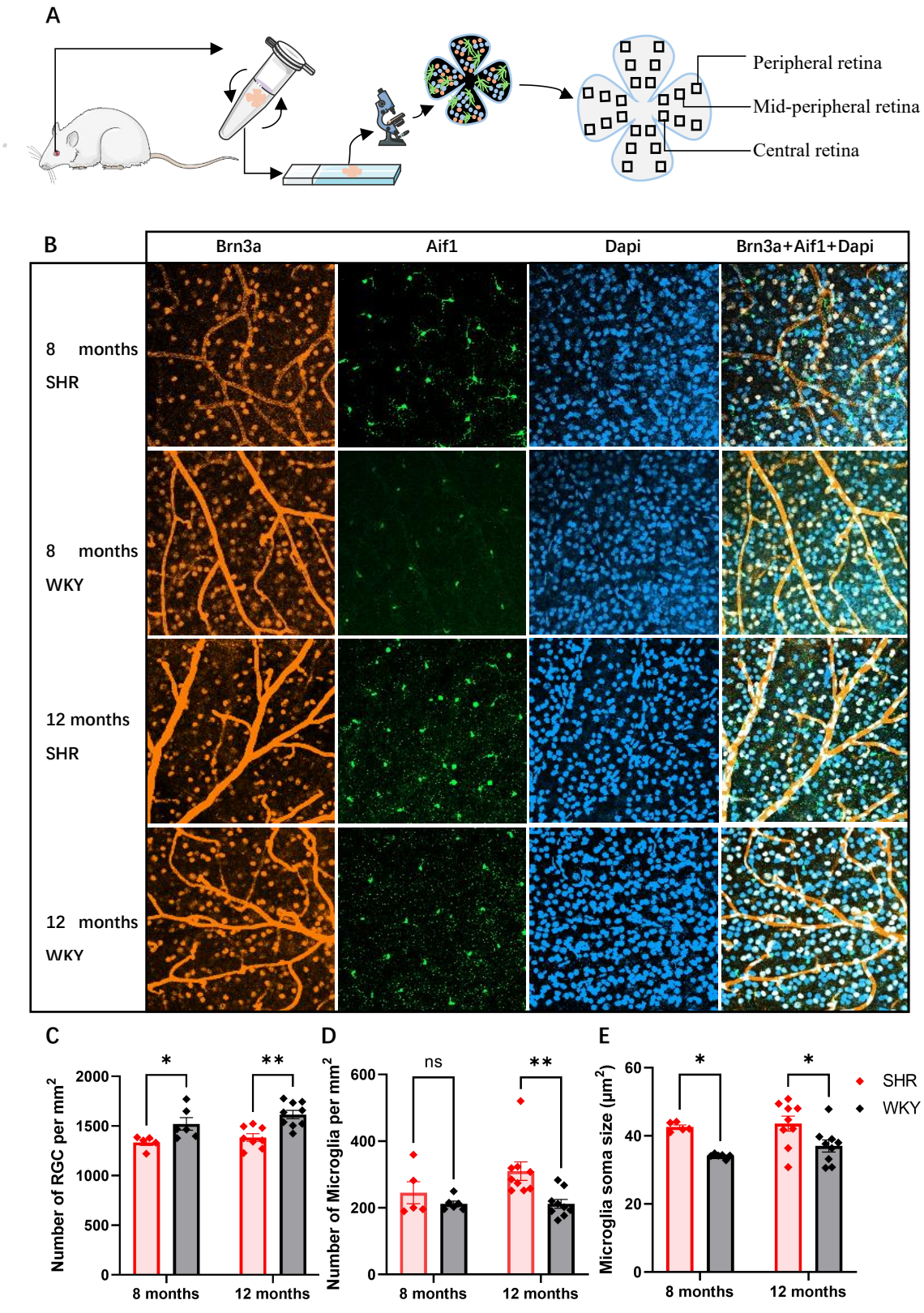

Figure 15. A. Experimental workflow of the mounting and staining process; **B.** Representative images from the 8- and 12-month-old SHR and WKY retinas; **C.** Retinal ganglion cell counts; **D.** Microglial cell counts; **E.** Microglial soma size measurements.

4.2.2. The Staining and ELISA Results of EDN2 and GFAP

Figure 16 illustrates the levels and expression of EDN2 and GFAP in 8-month-old SHR and WKY, with EDN2 and GFAP signals showing co-localization. Figure 16A presents images of cryosectioned retinal slides from both groups. For EDN2 staining, SHR exhibited higher fluorescence intensity compared to WKY. Our results suggested that astrocytes are a significant source of EDN2 secretion in the rat retina. Both the fluorescence intensity and weight percentage of EDN2 were elevated in SHR, while the GFAP weight percentage was higher by 30% in SHR, although this difference has not yet reached statistical significance. In summary, retinal expression of EDN2 was greater in SHR at both the mRNA and protein levels, and the overexpressed EDN2 is likely predominantly produced by astrocytes.

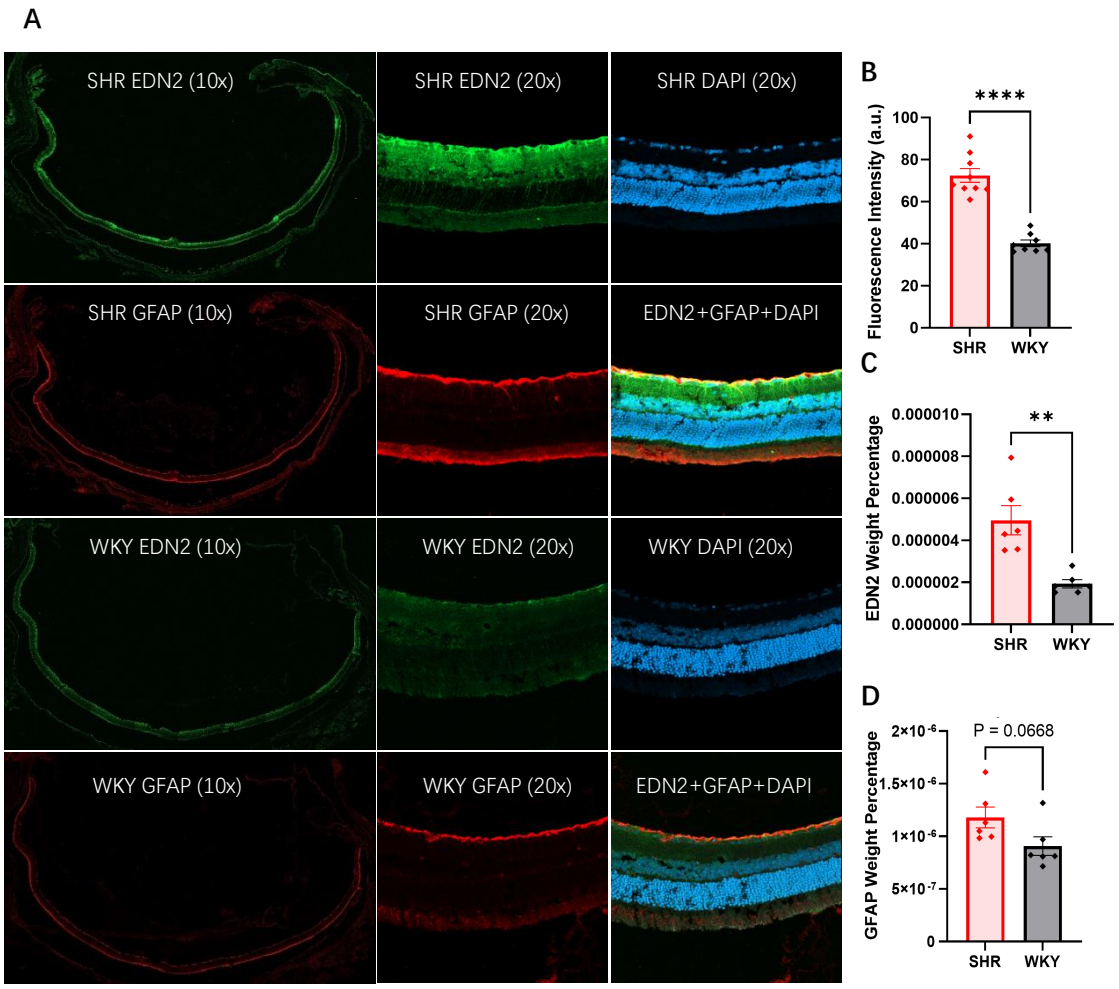

Figure 16. A. Representative images captured from cryosectioned retinal slides of 8-month-old SHR and WKY; **B.** Quantification of EDN2 fluorescence intensities; **C.** EDN2 weight percentage determined by ELISA; **D.** GFAP weight percentage determined by ELISA.

5. Discussion

In this study, we evaluated retinal changes in SHR relative to WKY from a biochemical perspective. Transcriptomic analyses, including qPCR and RNA sequencing, revealed significant alterations in gene expression at both 8 and 12 months.

At 8 months, the expression levels of IL-6, EDN2, CD68, TGFB1, complement components, TLRs, and CYBB were significantly upregulated in SHR, whereas NOS3 and TNF-α were downregulated. By 12 months, a broader range of genes, including IL-1β, IL-1α, CD68, endothelin elements, complement components, TLRs, CCL2, GFAP, and AIF1, were significantly elevated in SHR, while NOS2 expression was decreased. Pathway analyses via KEGG demonstrated that, at 8 months, several neuroinflammation-related pathways, such as leukocyte transendothelial migration, chemokine signaling, complement and coagulation cascades, and cytokine-cytokine receptor interaction, were upregulated in SHR. By 12 months, additional neuroinflammation pathways, including Toll-like receptor signaling and NF- κ B signaling, were also significantly elevated.

In addition, SHR exhibited a reduction in RGC counts at both 8 and 12 months compared to age-matched WKY controls. Microglial soma enlargement was observed in the retinas of SHR at both time points, with increased microglial counts detected at 12 months. These findings strongly suggest that RGCs degeneration begins as early as 8 months, accompanied by progressive microglial activation. Consistent with these changes, ELISA analyses showed overexpression of retinal EDN2 and GFAP in 8-month-old SHR. Immunohistochemical staining further revealed co-localization of EDN2 and GFAP signals in the retinas of both SHR and WKY, suggesting that astrocytes are a key source of EDN2 in the retina.

The results indicate increased retinal neuroinflammation in SHR compared to age-matched WKY at both time points. These findings suggest a mechanistic link

between HT and glaucoma at both transcriptomic and proteomic levels. Many inflammatory markers elevated in SHR are believed to play crucial roles in glaucoma progression. Histological studies have reported elevated levels of IL-6 and IL-1β in glaucomatous retinas (Gramlich, Beck et al. 2013). Retinal glia cells become activated during neuroinflammation, secreting various cytokines and chemokines, such as CCL2 and IL-6, which can further stimulate glia activation (Liddelow, Guttenplan et al. 2017). CD68, proposed to function as a scavenger receptor, promotes phagocytosis, clears cell debris, and activates macrophages (Rojas, Gallego et al. 2014). In a mouse OHT model, CD68 expression increased specifically in the retinal nerve fiber layer extending to the ganglion cell layer, potentially linking CD68 upregulation to RGC death (Rojas, Gallego et al. 2014). A human study analyzing optic nerve samples from glaucoma patients identified TGFB1 as one of the top upstream regulators elevated in the glaucomatous optic nerve (Becerra, Sabbagh et al. 2019). In addition, CYBB has been implicated in exacerbating oxidative stress, contributing to glaucoma pathogenesis (Fan Gaskin, Shah et al. 2021). Therefore, elevated levels of CD68, TGFB, and CYBB may contribute to the diminished RGC function observed in SHR. The role of the complement system in glaucoma is complex. For instance, C3 appears to mitigate early glaucoma progression in DBA/2J mice but may exacerbate degeneration during later stages (Bosco, Anderson et al. 2018). Among complement components, C3 is upregulated early; however, whether increased C3 expression is protective or detrimental in 8-month-old SHR remains uncertain. Regarding EDN2, evidence suggests it may compromise blood-retina barrier (BRB) integrity. Intravitreal injections of EDN2 in mice lead to enhanced vascular leakage and macrophage infiltration (Alrashdi, Deliyanti et al. 2018). Elevated EDN2 in SHR could thus reflect altered BRB function, correlating with increased leukocyte transendothelial migration and CD68 expression.

NOS3, primarily localized in vascular endothelial cells, supports neuroprotection by facilitating vasodilation and enhancing blood flow (Neufeld, Hernandez et al. 1997).

Its reduction in SHR aligns with impaired blood flow in the inner retina. Conversely, the reason for decreased TNF-α expression in SHR remains unclear. While TNF-α is known to induce RGCs apoptosis via caspase activation (Oliveira, Vasconcellos et al. 2014), it has also been proposed to exert neuroprotective effects by promoting survival signals (Mac Nair, Fernandes et al. 2014). Thus, its reduced expression might represent a compensatory protective response, although its precise role in SHR retina warrants further investigation. Toll-like receptors serve as upstream activators of immune cells and cytokine production (Luo, Yang et al. 2010). MYD88, a downstream regulator of TLRs, can activate NF-κB signaling, thereby amplifying inflammatory responses (Shestopalov, Spurlock et al. 2021). Studies have shown that C1QA mediates dendrite loss of RGC in DBA/2J mice and that C1 components contribute to dendritic and synaptic atrophy in OHT (Williams, Tribble et al. 2016). Moreover, increased C1QB and C3 accumulation occur in the RNFL and GCL in OHT eyes of both humans and rats. Furthermore, increased C1QB and C3 accumulate in the RNFL and GCL (Kuehn, Kim et al. 2006). Upstream complement proteins such as C1q and C4B may activate downstream components, including C5b and C6-C9, which form the membrane attack complex, thereby triggering inflammatory events that contribute to RGC degeneration in glaucoma. Indeed, higher expression levels of C7-C9 have been observed in the GCL and IPL (Tezel, Yang et al. 2010). Given that the complement system is upregulated in both glaucomatous and SHR retinas, it is plausible that RGC degeneration in glaucoma and SHR shares a common pathophysiological mechanism involving complement-mediated neuroinflammation. Lastly, activation of the endothelin system has been proposed as a detrimental factor for RGCs' survival (Chauhan 2008). Administration of EDN1 to the optic nerve causes decreased ocular blood flow, axonal loss, and reduced visual evoked potential (VEP) amplitude (Krupin, Orgül et al. 1996, Orgül, Cioffi et al. 1996, Oku, Sugiyama et al. 1999, Nagano, Wei et al. 2007, Wang, LeVatte et al. 2009). Elevated EDN2 is observed in the retinas of DBA/2J mice and is thought to contribute to glaucomatous degeneration in these mice (Howell, Macalinao et al. 2011, Howell, Soto et al. 2012).

Therefore, we suggest that the retinal degeneration observed in SHR might be caused by the activated endothelin system. A detailed discussion of the endothelin system and its implications will be discussed in the following chapter.

In contrast to the upregulated pathways observed in SHR, we also identified downregulation of oxidative phosphorylation at both 8 and 12 months. In addition, metabolic pathways were downregulated in 12-month-old SHR. ATP production is primarily carried out by the mitochondrial oxidative phosphorylation system (Smeitink, van den Heuvel et al. 2001). In the mitochondria, oxidative phosphorylation complexes I–IV, located at the inner membrane, pump protons into the intermembrane space to maintain the proton gradient necessary for ATP synthesis. Mitochondrial dysfunction leads to proton leakage, resulting in increased ROS production and decreased ATP generation. While mitochondria are a major source of ROS, they are also susceptible to oxidative damage. ROS-mediated apoptosis of RGCs and mitochondrial damage exacerbate glaucomatous neurodegeneration (Chrysostomou, Rezania et al. 2013). In 10-month-old DBA/2J mice, abnormal mitochondrial fission and reduced cristae volume have been observed in optic nerve head axons. Furthermore, cyclooxygenase immunoreactivity, a marker of mitochondrial activity, is decreased in the optic nerve head of these glaucomatous mice. Excessive mitochondrial fission impairs normal mitochondrial function and induces respiratory defects at the cellular level (Ju, Kim et al. 2008). Decreased mitochondrial respiratory activity and altered mitochondrial DNA have also been demonstrated in blood samples from POAG patients, indicating that mitochondrial dysfunction plays an important role in glaucoma development (Abu-Amero, Morales et al. 2006). Our findings of reduced oxidative phosphorylation in SHR are consistent with these reports and likely contribute to the functional loss of RGCs.

Chapter 4. Suppression of the Endothelin System Restores Retinal Functions in Spontaneously Hypertensive Rats

1. Introduction

1.1. The Association Between the Endothelin System and the Risk of Glaucoma

The potential relationship between the endothelin system and glaucoma risk has attracted considerable interest. The endothelin system comprises three isoforms, namely EDN1, EDN2, and EDN3. There are also two main receptor types: EDNRA and EDNRB. Each isoform exhibits distinct distribution and function in the body. EDN1 plays a critical role in cardiovascular regulation, EDN2 is primarily produced by the intestines and kidneys, and EDN3 is mainly found in the nervous system (Giaid, Gibson et al. 1991, Nakas-Icindic, Zaciragic et al. 2004).

Research has proposed a positive correlation between EDN1 and glaucoma risk, with particular attention to plasma and aqueous EDN1 levels in patients (Li, Zhang et al. 2016). Higher plasma EDN1 concentrations have consistently been observed in patients with NTG compared to control subjects (Cellini, Possati et al. 1997, Lee, Park et al. 2012). This trend suggests that elevated plasma EDN1 may be linked to an increased risk of glaucoma in these patients (Li, Zhang et al. 2016). However, the relationship between EDN1 and POAG remains elusive. Some studies report no significant difference in plasma EDN1 levels between POAG patients and control subjects (Tezel, Kass et al. 1997, Cellini and Caramazza 1999, Iwabe, Lamas et al. 2010, Choritz, Machert et al. 2012). However, other studies indicate that POAG patients, like those with NTG, may exhibit increased plasma EDN1 concentrations (Cellini, Strobbe et al. 2012, Chen, Chang et al. 2013). This inconsistency may stem from the complex and variable pathophysiology of POAG. For example, it has been suggested that elevated plasma EDN1 may be present primarily in POAG patients who have well-controlled IOP but continue to experience visual field deterioration (Cellini, Strobbe et al. 2012). Such findings imply that increased plasma EDN1 could

contribute to the underlying pathogenesis of both NTG and POAG (Tezel, Kass et al. 1997, Cellini and Caramazza 1999, Iwabe, Lamas et al. 2010, Cellini, Strobbe et al. 2012, Choritz, Machert et al. 2012, Chen, Chang et al. 2013, Li, Zhang et al. 2016).

Notably, several studies have consistently demonstrated that POAG patients have significantly higher aqueous EDN1 levels compared to healthy controls (Tezel, Kass et al. 1997, Iwabe, Lamas et al. 2010, Choritz, Machert et al. 2012). In contrast, evidence regarding EDN1 levels in the AH of NTG patients is mixed. While some studies report significantly increased levels, others do not find a significant difference when compared to controls (Iwabe, Lamas et al. 2010, Sin, Song et al. 2013).

1.2. The Influence of the Endothelin System on IOP

The distinct patterns of plasma and aqueous EDN1 levels observed in NTG and POAG patients suggest that EDN1 plays multiple roles in the pathogenesis of glaucoma, not only in regulating IOP, but also in mediating pressure-independent disease progression. EDN1 is known to influence IOP by affecting the dynamics of AH outflow (Korbmacher, Helbig et al. 1989, Matsumoto, Yorio et al. 1996, Taniguchi, Haque et al. 1996). Both the ciliary muscle and TM possess smooth muscle-like properties and are pivotal in IOP control. The TM and ciliary muscle function antagonistically. For example, TM contraction reduces outflow facility, while ciliary muscle contraction causes the TM to distend, thereby increasing outflow facility (Wiederholt, Thieme et al. 2000). Experimental evidence shows that EDN1 induces contraction in both the ciliary muscle and TM (Erickson-Lamy, Korbmacher et al. 1991, Lepple-Wienhues, Stahl et al. 1991, Matsumoto, Yorio et al. 1996, Taniguchi, Haque et al. 1996, Haque, Pang et al. 1998), likely through elevation of intracellular calcium (Ca^{2+}) via the EDNRA receptor subtype (Korbmacher, Helbig et al. 1989). For example, in cultured human ciliary muscle cells and TM cells, EDN1 stimulates intracellular Ca^{2+} mobilization and causes smooth muscle-like cell contraction (Korbmacher, Helbig et al. 1989, Matsumoto, Yorio et al. 1996, Haque,

Pang et al. 1998). Animal studies have also demonstrated that EDN1, when injected into the anterior chamber, increases outflow facility by inducing ciliary muscle contraction in monkeys (Erickson-Lamy, Korbmacher et al. 1991). In bovine ciliary muscle, administration of a low dose of EDN1 (0.1 nM) induces relaxation, whereas a higher dose (i.e., 1 nM) causes constriction. The relaxation is likely mediated by EDNRB, while the constriction is mediated by EDNRA (Kamikawatoko, Tokoro et al. 1995). Numerous animal studies have reported that EDNRA primarily contributes to IOP elevation, whereas EDNRB appears to regulate IOP reduction (Haque, Taniguchi et al. 1995, Hollo, Kothy et al. 2002, Wang, Podos et al. 2011). However, the precise mechanisms by which EDNRA and EDNRB modulate IOP are complex and influenced by factors such as drug concentration, animal species, and the sensitivity of the ciliary muscle and TM, all of which affect the final IOP values (Haque, Taniguchi et al. 1995, Hollo, Kothy et al. 2002, Wang, Podos et al. 2011). Studies with EDNRA-selective antagonists, e.g., BQ485 and SPP301, have been shown to prevent or reduce acute IOP elevation in animal models of glaucoma (Hollo, Kothy et al. 2002, Wang, Podos et al. 2011). On the contrary, administration of the selective EDNRB agonist Sarafotoxin S8C has been demonstrated to lower IOP in rabbits (Haque, Taniguchi et al. 1995).

These findings suggest a complex relationship between the endothelin system and glaucoma. Given the frequently elevated aqueous EDN1 levels observed in POAG, EDN1 likely contributes to both IOP-dependent and IOP-independent mechanisms of disease progression. Evidence indicates that EDN1-induced muscle contraction may affect AH dynamics, while its IOP-independent actions could involve retinal blood flow regulation and neuroprotection.

1.3. The Influence of EDN1 on the Optic Nerve

It has been hypothesized that optic nerve ischemia is another EDN1-involved pathogenic mechanism in glaucoma. EDN1 damages ocular tissues by constricting

blood vessels and causing hemodynamic disturbances. Administration of EDN1 to the retrobulbar optic nerve in rats decreases optic nerve blood flow (Wang, LeVatte et al. 2009). Similarly, EDN1 applied to the perineural region of the anterior optic nerve reduces optic nerve blood flow in monkeys and rabbits (Krupin, Orgül et al. 1996, Orgül, Cioffi et al. 1996). The microvasculature supplying the anterior optic nerve constricts in a dose-dependent manner in response to perineural EDN1 (Iwabe, Lamas et al. 2010). Intravitreal injection of EDN1 triggers decreased optic nerve blood flow, increased cup/disc ratio, axonal loss, and glial proliferation in rabbits (Oku, Sugiyama et al. 1999). It also leads to reduced visual evoked potential (VEP) amplitude and prolonged VEP N1 latency in rabbits (Oku, Sugiyama et al. 1999, Nagano, Wei et al. 2007). These reductions in VEP and optic nerve blood flow caused by EDN1 can be blocked by iganidipine, a Ca^{2+} channel blocker (Oku, Sugiyama et al. 2000, Waki, Sugiyama et al. 2001). Therefore, Ca^{2+}-mediated vasoconstriction contributes to EDN1-induced optic nerve disorders (Oku, Sugiyama et al. 2000). Given the relationship between EDN1 and decreased optic nerve blood flow, it is postulated that altered hemodynamics may explain the link between increased plasma EDN1 and NTG (Sugiyama, Moriya et al. 1995).

1.4. The Role of EDN2 in Glaucomatous Degeneration

For EDN2, only limited studies have investigated its impact on glaucoma (Sharma, Hingorani et al. 1999, Liefeldt, Rylski et al. 2010). Existing research indicates that in DBA/2J mice, the EDN2 gene is upregulated in the retina and optic nerve head during early glaucoma. EDN2 expression is localized to microglia/macrophage-like cells in the nerve fiber layer. Apart from the effects of EDN1, intravitreal administration of EDN2 induces RGC damage and vasoconstriction (Howell, Macalinao et al. 2011). A reduction in the lumen-to-total blood vessel area has been observed in the retina of DBA/2J mice, likely due to vasoconstriction caused by elevated EDN2 levels (Howell, Macalinao et al. 2011). Additional studies demonstrate that x-ray treatment can prevent proinflammatory

monocytes infiltration into the optic nerve, thereby mitigating glaucomatous damage in DBA/2J mice. However, intravitreal EDN2 injections counteract the axon preservation achieved by x-ray treatment in these mice (Howell, Soto et al. 2012). As a result, EDN2 was proposed to be a detrimental factor during glaucoma progression (Howell, Soto et al. 2012). To explore how EDN2 may influence the retinal biochemical environment, we analyzed data from the human transcriptomic database GSE115828, focusing on subjects with mild AMD (Mgs level 1-2). We found that EDN2 positively correlates with complement components, including C1R, C1S, C1QA, C1QB, C1QC, C2, C3, C4A, and C4B, with $r > 0.3$ and $P < 0.05$ (Figure 17A, C-I). C3 and C5AR2 also show significant, albeit weaker, correlations with EDN2 ($r > 0.2$, $P < 0.05$) (Figure 17B and 17I). Notably, positive correlations were also observed between EDN2 and markers such as CD68, GFAP, TGFB1, and IL-6 (Figure 17K-N). Moreover, EDN2 exhibits a weak but statistically significant correlation with age ($r > 0.1$, $P < 0.05$) (Figure 17O). A heatmap illustrating data from 322 subjects is presented in Figure 17P. Based on these findings, we hypothesize that EDN2 may be associated with the activation of the complement system as well as with the expression of inflammatory and glial markers CD68, GFAP, TGFB1, and IL-6.

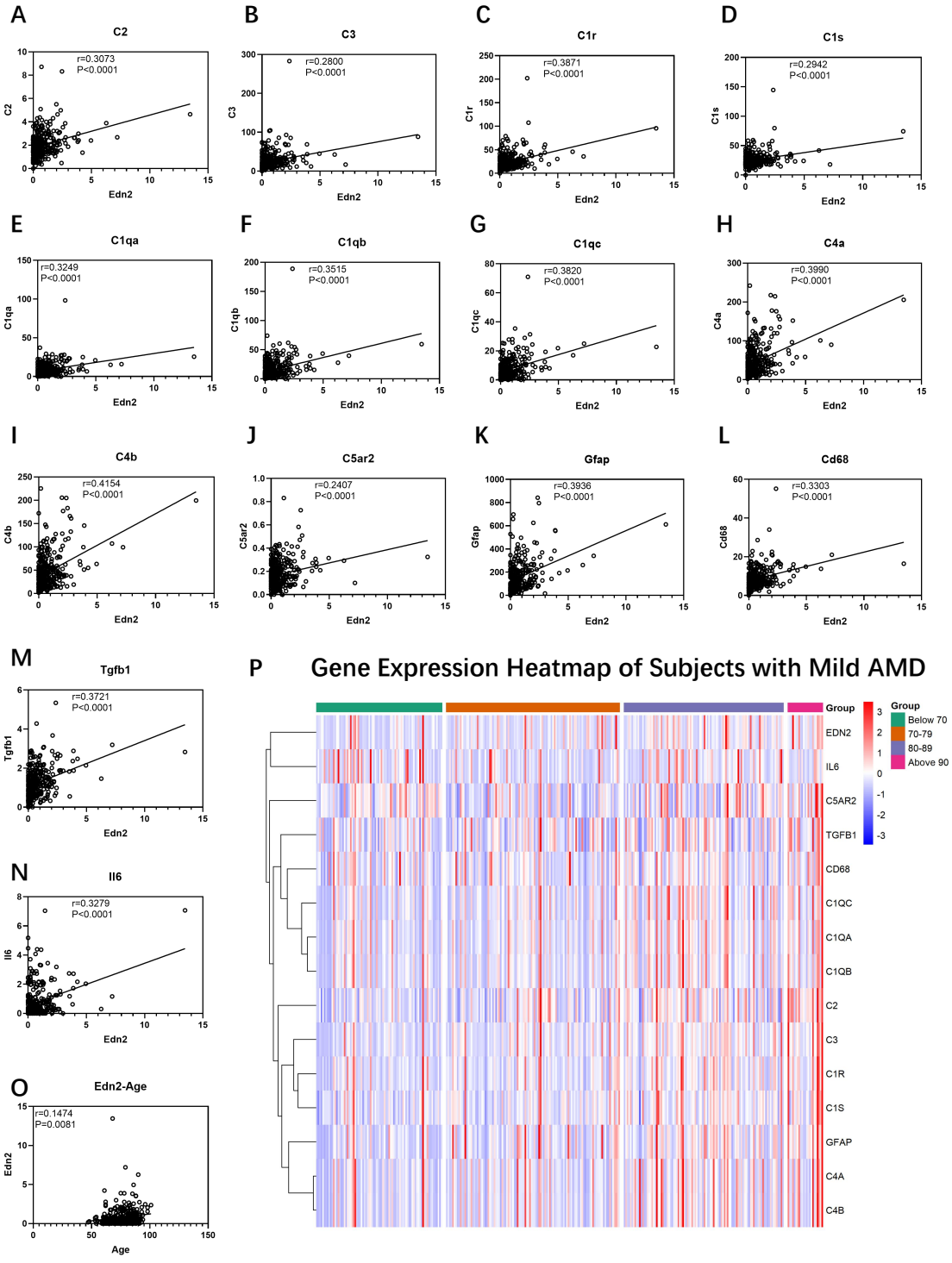

Figure 17. A-J. The correlation between EDN2 and complement elements in the human retina with mild AMD; **K-N.** The correlation between EDN2 and GFAP, CD68, TGFB1, and IL-6 in the human retina; **O.** The correlation between EDN2 and age in the human retina; **P.** A heatmap of the aforementioned targets, with subjects categorized by different age groups.

2. Objectives

In the transcriptomic studies, we revealed an activated endothelin system in SHR. At 8 months, SHR exhibited increased EDN2 expression. By 12 months, the levels of EDN1, EDN2, EDN3, and EDNRA were elevated in SHR. Furthermore, we observed that EDN2 expression positively correlates with complement elements, including C1QA, C1QB, C1QC, C1S, C1R, C2, C3, C4A, and C4B in human retina with mild AMD. Based on these findings, we postulate that the endothelin system may contribute to the neurodegenerative process in the SHR retina, leading to decreased retinal functional responses. The primary aim of this work is to determine whether the endothelin system contributes to retinal degeneration in SHR and whether it serves as a key mechanistic link between HT and glaucoma. In addition, although EDN1 has been suggested to influence optic nerve blood flow, it remains unclear whether EDNRA or EDNRB mediates this response. While EDN2 is proposed as a detrimental factor in glaucoma pathogenesis, the precise mechanisms by which EDN2 causes neurodegeneration remain largely unknown.

Our study has two main objectives:

- To investigate how EDN2 affects IOP, retinal function responses, retinal structures, and inflammation in SHR and WKY by knocking out EDN2; and
- To examine the effects of EDNRA and EDNRB on IOP and retinal responses through intravitreal injections of their antagonists in SHR and WKY.

3. Methods

3.1. Intravitreal Injection of AAV to Knock Out EDN2

To investigate the role of EDN2 in the eye, we used AAV to knock out EDN2 in the eyes of SHR and WKY. Since elevated EDN2 expression was detected in 8-month-old SHR, we selected 8-month-old SHR and WKY for the experiments described in this chapter. The AAV used was sgRNA AAV2 (WZ Biosciences Inc.). Unilateral intravitreal injections of either EDN2 KO AAV or control AAV were performed after measuring baseline IOP, retinal function, SBP, and DBP. Both types of AAV were diluted in PBS to a concentration of 5 x 10^{10} vg/ml. During treatment, 1 µl of the diluted AAV was injected. Animals were fully anesthetized with a ketamine-xylazine mixture, and pupils were dilated using 0.5% tropicamide (Mydrin-P, Santen Pharmaceutical, Japan). For the experimental treatment eye, a hole was punctured in the sclera 0.5 mm posterior to the limbus using a 30 G needle. The diluted AAV was then injected into the vitreous chamber through the puncture site with a glass micropipette, taking care to avoid contact with the crystalline lens. After injection, topical antibiotics such as levofloxacin were applied to the puncture site to prevent infection. Post-treatment assessments of IOP, SBP, DBP, and retinal function were conducted 26 to 30 Days after injection. Retinas were collected 31 to 35 Days post-treatment for transcriptomic analysis, ELISA, and immunohistochemistry staining. We employed qPCR and RNA sequencing to examine how EDN2 influences retinal function. ELISA and immunohistochemistry staining of EDN2 were performed to evaluate the efficacy of the EDN2 KO AAV at the protein level. An overview of the experimental protocol is illustrated in Figure 19A.

3.2. Intravitreal Injection of Endothelin Antagonists

Local blockade of EDNRA and EDNRB in the retinas of SHR and WKY was achieved through intravitreal injections of Bq123 and Bq788, respectively. Bq123 is a selective antagonist of EDNRA, while Bq788 selectively antagonizes EDNRB (Fukuroda, Ozaki et al. 1994). The molecular formulas for Bq123 and Bq788 are

$C_{31}H_{41}N_6O_7Na$ and $C_{34}H_{50}N_5NaO_7$, respectively. Both compounds were obtained from Sigma-Aldrich (USA) and stored as sodium salt powders at -20°C. The structures of Bq123 and Bq788 are shown in Figure 18. Prior to administration, baseline IOP and retinal functional responses were measured in all animals. For drug treatment, Bq123 or Bq788 was unilaterally injected into the experimental eye on Day 0 and Day 10. Each injection consisted of 1 µl of Bq123 or Bq788 diluted to 10 µM in PBS. Control groups received 1 µl of PBS. The injection procedures followed the same protocol as described for the AAV injections. IOP was measured on Day 8 following the first injection, and retinal function was evaluated on Day 9. The second injection was administered on Day 10 at the same dose as the first. Subsequent measurements of IOP and retinal responses were performed on Days 18 and 19, respectively. Animals were sacrificed on Day 20, and retinal tissues from the experimental eye were collected for qPCR analysis. The experimental design for the Bq123 and Bq788 treatment is illustrated in Figure 23A.

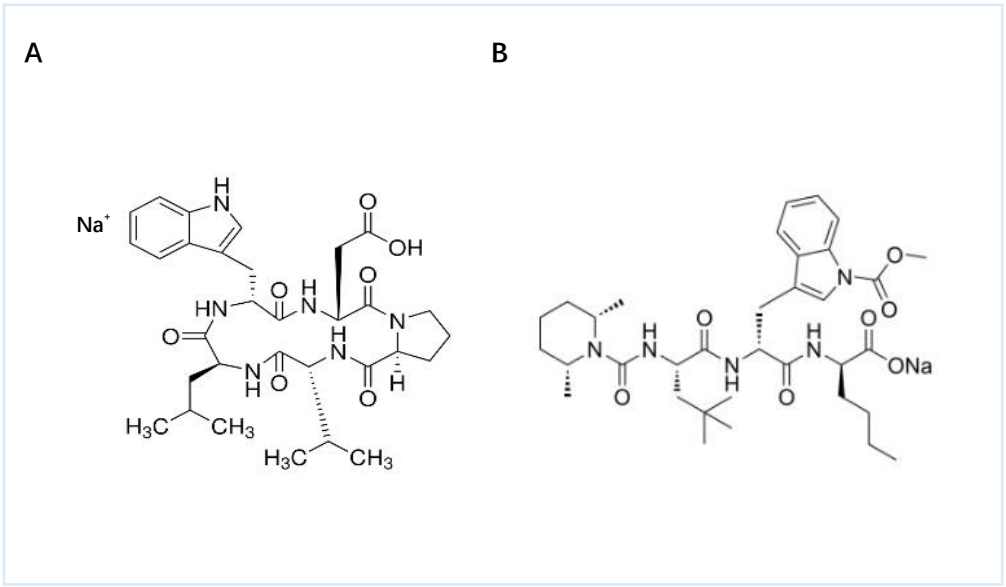

Figure 18. Molecular structures of **A**. Bq123 and **B**. Bq788 sodium salts.

4. Results

4.1. The Influence of EDN2 KO on BP and Ocular Phenotypes in SHR and WKY

The effects of EDN2 KO AAV and control AAV on SBP, DBP, IOP, and retinal responses in SHR and WKY are summarized in Figure 19B-G. We observed that injection of EDN2 KO AAV did not affect SBP, DBP, or IOP in SHR. SHR receiving the control AAV showed a slight increase in SBP. In WKY, neither type of AAV injection impacted SBP, DBP, or IOP. In SHR treated with EDN2 KO AAV, the treated eye exhibited increases of 33%, 29%, and 48% in the amplitudes of the pSTR, a-wave, and b-wave, respectively. The control AAV did not cause significant changes in retinal responses in SHR. No notable changes in retinal responses were observed after either injection in WKY.

AAV injections did not significantly alter total retinal thickness in either SHR or WKY (Figure 20A). EDN2 KO increased retinal artery lumen area by 61% in SHR and 31% in WKY (Figure 20C). Retinal vein lumen area increased by 62% in SHR post-EDN2 KO (P=0.1580), with no significant changes in WKY (Figure 20D). The control AAV retinas showed no alterations in retinal hemodynamics.

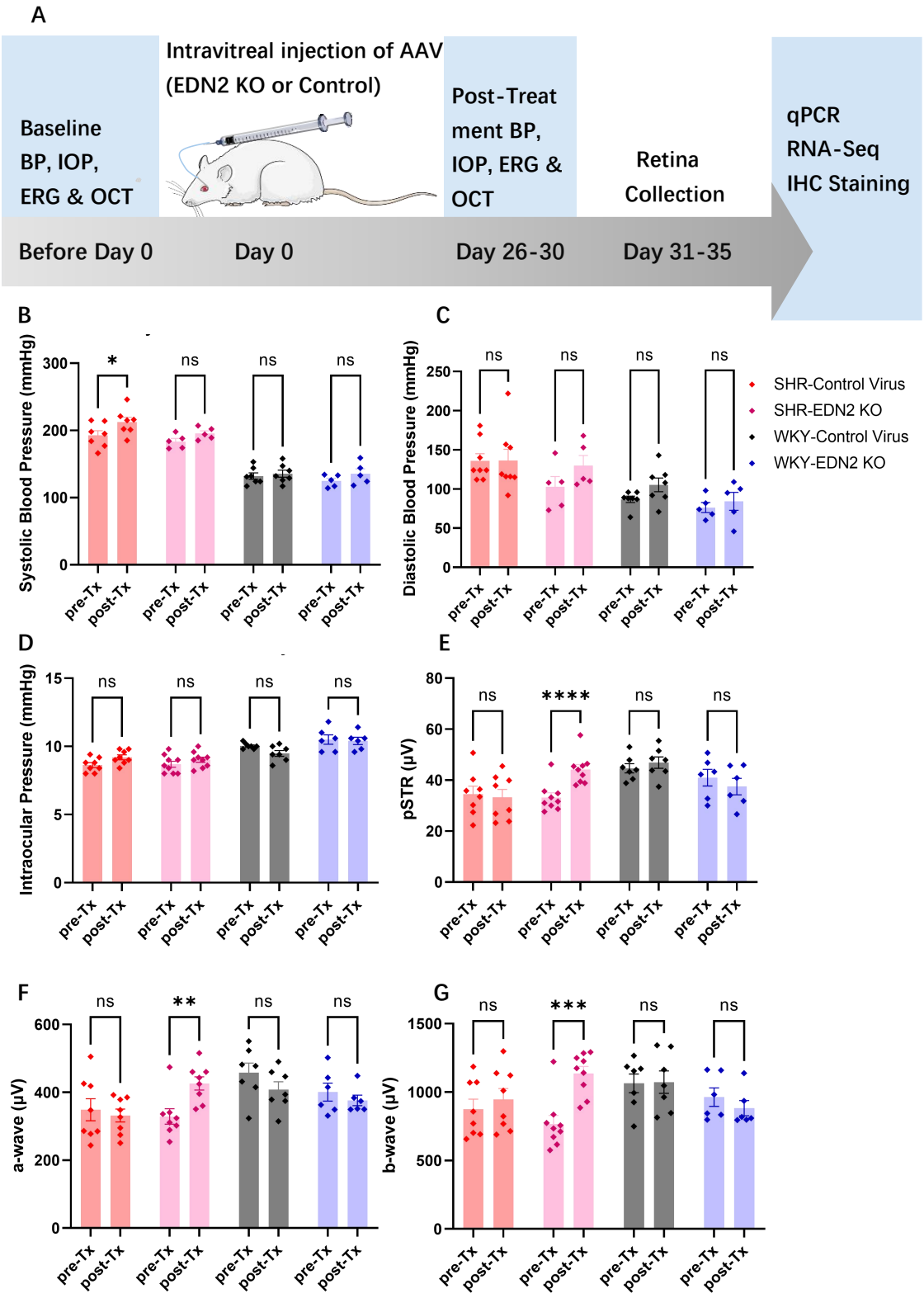

Figure 19. A. Experimental protocol for AAV treatment and measurements. **B-G.** Pre- and post-treatment measurements of SBP, DBP, IOP, pSTR, a-wave, and b-wave in SHR and WKY.

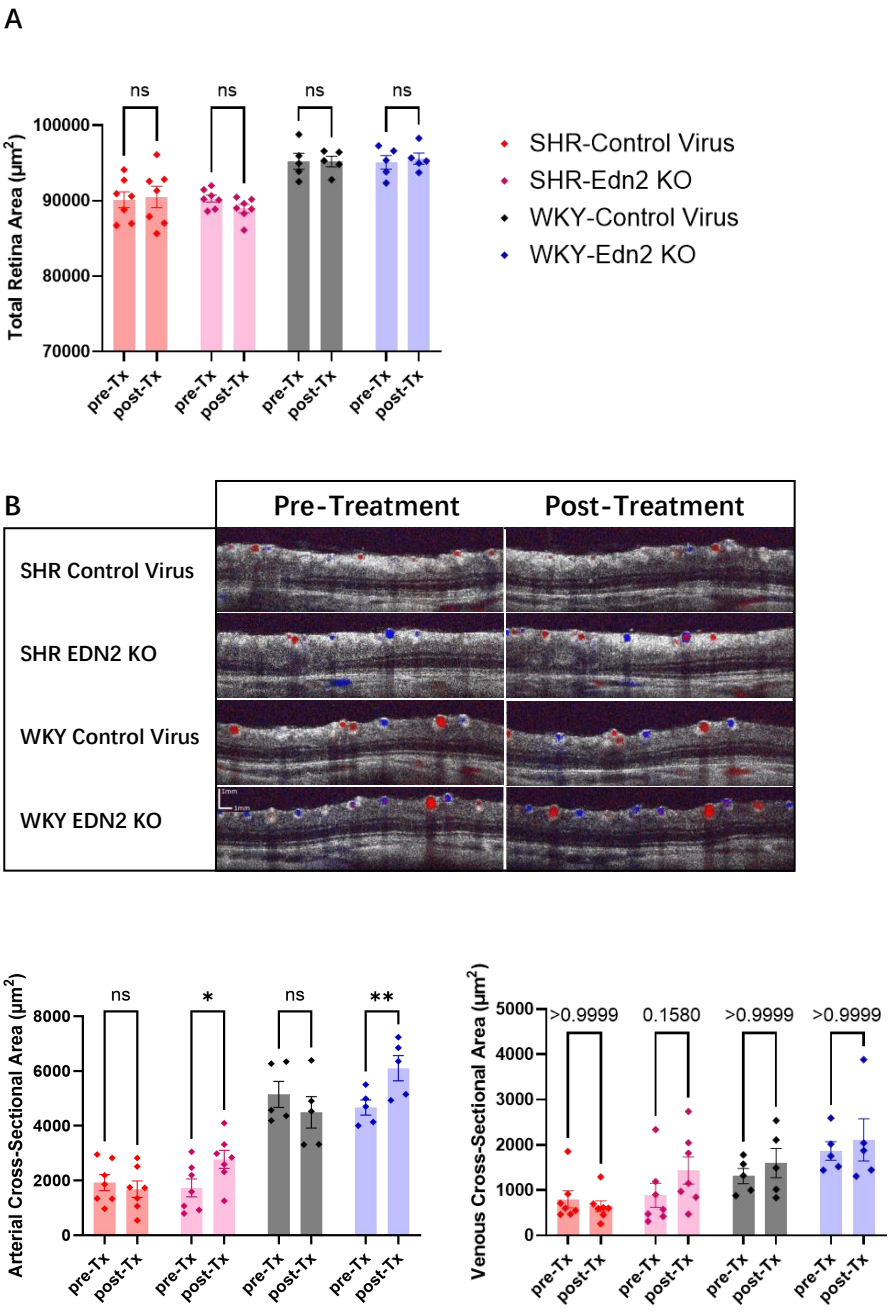

Figure 20. A. Pre- and post-treatment measurements of total retinal area in SHR and WKY; **B.** Representative images of pre- and post-treatment lumen areas of retinal arteries and veins from SHR and WKY; **C-D.** Pre- and post-treatment measurements of lumen areas of retinal arteries and veins in SHR and WKY. Data are shown as mean ± SEM. * $P < 0.5$; ** $P < 0.01$ (Two-way ANOVA with Bonferroni's multiple comparisons test).

4.2. The Transcriptomic Changes after EDN2 KO in SHR and WKY

The qPCR and RNA sequencing results of SHR injected with EDN2 KO AAV and control AAV are summarized in Figure 20. Our results showed that injection of EDN2 KO AAV successfully downregulated EDN2 mRNA expression (Figure 20A-C). In addition, qPCR results revealed downregulation of EDN3, EDNRB, IL-1α, IL-1β, C3, C1QA, and TNF-α in SHR treated with EDN2 KO AAV. Consistent with the qPCR results, RNA sequencing demonstrated downregulation of C1R, C1S, C1QA, C1QB, C1QC, C2, C3, C4A, C4B, C5AR2, NOS3, TLR13, TLR7, TLR8, TLR2, AIF1, CD68, GFAP, TGFB1, EDN3, MYD88, CCL2, and CYBB in SHR following EDN2 KO AAV injection. KEGG pathway analysis indicated suppression of complement and coagulation cascades, as well as cytokine-cytokine receptor interaction pathways, in SHR receiving EDN2 KO AAV injection. Furthermore, metabolic pathways were upregulated in SHR injected with EDN2 KO AAV.

The qPCR and RNA sequencing results of WKY injected with EDN2 KO AAV and control AAV are presented in Figure 21. Similar to the findings in SHR, EDN2 KO AAV significantly decreased EDN2 mRNA expression in WKY. EDN1 expression was shown to increase in WKY receiving EDN2 KO AAV. RNA sequencing revealed downregulation of EDN3, EDNRB, C1QA, C1QC, C1R, C3, C1S, C4A, C4B, GFAP, TLR7, TLR8, AIF1, CYBB, and TNF-α in WKY after EDN2 KO AAV treatment. The downregulated KEGG pathways included complement and coagulation cascades, as well as cytokine-cytokine receptor interactions. Notably, fewer genes were affected in WKY compared to SHR.

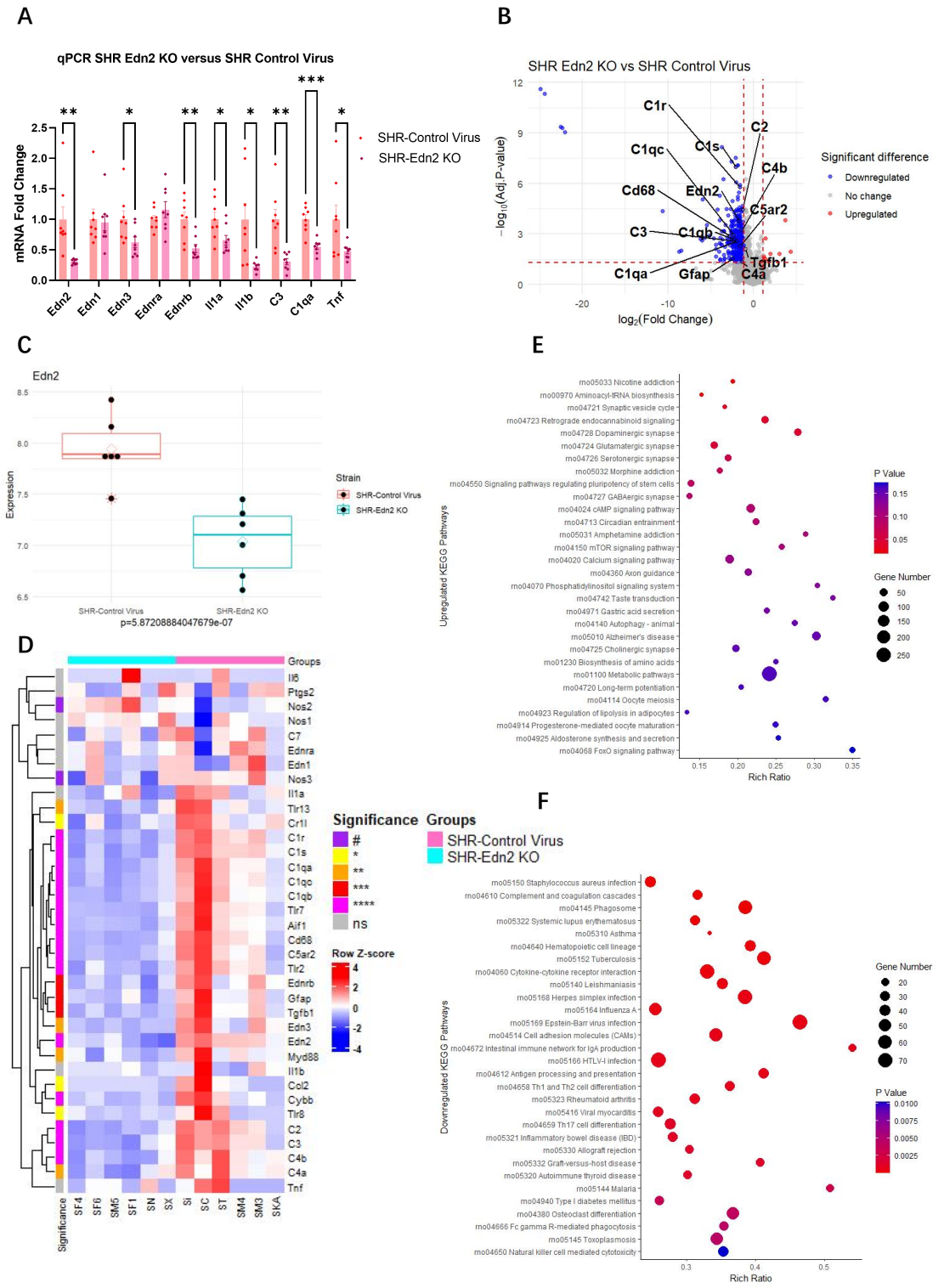

Figure 21. A. qPCR results of SHR injected with either EDN2 KO AAV or control AAV; **B.** Volcano plots showing downregulated targets in SHR treated with EDN2 KO AAV; **C.** EDN2 expression examined by RNA sequencing in SHR treated with EDN2 KO AAV and control AAV; **D.** Heatmap of the targets of interest; **E-F.** Upregulated and downregulated KEGG pathways in SHR injected with EDN2 KO AAV compared to those injected with control AAV.

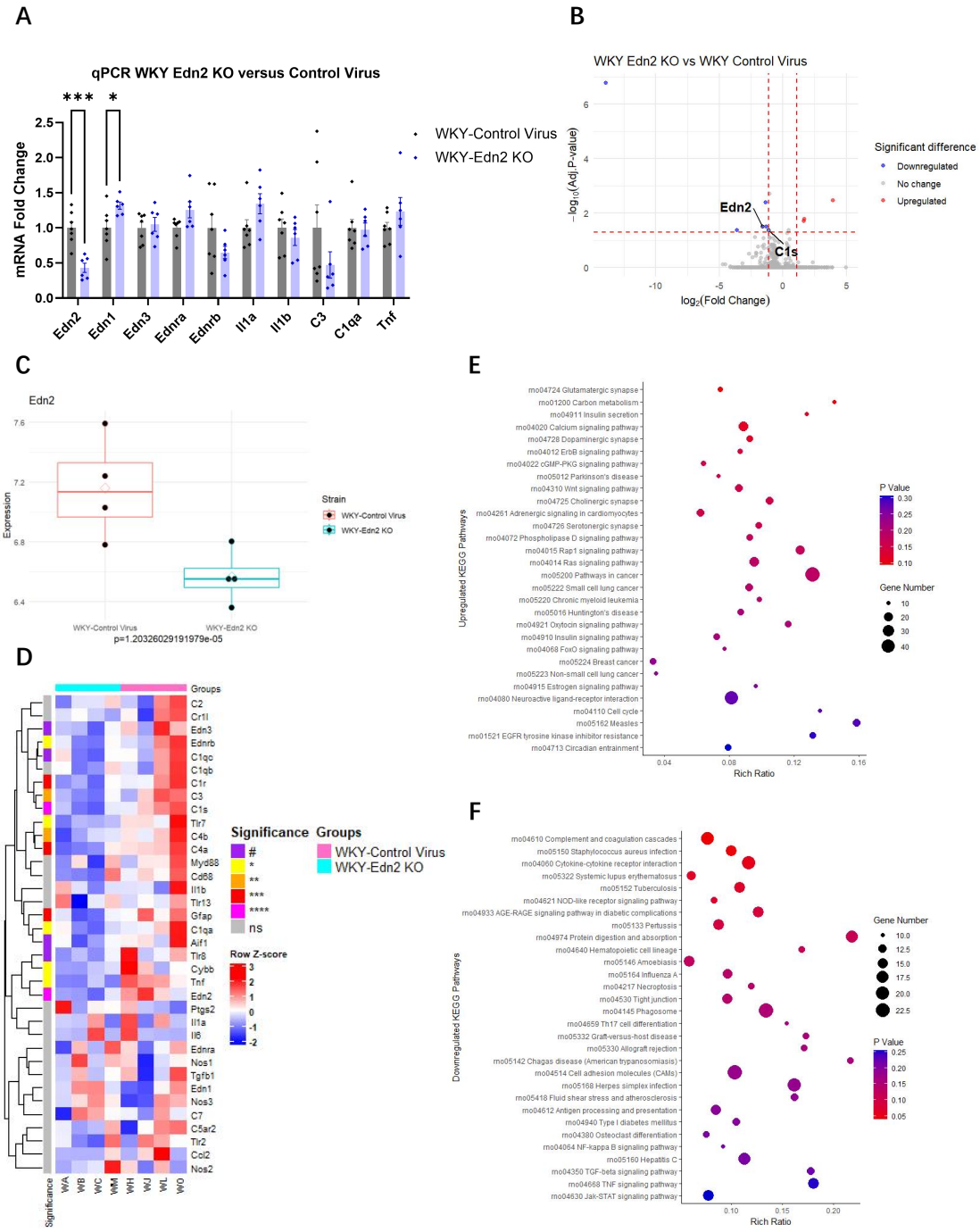

Figure 22. A. qPCR results showing WKY injected with EDN2 KO AAV compared to WKY injected with control AAV; **B.** Volcano plots illustrating differentially expressed targets in WKY injected with EDN2 KO AAV versus control AAV; **C.** EDN2 expressions analyzed by RNA sequencing in WKY injected with EDN2 KO AAV and control AAV; **D.** Heatmap of the targets of interest; **E-F.** Upregulated and downregulated KEGG pathways in WKY injected with EDN2 KO AAV compared to control AAV.

4.3. Influence of EDN2 KO on RGCs and Microglia in SHR and WKY

Representative post-treatment retinal images are shown in Figure 23A. In SHR, EDN2 KO AAV injection produced a mild but significant increase in RGC counts (Figure 23B). Retinas from SHR receiving EDN2 KO AAV also exhibited significantly fewer microglia and smaller microglia soma sizes, compared to control AAV-treated SHR (Figures 23D and 23F). These changes were absent in WKY receiving EDN2 KO AAV versus controls (Figures 23C, 23E, and 23G). Therefore, EDN KO reduced retinal neuroinflammation at both transcriptomic and protein levels in SHR, while significantly protecting RGCs from degeneration.

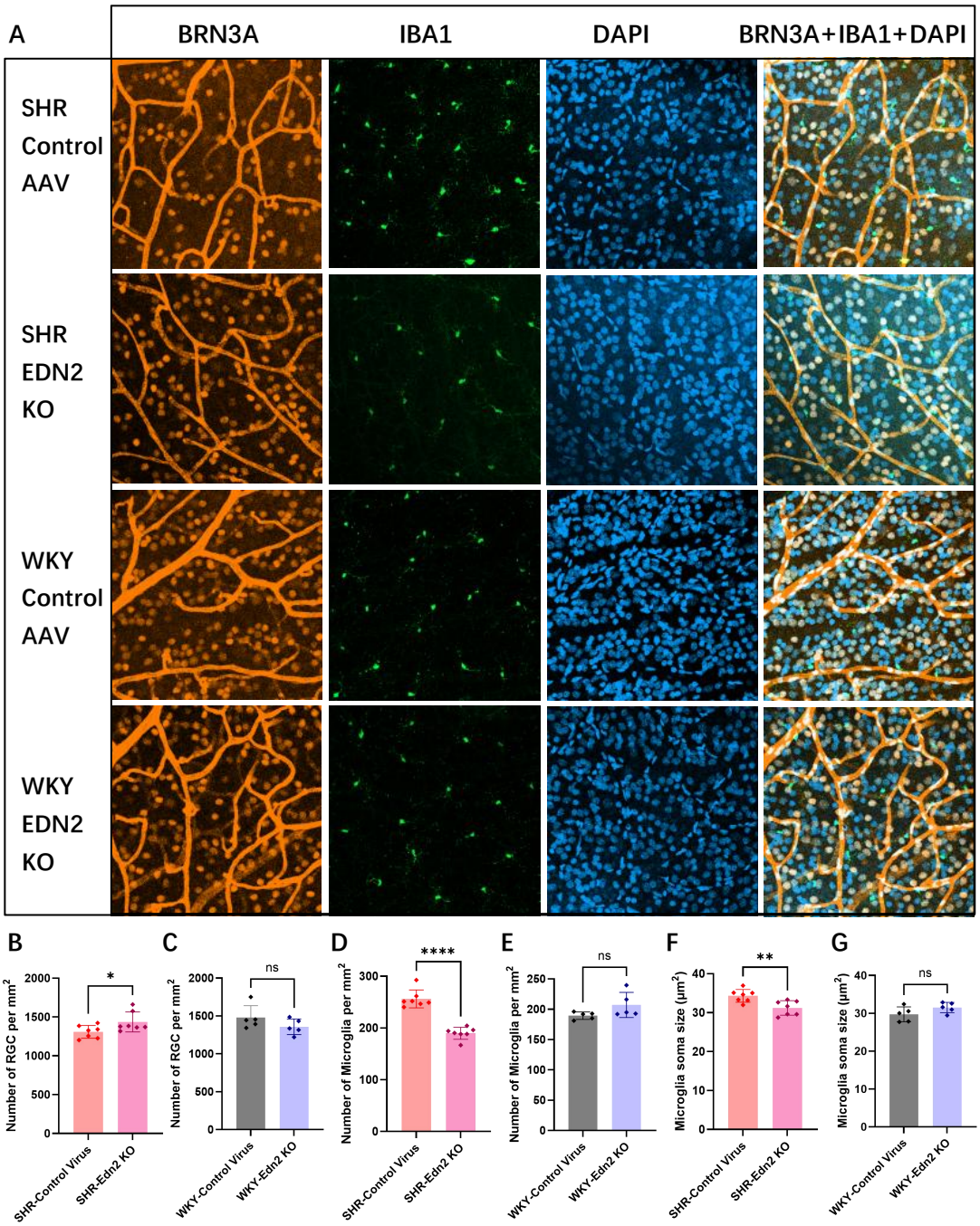

Figure 23. A. Representative images from post-treatment SHR and WKY retinas; **B-C.** Retinal ganglion cell counts from post-treatment SHR and WKY retinas; **D-E.** Microglial cell counts from post-treatment SHR and WKY retinas; **F-G.** Microglial soma size measurements from post-treatment SHR and WKY retinas. Data are shown as mean ± SEM. * $P < 0.5$; ** $P < 0.01$; **** $P < 0.0001$ (Student's T-test).

4.4. The Efficacy of EDN2 Inhibition at the Protein Level in SHR and WKY

To confirm the effectiveness of EDN2 KO AAV in SHR and WKY at the protein level, we measured EDN2 levels in the retina using ELISA and immunohistochemistry (IHC) staining. As shown in Figure 22A-B, the IHC fluorescence intensity in SHR treated with EDN2 KO AAV was significantly lower than in those receiving the control virus. In WKY, the reduction in EDN2 expression in the KO group was not statistically significant. The ELISA results were consistent with the IHC findings, showing a significant decrease in EDN2 levels in SHR injected with EDN2 KO AAV. In WKY, no significant difference was observed between the EDN2 KO and control AAV groups (Figure 22C). For GFAP expression, no significant differences were observed among the four groups (Figure 22D).

Taken together, EDN2 KO AAV injection led to a significant reduction in EDN2 expression in SHR at both mRNA and protein levels. However, in WKY, the effect of EDN2 KO AAV was only detected at the mRNA level. This difference might be due to the low baseline level of EDN2 in WKY, which limits further reduction.

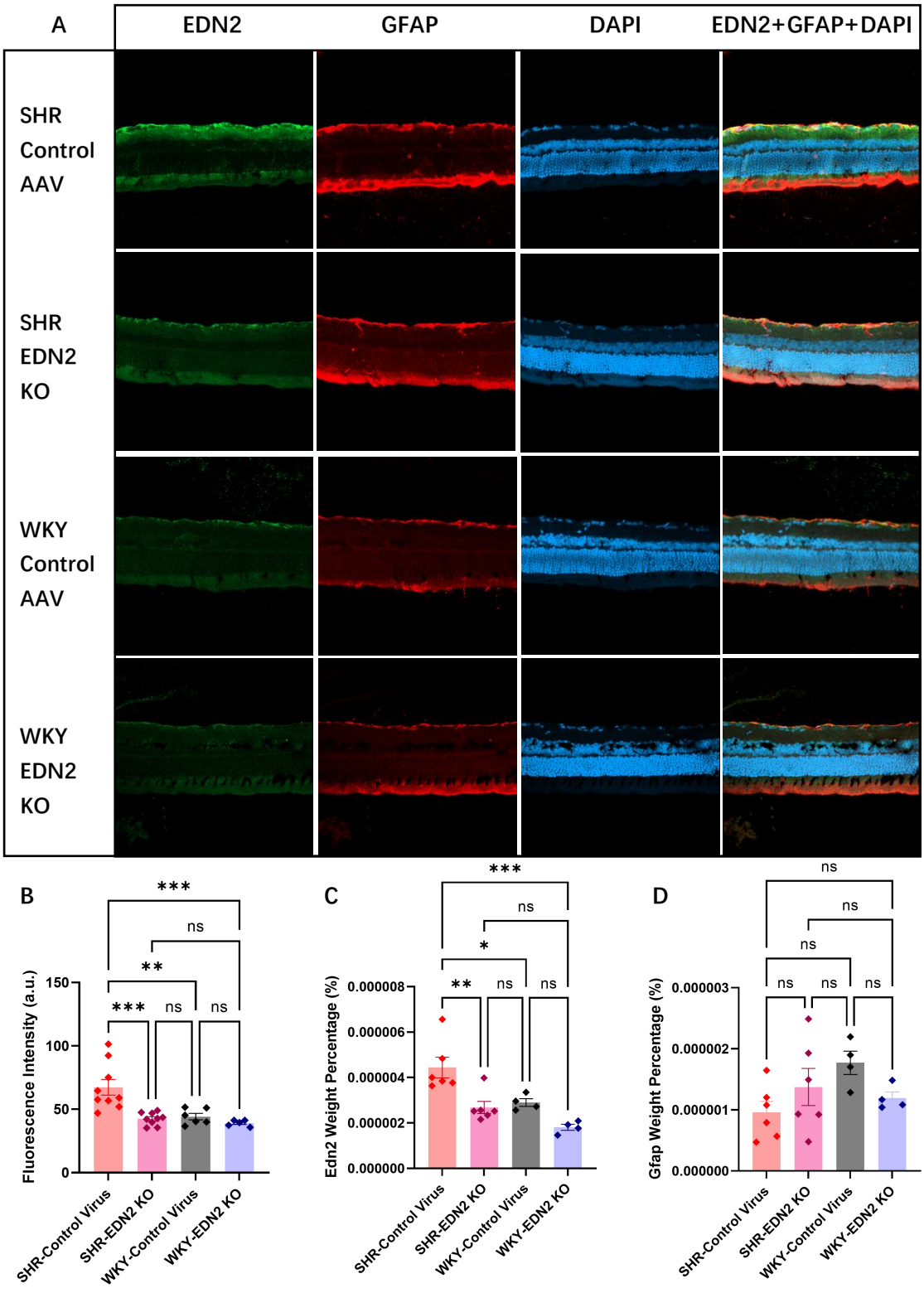

Figure 24. **A**. Representative images of SHR and WKY injected with EDN2 KO AAV or control AAV; **B**. Quantification of EDN2 fluorescence intensities; **C**. EDN2 protein levels measured by ELISA; **D**. GFAP protein levels measured by ELISA (expressed as a percentage of total protein).

4.5. The Influence of Bq123 and Bq788 on the Retina in SHR and WKY

The effects of intravitreal administration of Bq123 and Bq788 on IOP and retinal responses in SHR and WKY are summarized in Figure 23. Neither Bq123 nor Bq788 affected IOP in SHR. In WKY, Bq123 significantly lowered IOP in the treated eye, with the mean IOP decreasing from 10.0 mmHg to 9.3 mmHg on Day 8 and to 9.1 mmHg on Day 18. Bq123 improved functional retinal responses in SHR but not in WKY. In SHR, the pSTR increased by 32% and 58% compared to baseline on Day 9 and Day 19, respectively. In addition, Bq123 treatment enhanced the amplitudes of the a-wave and b-wave in SHR. On Day 19, the a-wave in the treated eye of SHR increased by 20% from baseline, and the b-wave showed a 21% increase over baseline on the same Day. In WKY, Bq123 treatment did not cause significant changes in retinal responses. On the other hand, Bq788 did not produce detectable changes in retinal responses in either SHR or WKY.

The qPCR results are presented in Figure 23F-I, comparing eyes with Bq123 or Bq788 injections to those receiving only PBS. In SHR eyes treated with Bq123, retinas showed decreased expression of IL-1α, EDN1, and EDNRA. In WKY, only EDN1 levels were significantly reduced after Bq123 treatment. Interestingly, EDN3 was upregulated in the retinas of WKY treated with Bq123. For Bq788 treatment, no significant changes were observed in either SHR or WKY.

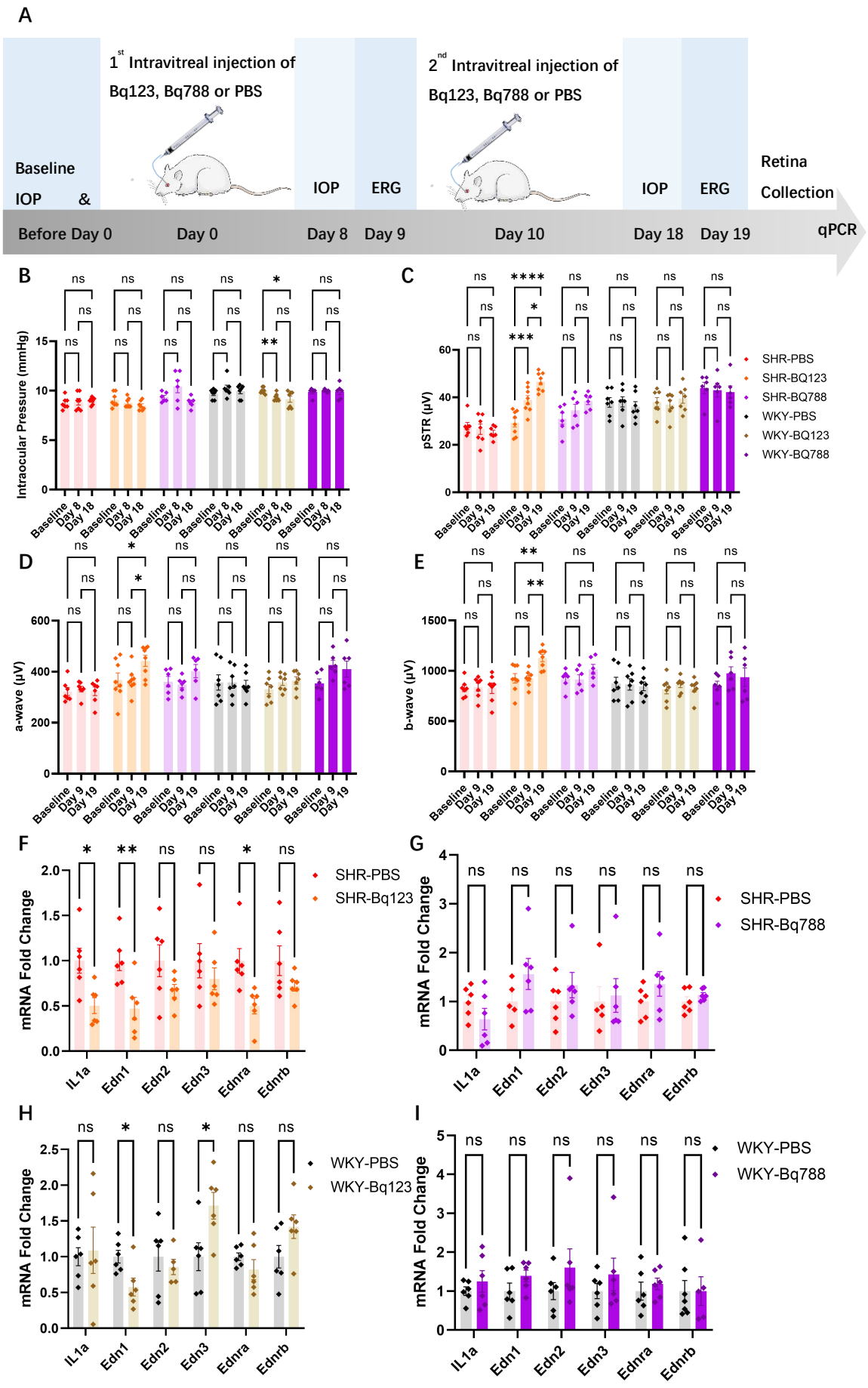
A
1st Intravitreal injection of Bq123, Bq788 or PBS
2nd Intravitreal injection of Bq123, Bq788 or PBS
Baseline IOP &
IOP
ERG
IOP
ERG
Retina Collection
qPCR
Before Day 0
Day 0
Day 8
Day 9
Day 10
Day 18
Day 19
B
Intraocular Pressure (mmHg)
C
pSTR (μV)
SHR-PBS
SHR-BQ123
SHR-BQ788
WKY-PBS
WKY-BQ123
WKY-BQ788
D
a-wave (μV)
E
b-wave (μV)
F
mRNA Fold Change
SHR-PBS
SHR-Bq123
G
SHR-PBS
SHR-Bq788
H
WKY-PBS
WKY-Bq123
I
WKY-PBS
WKY-Bq788
IL1a
Edn1
Edn2
Edn3
Ednra
Ednrb

Figure 25. A. Experimental design for treatment with Bq123 and Bq788 in SHR and WKY; **B-E.** IOP and functional retinal responses of SHR and WKY following injections of Bq123, Bq788, or PBS; **F-G.** qPCR results for SHR injected with Bq123 or Bq788 compared to SHR injected with PBS; **H-I.** qPCR results for WKY injected with Bq123 or Bq788 compared to WKY injected with PBS.

5. Discussion

We investigated the effects of EDN2 and endothelin receptor antagonists on IOP, functional retinal responses, and retinal biochemical changes. Our transcriptomic results revealed that at 8 months, SHR exhibited increased EDN2 expression, and at 12 months, EDN1, EDN2, EDN3, and EDNRA were all elevated in SHR. These results strongly suggest that activation of these endothelin components may play an important role in retinal degeneration in SHR. By knocking out retinal EDN2 using AAV, we observed significant improvements in functional retinal responses in SHR. Transcriptomic analysis identified downregulation of C1R, C1S, C1QA, C1QB, C1QC, C2, C3, C4A, C4B, C5AR2, NOS3, TLR13, TLR7, TLR8, TLR2, AIF1, CD68, GFAP, TGFB1, EDN3, MYD88, CCL2, and CYBB, as well as suppression of complement and coagulation cascades and cytokine-cytokine receptor interactions in SHR injected with EDN2 KO AAV. In WKY, EDN2 KO did not significantly rescue functional retinal responses. Nonetheless, we detected downregulation of EDN3, EDNRB, C1QA, C1QC, C1R, C3, C1S, C4A, C4B, GFAP, TLR7, TLR8, AIF1, CYBB, and TNF-α in WKY receiving EDN2 KO AAV. Complement and coagulation cascades and cytokine-cytokine receptor interactions were also suppressed in WKY, albeit with fewer affected genes compared to SHR. IOP remained unaffected by EDN2 KO AAV injection in both SHR and WKY. The lumen area of retinal arteries increased significantly in both SHR and WKY after EDN2 KO. Fewer and smaller retinal microglia were observed in SHR receiving EDN2 KO AAV. The RGCs' counts were also mildly higher in SHR receiving EDN2 KO AAV. Furthermore, intravitreal injection of Bq123 improved the functional retinal responses in SHR, and this effect was independent of IOP reduction. qPCR results showed that Bq123 administration decreased retinal expressions of IL-1α, EDN1, and EDNRA in SHR. In WKY, Bq123 reduced EDN1 expression but increased EDN3 levels. Treatment with Bq788 produced no significant effects on functional retinal responses or biochemical changes in either SHR or WKY.

Previous research on the functional role of EDN2 in the retina is limited. It has been suggested that EDN2 acts as a detrimental factor in glaucoma development, with elevated levels observed in the retina and optic nerve of DBA/2J mice (Howell, Macalinao et al. 2011). However, the precise mechanism by which EDN2 induces retinal degeneration remains largely unclear. We revealed a positive correlation between EDN2 and the complement and coagulation cascades. Utilizing a human retinal RNA sequencing database, we observed positive correlations between retinal EDN2 and C1R, C1S, C1QA, C1QB, C1QC, C2, C3, C4A, C4B, CD68, GFAP, TGFB1, and IL-6. These human findings are consistent with our experimental results obtained in rats, suggesting that EDN2 may influence functional retinal responses in SHR through activation of the complement system and other inflammatory components. Furthermore, immunohistochemistry revealed co-localization of retinal EDN2 and GFAP, indicating that astrocytes may be the primary source of retinal EDN2 secretion. It is possible that increased EDN2 in SHR is secreted by astrocytes and acts on other cell types, including RGCs. By activating the complement system and promoting inflammation, EDN2 leads to decreased functional retinal responses in SHR.

Previous studies have demonstrated that blocking EDNRA reduces IOP in rabbits and monkeys (Hollo, Kothy et al. 2002, Wang, Podos et al. 2011). However, in our study, administration of Bq123 did not produce a significant IOP reduction in SHR, whereas it caused a small but statistically significant decrease of < 1 mmHg in WKY. The reason for this discrepancy remains unclear but may be attributed to species differences and/or the relatively low baseline IOP in SHR, making it more challenging to detect measurable changes.

Conversely, our results show that blocking EDNRA with Bq123 can restore retinal functional responses in SHR. This effect may be mediated by the suppression of IL-1α, EDN1, and EDNRA expression. These findings support the hypothesis that

Bq123-induced EDNRA blockade leads to an improvement in retinal function independent of IOP reduction. Previous research suggests that it contributes to retinal degeneration through mechanisms involving glial activation and apoptosis. For instance, EDN1 promotes the proliferation of human optic nerve head astrocytes via both EDNRA and EDNRB (Prasanna, Krishnamoorthy et al. 2002). Moreover, in mice overexpressing EDN1 in vascular endothelial cells, astrocytes surrounding retinal blood vessels exhibit enlarged end feet. This swelling is believed to compromise the blood-retinal barrier, thereby leading to retinal degeneration (Mi, Zhang et al. 2012).

Literature suggests that EDNRB is a key mediator of RGC loss in glaucoma. Human glaucomatous optic nerves exhibit higher EDNRB expression compared to those from healthy controls, with EDNRB expression colocalizing with astrocytic processes in glaucomatous eyes (Wang, Fortune et al. 2006). In line with this, EDNRB-deficient rats exhibit less optic nerve degeneration under OHT than wild-type controls (Minton, Phatak et al. 2012). It has been reported that EDN1 induces apoptosis in cultured RGCs. This effect is significantly attenuated by EDNRB antagonists, but not by EDNRA antagonists. Further implicating EDNRB in RGC loss. However, in our experiments, Bq788 showed no significant effect on retinal functional responses or inflammation. This suggests that EDNRB does not mediate HT-related retinal degeneration in our model. As described in Chapter 3, EDNRA and EDNRB generally mediate vasoconstriction and vasodilation, respectively (Schiffrin 2005). We speculate that in the retina of SHR, the vasodilatory and potentially protective effects of EDNRB may outweigh its detrimental effects. Alternatively, the 20-Day treatment period may be insufficient to observe the benefits of EDNRB blockade.

In contrast, substantial evidence indicates a harmful role for EDNRA in glaucoma. OHT causes EDNRA accumulation in the GCL, IPL, and OPL in rats (McGrady, Minton et al. 2017). EDNRA may lead to retinal damage by compromising the blood

supply. For example, intravitreal EDN1 injections induce RGC death in mice, which is effectively prevented by systemic deletion of EDNRA and its deletion specifically from vascular mural cells. This indicates that EDNRA-mediated vasoconstriction in vascular mural cells leads to RGC death following EDN1 administration (Marola, Howell et al. 2022). Consistent with these findings, specific EDNRA blockade in our study significantly improved retinal function in SHR. The beneficial effects of Bq123 may be attributed to increased blood flow. Moreover, EDNRA blocking in SHR was associated with reduced retinal levels of IL-1α, a neuroinflammation marker primarily produced by activated microglia and observed to be slightly elevated in 12-month-old SHR (Liddelow, Guttenplan et al. 2017). Our results suggest that EDNRA inhibition may mitigate retinal inflammation, with lowered IL-1α as an early indicator.

In conclusion, retinal EDN2 KO rescued the functional retinal responses and RGC counts in SHR by improving blood flow and reducing complement components and other inflammatory mediators. Bq123 treatment restored retinal function by suppressing EDN1, EDNRA, and IL-1α expression in the retina. In summary, HT-induced functional retinal loss in SHR can be mitigated by suppressing the endothelin system, particularly EDN2 and EDNRA. Blocking EDN2 and EDNRA may restore functional retinal responses by reducing retinal inflammation.

Chapter 5. Conclusion

Glaucoma is the leading cause of irreversible blindness worldwide (Dandona and Dandona 2006). Current treatments for glaucoma, including eye drops, surgical procedures, and laser therapy, aim to delay disease progression primarily by lowering IOP (Tribble, Hui et al. 2023). However, no disease-modifying agent exists for glaucoma, and many patients continue to lose eyesight despite achieving controlled IOP (Chauhan and Drance 1992). The pathophysiology of glaucoma is thought to involve both mechanical and vascular mechanisms (Cui, Pan et al. 2022). The mechanical theory proposes that elevated IOP compresses ocular structures, damaging RGCs (Cui, Pan et al. 2022). The vascular theory suggests that insufficient blood flow to the optic nerve causes RGC injury. These two theories are interconnected, indicating a multifactorial pathogenesis (Cui, Pan et al. 2022). HT is a highly prevalent condition and the leading cause of premature death worldwide (Mills, Stefanescu et al. 2020). Its pathophysiology involves abnormal activation of the sympathetic nervous system, dysregulated vasoactive hormones, and vascular endothelial dysfunction, which lead to arterial wall thickening and impaired autoregulation (Hall, Granger et al. 2012, Hall, Omoto et al. 2024). The relationship between HT and glaucoma risk remains unclear, with studies showing both positive and negative associations (Peräsalo and Raitta 1990, Dielemans, Vingerling et al. 1995, Bonomi, Marchini et al. 2000, Leske, Wu et al. 2002, Mitchell, Lee et al. 2004, Plange, Kaup et al. 2006, Orzalesi, Rossetti et al. 2007, Wierzbowska, Wierzbowski et al. 2012, Gangwani, Chan et al. 2013, Bae, Lee et al. 2014, Asefa, Neustaeter et al. 2020). This inconsistency may relate to variations in patient demographics, stage of the disease, and timing of antihypertensive treatment. Similarly, the effect of BP on IOP remains uncertain (Bonomi, Marchini et al. 2000, Chen and Lai 2005, Wu, Nemesure et al. 2006, Xu, Wang et al. 2007, Zhao, Cho et al. 2014).

This study examined the effects of chronic HT on IOP, functional retinal responses, and retinal hemodynamics, both cross-sectionally and longitudinally. SHR were used

as the chronic HT model, with WKY serving as normal controls. Measurements of IOP, retinal responses, inner lumen area of retinal arteries and veins, and blood velocities in the central retinal artery were taken at 4, 8, and 12 months in both groups. SHR consistently exhibited higher BP but lower IOP compared to WKY. At 4 months, retinal responses were similar between groups, but by 8 and 12 months, SHR showed declines relative to WKY. Longitudinal and cross-sectional findings were consistent. Inner lumen area of retinal arteries and veins was significantly reduced in SHR, while mean blood velocity in the central retinal artery was comparable between groups. Despite increased OPP in SHR, their inner retinal blood flow remained lower than WKY, suggesting that HT-induced elevated OPP does not necessarily increase retinal blood flow. Chronic HT is associated with increased vascular resistance and endothelial dysfunction (Intengan and Schiffrin 2000, Resch, Garhofer et al. 2009), which may underlie decreased retinal blood flow and subsequent retinal dysfunction in SHR.

Systemic inflammation and oxidative stress are believed to contribute to HT development (Patel, Cardneau et al. 2006, Dinh, Drummond et al. 2014, Tanase, Gosav et al. 2019). Neuroinflammation and oxidative stress have been shown to play important roles in glaucoma development. We hypothesize shared pathophysiological mechanisms between HT and glaucoma. Our goal was to identify early retinal changes caused by chronic HT. At 8 months, SHR retinas showed increased expression of key inflammatory and complement markers such as Cd68, TGFB1, CYBB, EDN2, C2, C3, C1R, C1S, TLR2, TLR7, TLR8, and MYD88. By 12 months, additional inflammatory genes (IL-1β, IL-1α, EDN1, EDN3, EDNRA, CCL2, GFAP, AIF1), and complement factors (C1QA, C1QB, C1QC, C1R, C4A, C4B, C5AR2, C7) were upregulated. KEGG pathway analysis revealed activation of leukocyte transendothelial migration, chemokine signaling, complement and coagulation cascades, and cytokine-cytokine receptor interaction, Toll-like receptor signaling, and NF-kappa B signaling in SHR. RGC counts were reduced in SHR at 8 and 12 months

versus WKY. Microglial enlargement occurred at both 8 and 12 months, with increased microglial counts at 12 months. Elevated retinal EDN2 and GFAP protein levels were confirmed at 8 months, and these markers colocalized in retinal tissues of both SHR and WKY. Collectively, these data strongly suggest that HT-induced retinal functional decline in SHR is mediated by increased neuroinflammation.

Endothelin components are hypothesized to contribute importantly to retinal neurodegeneration (Howell, Macalinao et al. 2011, Marola, Howell et al. 2022). We found that SHR exhibited increased EDN2 expression at the gene and protein levels at 8 months, with further upregulation of EDN1, EDN2, EDN3, and EDNRA at 12 months. Using a genetic approach, we conducted Edn2 KO via sgRNA AAV in both SHR and WKY to investigate its retinal effects. Edn2 KO in SHR increased RGC counts and retinal blood supply, improved retinal function, and decreased key inflammatory and complement genes, including C1R, C1S, C1QA, C1QB, C1QC, C2, C3, C4A, C4B, C5AR2, TLR2, TLR7, TLR8, Cd68, CYBB, and TGFB1. This was accompanied by suppression of complement and coagulation cascades and cytokine-cytokine receptor interactions. In WKY, Edn2 KO did not significantly affect retinal functional responses but did reduce expression of complement factors and inflammatory markers, although to a lesser degree than in SHR. Importantly, IOP remained unchanged by EDN2 KO in both strains.

In addition to the genetic approach, we used a pharmacological approach by blocking EDNRA and EDNRB. Intravitreal injection of Bq123, an EDNRA antagonist, alleviated HT-induced declines in retinal function, including pSTR, a-wave, and b-wave amplitudes, in SHR but had no effects in WKY. This improvement was independent of IOP changes. qPCR showed Bq123 administration downregulated IL-1α, EDN1, and EDNRA expression in SHR retinas. Administration of Bq123 did not cause a significant change in EDN2 expression. One possible explanation is that EDNRA is a downstream receptor of EDN2, and it does not significantly affect the

production of EDN2. Conversely, EDN2 may exert a detrimental effect on the retina mediated primarily by EDNRA. On the other hand, intravitreal injection of Bq788, an EDNRB antagonist, had no significant effect on retinal responses in either strain. These findings indicate that endothelin components, particularly EDN2 and EDNRA, play critical roles in retinal degeneration and functional loss induced by HT in SHR. Our observations indicate that EDN2 KO in SHR rescues retinal functional degeneration, potentially through the restoration of retinal blood supply and downregulation of complement components. This promising finding highlights the need for future studies to better understand the role of complement components in HT-induced retinal degeneration. Furthermore, since EDN2 is associated with several inflammatory markers, including AIF1 and CD68, it may represent a valuable therapeutic target for other retinal diseases caused by neuroinflammation. Overall, targeting the endothelin system presents as a novel approach for treating inflammation-related retinal disorders and warrants further investigation.

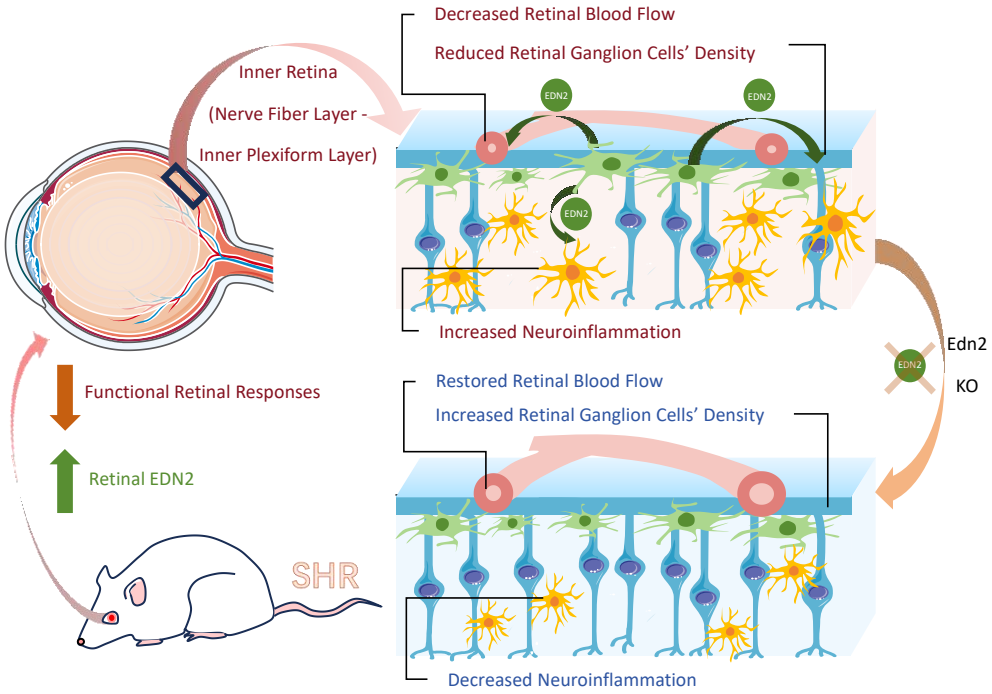

Figure 26. A schematic diagram summarizing the major findings.

References

Abu-Amero, K. K., J. Morales and T. M. Bosley (2006). "Mitochondrial abnormalities in patients with primary open-angle glaucoma." Invest Ophthalmol Vis Sci 47(6): 2533–2541.

Adornetto, A., R. Russo and V. Parisi (2019). "Neuroinflammation as a target for glaucoma therapy." Neural Regen Res 14(3): 391–394.

Agar, A., S. S. Yip, M. A. Hill and M. T. Coroneo (2000). "Pressure related apoptosis in neuronal cell lines." J Neurosci Res 60(4): 495–503.

Agarwal, R., S. K. Gupta, P. Agarwal, R. Saxena and S. S. Agrawal (2009). "Current concepts in the pathophysiology of glaucoma." Indian J Ophthalmol 57(4): 257–266.

Ahmad, S. S. (2024). "The mechanical theory of glaucoma in terms of prelaminar, laminar, and postlaminar factors." Taiwan J Ophthalmol 14(3): 376–386.

Akay, F., F. C. Gundogan, U. Yolcu, S. Toyran, E. Tunc and S. Uzun (2016). "Retinal structural changes in systemic arterial hypertension: an OCT study." Eur J Ophthalmol 26(5): 436–441.

Alrashdi, S. F., D. Deliyanti, D. M. Talia and J. L. Wilkinson-Berka (2018). "Endothelin-2 Injures the Blood-Retinal Barrier and Macroglial Muller Cells: Interactions with Angiotensin II, Aldosterone, and NADPH Oxidase." Am J Pathol 188(3): 805–817.

Amerasinghe, N., T. Aung, N. Cheung, C. W. Fong, J. J. Wang, P. Mitchell, S. M. Saw and T. Y. Wong (2008). "Evidence of retinal vascular narrowing in glaucomatous eyes in an Asian population." Invest Ophthalmol Vis Sci 49(12): 5397–5402.

Anderson, D. R. and A. Hendrickson (1974). "Effect of intraocular pressure on rapid axoplasmic transport in monkey optic nerve." Invest Ophthalmol Vis Sci 13(10): 771–783.

Asefa, N. G., A. Neustaeter, N. M. Jansonius and H. Snieder (2020). "Autonomic dysfunction and blood pressure in glaucoma patients: the Lifelines Cohort Study." Invest Ophthalmol Vis Sci 61(11): 25.

Azizi, M., M. Sapoval, P. Gosse, M. Monge, G. Bobrie, P. Delsart, M. Midulla, C.

Mounier-Vehier, P. Y. Courand, P. Lantelme, T. Denolle, C. Dourmap-Collas, H. Trillaud, H. Pereira, P. F. Plouin, G. Chatellier and i. Renal Denervation for Hypertension (2015). "Optimum and stepped care standardised antihypertensive treatment with or without renal denervation for resistant hypertension (DENERHTN): a multicentre, open-label, randomised controlled trial." Lancet 385(9981): 1957–1965.

Bae, H. W., N. Lee, H. S. Lee, S. Hong, G. J. Seong and C. Y. Kim (2014). "Systemic hypertension as a risk factor for open-angle glaucoma: a meta-analysis of population-based studies." PLoS One 9(9): e108226.

Banerjee, D., A. Banerjee, S. Mookherjee, M. Vishal, A. Mukhopadhyay, A. Sen, A. Basu and K. Ray (2013). "Mitochondrial genome analysis of primary open angle glaucoma patients." PLoS One 8(8): e70760.

Barbaro, N. R., T. M. de Araújo, J. E. Tanus-Santos, G. F. Anhê, V. Fontana and H. Moreno (2015). "Vascular damage in resistant hypertension: TNF-alpha inhibition effects on endothelial cells." Biomed Res Int 2015: 1–8.

Barbaro, N. R., V. Fontana, R. Modolo, A. P. De Faria, A. R. Sabbatini, F. H. Fonseca, G. F. Anhe and H. Moreno (2015). "Increased arterial stiffness in resistant hypertension is associated with inflammatory biomarkers." Blood Press 24(1): 7–13.

Bautista, L. E., L. M. Vera, I. A. Arenas and G. Gamarra (2005). "Independent association between inflammatory markers (C-reactive protein, interleukin-6, and TNF-alpha) and essential hypertension." J Hum Hypertens 19(2): 149–154.

Becerra, C. C., A. Sabbagh, J. Aljabban, S. Frank, A. Tahboub and D. Hadley (2019). "Meta-Analysis of Genetic Expression Profiles in Glaucoma." Invest Ophthalmol Vis Sci 60(9): 6068–6068.

Bednarczyk, E. M., B. Remler, C. Weikart, A. D. Nelson and R. C. Reed (1998). "Global cerebral blood flow, blood volume, and oxygen metabolism in patients with migraine headache." Neurology 50(6): 1736–1740.

Bhatt, Y., D. M. Hunt and L. S. Carvalho (2023). "The origins of the full-field flash electroretinogram b-wave." Front Mol Neurosci 16: 1153934.

Blanton, F. M. (1964). "Anterior Chamber Angle Recession and Secondary Glaucoma. A Study of the Aftereffects of Traumatic Hyphemas." Arch Ophthalmol 72: 39–43.

Bonomi, L., G. Marchini, M. Marraffa, P. Bernardi, R. Morbio and A. Varotto (2000). "Vascular risk factors for primary open angle glaucoma: the Egna-Neumarkt Study." Ophthalmology 107(7): 1287–1293.

Bosco, A., S. R. Anderson, K. T. Breen, C. O. Romero, M. R. Steele, V. A. Chiodo, S. L. Boye, W. W. Hauswirth, S. Tomlinson and M. L. Vetter (2018). "Complement C3-Targeted Gene Therapy Restricts Onset and Progression of Neurodegeneration in Chronic Mouse Glaucoma." Mol Ther 26(10): 2379–2396.

Bosco, A., M. R. Steele and M. L. Vetter (2011). "Early microglia activation in a mouse model of chronic glaucoma." J Comp Neurol 519(4): 599–620.

Bourke, K., M. R. Patel, L. M. Prisant and D. M. Marcus (2004). "Hypertensive choroidopathy." J Clin Hypertens (Greenwich) 6(8): 471–472.

Bulpitt, C. J., C. Hodes and M. G. Everitt (1975). "Intraocular pressure and systemic blood pressure in the elderly." Br J Ophthalmol 59(12): 717–720.

Cai, Q. and Z. H. Sheng (2009). "Molecular motors and synaptic assembly." Neuroscientist 15(1): 78–89.

Calkins, D. J. (2012). "Critical pathogenic events underlying progression of neurodegeneration in glaucoma." Prog Retin Eye Res 31(6): 702–719.

Calkins, D. J. (2013). "Age-related changes in the visual pathways: blame it on the axon." Invest Ophthalmol Vis Sci 54(14): ORSF37–41.

Cellini, M. and R. Caramazza (1999). "Chronic open angle glaucoma and low tension glaucoma: endothelin - 1 levels in plasma and aqueous humour." Acta Odontol Scand 77: 7–8.

Cellini, M., G. L. Possati, V. Profazio, M. Sbrocca, N. Caramazza and R. Caramazza (1997). "Color Doppler imaging and plasma levels of endothelin-1 in low-tension glaucoma." Acta Ophthalmol Scand Suppl(224): 11–13.

Cellini, M., E. Strobbe, C. Gizzi, N. Balducci, P. G. Toschi and E. C. Campos (2012). "Endothelin-1 plasma levels and vascular endothelial dysfunction in primary open

angle glaucoma." Life Sci 91(13-14): 699–702.

Charlson, M. E., C. G. de Moraes, A. Link, M. T. Wells, G. Harmon, J. C. Peterson, R. Ritch and J. M. Liebmann (2014). "Nocturnal systemic hypotension increases the risk of glaucoma progression." Ophthalmology 121(10): 2004–2012.

Chatterjee, S., S. Chattopadhyay, M. Hope-Ross and P. L. Lip (2002). "Hypertension and the eye: changing perspectives." J Hum Hypertens 16(10): 667–675.

Chauhan, B. C. (2008). "Endothelin and its potential role in glaucoma." Can J Ophthalmol 43(3): 356–360.

Chauhan, B. C. and S. M. Drance (1992). "The relationship between intraocular pressure and visual field progression in glaucoma." Graefes Arch Clin Exp Ophthalmol 230(6): 521–526.

Chen, H. Y., Y. C. Chang, W. C. Chen and H. Y. Lane (2013). "Association between plasma endothelin-1 and severity of different types of glaucoma." J Glaucoma 22(2): 117–122.

Chen, H. Y. and S. W. Lai (2005). "Relation between intraocular pressure and systemic health parameters in Taiwan." South Med J 98(1): 28–32.

Chen, K. G., R. R. Kang, Q. Sun, C. Liu, Z. Ma, K. Liu, Y. Deng, W. Liu and B. Xu (2020). "Resveratrol ameliorates disorders of mitochondrial biogenesis and mitophagy in rats continuously exposed to benzo(a)pyrene from embryonic development through adolescence." Toxicology 442: 152532.

Chobanian, A. V., G. L. Bakris, H. R. Black, W. C. Cushman, L. A. Green, J. L. Izzo, Jr., D. W. Jones, B. J. Materson, S. Oparil, J. T. Wright, Jr., E. J. Roccella, L. National Heart, D. E. Blood Institute Joint National Committee on Prevention, P. Treatment of High Blood and C. National High Blood Pressure Education Program Coordinating (2003). "The Seventh Report of the Joint National Committee on Prevention, Detection, Evaluation, and Treatment of High Blood Pressure: the JNC 7 report." JAMA 289(19): 2560–2572.

Choi, H., J. Y. Kim, K. H. Lee, J. S. Kim, J. Y. Lee, E. K. Choi, H. J. Seong, G. Kim, H. Park, E. Jung, S. H. Hong, A. Kronbichler, M. Eisenhut, A. Koyanagi, L. Jacob, D.

K. Yon, S. W. Lee, M. S. Kim, K. Kostev, J. I. Shin, J. W. Yang and L. Smith (2021). "Omega-3 fatty acids supplementation on major cardiovascular outcomes: an umbrella review of meta-analyses of observational studies and randomized controlled trials." Eur Rev Med Pharmacol Sci 25(4): 2079–2092.

Choi, J., K. H. Kim, J. Jeong, H. S. Cho, C. H. Lee and M. S. Kook (2007). "Circadian fluctuation of mean ocular perfusion pressure is a consistent risk factor for normal-tension glaucoma." Invest Ophthalmol Vis Sci 48(1): 104–111.

Choplin, N. T. and C. E. Traverso (2014). Atlas of glaucoma, CRC Press.

Chopra, A., A. Sharma, S. Singh and V. Bahl (2014). "Changing Perspectives in Classifications of Hypertensive Retinopathy." IOSR J Dent Med Sci 13: 51–54.

Choritz, L., M. Machert and H. Thieme (2012). "Correlation of endothelin-1 concentration in aqueous humor with intraocular pressure in primary open angle and pseudoexfoliation glaucoma." Invest Ophthalmol Vis Sci 53(11): 7336–7342.

Chrysostomou, V., F. Rezania, I. A. Trounce and J. G. Crowston (2013). "Oxidative stress and mitochondrial dysfunction in glaucoma." Curr Opin Pharmacol 13(1): 12–15.

Chua, J., C. Y.-L. Cheung, L. Schmetterer and T. Y. Wong (2020). Hypertensive Fundus Changes. Retinal Vascular Disease. A. Sheyman and A. A. Fawzi. Singapore, Springer Nature Singapore: 85–97.

Chua, J., C. W. L. Chin, J. Hong, M. L. Chee, T. T. Le, D. S. W. Ting, T. Y. Wong and L. Schmetterer (2019). "Impact of hypertension on retinal capillary microvasculature using optical coherence tomographic angiography." J Hypertens 37(3): 572–580.

Chung, H. S., A. Harris, L. Kagemann and B. Martin (1999). "Peripapillary retinal blood flow in normal tension glaucoma." Br J Ophthalmol 83(4): 466–469.

Civan, M. M., D. Benos and S. Simon (2008). The eye's aqueous humor, Elsevier.

Costa, V. P., E. S. Arcieri and A. Harris (2009). "Blood pressure and glaucoma." Br J Ophthalmol 93(10): 1276–1282.

Costa, V. P., A. Harris, D. Anderson, R. Stodtmeister, F. Cremasco, H. Kergoat, J. Lovasik, I. Stalmans, O. Zeitz, I. Lanzl, K. Gugleta and L. Schmetterer (2014).

"Ocular perfusion pressure in glaucoma." Acta Ophthalmol 92(4): e252–266.

Costa, V. P., J. Jimenez-Roman, F. G. Carrasco, A. Lupinacci and A. Harris (2010). "Twenty-four-hour ocular perfusion pressure in primary open-angle glaucoma." Br J Ophthalmol 94(10): 1291–1294.

Costagliola, C., R. Di Benedetto, L. De Caprio, R. Verde and L. Mastropasqua (1995). "Effect of oral captopril (SQ 14225) on intraocular pressure in man." Eur J Ophthalmol 5(1): 19–25.

Costagliola, C., M. Verolino, M. L. De Rosa, G. Iaccarino, M. Ciancaglini and L. Mastropasqua (2000). "Effect of oral losartan potassium administration on intraocular pressure in normotensive and glaucomatous human subjects." Exp Eye Res 71(2): 167–171.

Crowley, S. D., S. B. Gurley, M. J. Herrera, P. Ruiz, R. Griffiths, A. P. Kumar, H. S. Kim, O. Smithies, T. H. Le and T. M. Coffman (2006). "Angiotensin II causes hypertension and cardiac hypertrophy through its receptors in the kidney." Proc Natl Acad Sci U S A 103(47): 17985–17990.

Cui, Y. K., L. Pan, T. Lam, C. Y. Wen and C. W. Do (2022). "Mechanistic links between systemic hypertension and open angle glaucoma." Clin Exp Optom 105(4): 362–371.

Cursiefen, C., M. Wisse, S. Cursiefen, A. Junemann, P. Martus and M. Korth (2000). "Migraine and tension headache in high-pressure and normal-pressure glaucoma." Am J Ophthalmol 129(1): 102–104.

Dandona, L. and R. Dandona (2006). "What is the global burden of visual impairment?" BMC Med 4: 6.

Dengler-Crish, C. M., M. A. Smith, D. M. Inman, G. N. Wilson, J. W. Young and S. D. Crish (2014). "Anterograde transport blockade precedes deficits in retrograde transport in the visual projection of the DBA/2J mouse model of glaucoma." Front Neurosci 8: 290.

Dhingra, D. and S. Bhartiya (2020). "Evaluating glaucoma surgeries in the MIGS context." Rom J Ophthalmol 64(2): 85–95.

Dielemans, I., J. R. Vingerling, D. Algra, A. Hofman, D. E. Grobbee and P. T. de Jong (1995). "Primary open-angle glaucoma, intraocular pressure, and systemic blood pressure in the general elderly population: the Rotterdam Study." Ophthalmology 102(1): 54–60.

Dinh, Q. N., G. R. Drummond, C. G. Sobey and S. Chrissobolis (2014). "Roles of inflammation, oxidative stress, and vascular dysfunction in hypertension." Biomed Res Int 2014: 406960.

Dong, L., Y. Hu, L. Zhou and X. Cheng (2018). "P2X7 receptor antagonist protects retinal ganglion cells by inhibiting microglial activation in a rat chronic ocular hypertension model." Mol Med Rep 17(2): 2289–2296.

Dong, Y. R., C. E. Gustafson, J. Wang, J. Z. Cui and T. Yoshitomi (2019). "Remodeled structure and reduced contractile responsiveness of ocular ciliary artery in spontaneously hypertensive rats." Int J Ophthalmol 12(3): 363–368.

Du, R., X. Wang and S. He (2020). "BDNF improves axon transportation and rescues visual function in a rodent model of acute elevation of intraocular pressure." Sci China Life Sci 63(9): 1337–1346.

Duerrschmidt, N., N. Wippich, W. Goettsch, H. J. Broemme and H. Morawietz (2000). "Endothelin-1 induces NAD(P)H oxidase in human endothelial cells." Biochem Biophys Res Commun 269(3): 713–717.

Duke-Elder, W. S. (1926). "The Ocular Circulation: Its Normal Pressure Relationships and Their Physiological Significance." Br J Ophthalmol 10(10): 513–572.

Duke-Elder, W. S. (1926). "The venous pressure of the eye and its relation to the intra-ocular pressure." J Physiol 61(3): 409–418.

Echevarria, F. D., C. R. Formichella and R. M. Sappington (2017). "Interleukin-6 Deficiency Attenuates Retinal Ganglion Cell Axonopathy and Glaucoma-Related Vision Loss." Front Neurosci 11: 318.

Erickson-Lamy, K., C. Korbmacher, J. S. Schuman and J. A. Nathanson (1991). "Effect of endothelin on outflow facility and accommodation in the monkey eye in vivo." Invest Ophthalmol Vis Sci 32(3): 492–495.

Fan Gaskin, J. C., M. H. Shah and E. C. Chan (2021). "Oxidative Stress and the Role of NADPH Oxidase in Glaucoma." Antioxidants (Basel) 10(2).

Fernandez-Albarral, J. A., A. I. Ramirez, R. de Hoz, J. A. Matamoros, E. Salobrar-Garcia, L. Elvira-Hurtado, I. Lopez-Cuenca, L. Sanchez-Puebla, J. J. Salazar and J. M. Ramirez (2024). "Glaucoma: from pathogenic mechanisms to retinal glial cell response to damage." Front Cell Neurosci 18: 1354569.

Fisher, J., T. Mizrahi, H. Schori, E. Yoles, H. Levkovitch-Verbin, S. Haggiag, M. Revel and M. Schwartz (2001). "Increased post-traumatic survival of neurons in IL-6-knockout mice on a background of EAE susceptibility." J Neuroimmunol 119(1): 1–9.

Flammer, J. (1994). "The vascular concept of glaucoma." Surv Ophthalmol 38 Suppl: S3–6.

Flammer, J. and S. Orgul (1998). "Optic nerve blood-flow abnormalities in glaucoma." Prog Retin Eye Res 17(2): 267–289.

Fleenor, D. L., A. R. Shepard, P. E. Hellberg, N. Jacobson, I. H. Pang and A. F. Clark (2006). "TGFbeta2-induced changes in human trabecular meshwork: implications for intraocular pressure." Invest Ophthalmol Vis Sci 47(1): 226–234.

Forouzanfar, M. H., P. Liu, G. A. Roth, M. Ng, S. Biryukov, L. Marczak, L. Alexander, K. Estep, K. Hassen Abate, T. F. Akinyemiju, R. Ali, N. Alvis-Guzman, P. Azzopardi, A. Banerjee, T. Barnighausen, A. Basu, T. Bekele, D. A. Bennett, S. Biadgilign, F. Catala-Lopez, V. L. Feigin, J. C. Fernandes, F. Fischer, A. A. Gebru, P. Gona, R. Gupta, G. J. Hankey, J. B. Jonas, S. E. Judd, Y. H. Khang, A. Khosravi, Y. J. Kim, R. W. Kimokoti, Y. Kokubo, D. Kolte, A. Lopez, P. A. Lotufo, R. Malekzadeh, Y. A. Melaku, G. A. Mensah, A. Misganaw, A. H. Mokdad, A. E. Moran, H. Nawaz, B. Neal, F. N. Ngalesoni, T. Ohkubo, F. Pourmalek, A. Rafay, R. K. Rai, D. Rojas-Rueda, U. K. Sampson, I. S. Santos, M. Sawhney, A. E. Schutte, S. G. Sepanlou, G. T. Shifa, I. Shiue, B. A. Tedla, A. G. Thrift, M. Tonelli, T. Truelsen, N. Tsilimparis, K. N. Ukwaja, O. A. Uthman, T. Vasankari, N. Venketasubramanian, V. V. Vlassov, T. Vos, R. Westerman, L. L. Yan, Y. Yano, N. Yonemoto, M. E. Zaki and C. J. Murray (2017).

"Global Burden of Hypertension and Systolic Blood Pressure of at Least 110 to 115 mm Hg, 1990-2015." JAMA 317(2): 165–182.

Forte, P., M. Copland, L. M. Smith, E. Milne, J. Sutherland and N. Benjamin (1997). "Basal nitric oxide synthesis in essential hypertension." Lancet 349(9055): 837–842.

Fortune, B., B. V. Bui, J. C. Morrison, E. C. Johnson, J. Dong, W. O. Cepurna, L. Jia, S. Barber and G. A. Cioffi (2004). "Selective ganglion cell functional loss in rats with experimental glaucoma." Invest Ophthalmol Vis Sci 45(6): 1854–1862.

Freddo, T. F., M. Civan and H. Gong (2021). Aqueous humor and the dynamics of its flow: mechanisms and routes of aqueous humor drainage. Albert and Jakobiec's Principles and Practice of Ophthalmology, Springer: 1–46.

Fukuroda, T., S. Ozaki, M. Ihara, K. Ishikawa, M. Yano and M. Nishikibe (1994). "Synergistic inhibition by BQ-123 and BQ-788 of endothelin-1-induced contractions of the rabbit pulmonary artery." Br J Pharmacol 113(2): 336–338.

Funk, R. and J. Rohen (1985). "Comparative morphological studies on blood vessels in eyes of normotensive and spontaneously hypertensive rats." Exp Eye Res 40(2): 191–203.

Funk, R., J. W. Rohen and K. Skolasinska (1985). "Intraocular pressure and systemic blood pressure after administration of vasoactive substances in hypertensive and normal rats." Graefes Arch Clin Exp Ophthalmol 223(3): 145–149.

Gangwani, R. A., J. Chan, J. Lee, A. Kwong and J. S. Lai (2013). "Detection of glaucoma in a cohort of chinese subjects with systemic hypertension." J Ophthalmol 2013: 463710.

Garcia-Valenzuela, E., S. Shareef, J. Walsh and S. C. Sharma (1995). "Programmed cell death of retinal ganglion cells during experimental glaucoma." Exp Eye Res 61(1): 33–44.

Garg, A. and G. Gazzard (2020). "Treatment choices for newly diagnosed primary open angle and ocular hypertension patients." Eye (Lond) 34(1): 60–71.

Gazzard, G., E. Konstantakopoulou, D. Garway-Heath, A. Garg, V. Vickerstaff, R. Hunter, G. Ambler, C. Bunce, R. Wormald, N. Nathwani, K. Barton, G. Rubin, M.

Buszewicz and G. H. T. T. S. G. Li (2019). "Selective laser trabeculoplasty versus eye drops for first-line treatment of ocular hypertension and glaucoma (LiGHT): a multicentre randomised controlled trial." Lancet 393(10180): 1505–1516.

Gensheimer, T., D. Veerman, E. M. van Oosten, L. Segerink, A. Garanto and A. D. van der Meer (2025). "Retina-on-chip: engineering functional in vitro models of the human retina using organ-on-chip technology." Lab Chip 25(5): 996–1014.

Gerstenblith, A. T. and M. P. Rabinowitz (2012). The wills eye manual: office and emergency room diagnosis and treatment of eye disease, Lippincott Williams & Wilkins.

Giaid, A., S. J. Gibson, M. T. Herrero, S. Gentleman, S. Legon, M. Yanagisawa, T. Masaki, N. B. Ibrahim, G. W. Roberts, M. L. Rossi and et al. (1991). "Topographical localisation of endothelin mRNA and peptide immunoreactivity in neurones of the human brain." Histochemistry 95(3): 303–314.

Giardina, J. B., G. M. Green, K. L. Cockrell, J. P. Granger and R. A. Khalil (2002). "TNF-alpha enhances contraction and inhibits endothelial NO-cGMP relaxation in systemic vessels of pregnant rats." Am J Physiol Regul Integr Comp Physiol 283(1): R130–143.

Gibbons, G. H., R. E. Pratt and V. J. Dzau (1992). "Vascular smooth muscle cell hypertrophy vs. hyperplasia. Autocrine transforming growth factor-beta 1 expression determines growth response to angiotensin II." J Clin Invest 90(2): 456–461.

Goddard, J., N. R. Johnston, M. F. Hand, A. D. Cumming, T. J. Rabelink, A. J. Rankin and D. J. Webb (2004). "Endothelin-A receptor antagonism reduces blood pressure and increases renal blood flow in hypertensive patients with chronic renal failure: a comparison of selective and combined endothelin receptor blockade." Circulation 109(9): 1186–1193.

Goldberg, I., F. C. Hollows, M. A. Kass and B. Becker (1981). "Systemic factors in patients with low-tension glaucoma." Br J Ophthalmol 65(1): 56–62.

Graham, S. L. and S. M. Drance (1999). "Nocturnal hypotension: role in glaucoma progression." Surv Ophthalmol 43 Suppl 1: S10–16.

Graham, S. L., S. M. Drance, K. Wijsman, G. R. Douglas and F. S. Mikelberg (1995). "Ambulatory blood pressure monitoring in glaucoma. The nocturnal dip." Ophthalmology 102(1): 61–69.

Gramlich, O. W., S. Beck, N. von Thun Und Hohenstein-Blaul, N. Boehm, A. Ziegler, J. M. Vetter, N. Pfeiffer and F. H. Grus (2013). "Enhanced insight into the autoimmune component of glaucoma: IgG autoantibody accumulation and pro-inflammatory conditions in human glaucomatous retina." PLoS One 8(2): e57557.

Griendling, K. K., D. Sorescu and M. Ushio-Fukai (2000). "NAD(P)H oxidase: role in cardiovascular biology and disease." Circ Res 86(5): 494–501.

Grunwald, J. E., J. Piltz, S. M. Hariprasad, J. Dupont and M. G. Maguire (1999). "Optic nerve blood flow in glaucoma: effect of systemic hypertension." Am J Ophthalmol 127(5): 516–522.

Guo, L., S. E. Moss, R. A. Alexander, R. R. Ali, F. W. Fitzke and M. F. Cordeiro (2005). "Retinal ganglion cell apoptosis in glaucoma is related to intraocular pressure and IOP-induced effects on extracellular matrix." Invest Ophthalmol Vis Sci 46(1): 175–182.

Guzik, T. J., N. E. Hoch, K. A. Brown, L. A. McCann, A. Rahman, S. Dikalov, J. Goronzy, C. Weyand and D. G. Harrison (2007). "Role of the T cell in the genesis of angiotensin II induced hypertension and vascular dysfunction." J Exp Med 204(10): 2449–2460.

Haga, C., T. Waller, A. S. Ahuja, B. Farford, N. Dawson and M. Yin (2022). "There's Danger in the Drops: Systemic Effects of Ophthalmic Drops Used to Treat Glaucoma." Cureus 14(1): e20945.

Hall, J. E., J. P. Granger, J. M. do Carmo, A. A. da Silva, J. Dubinion, E. George, S. Hamza, J. Speed and M. E. Hall (2012). "Hypertension: physiology and pathophysiology." Compr Physiol 2(4): 2393–2442.

Hall, J. E., A. C. Guyton, T. G. Coleman, H. L. Mizelle and L. L. Woods (1986). "Regulation of arterial pressure: role of pressure natriuresis and diuresis." Fed Proc 45(13): 2897–2903.

Hall, J. E., A. C. M. Omoto, Z. Wang, A. Mouton, X. Li and M. E. Hall (2024). 5 - Pathophysiology of Hypertension. Hypertension (Fourth Edition). G. L. Bakris, M. J. Sorrentino and L. J. Laffin. New Delhi, Elsevier: 71–86.

Haque, M. S., I. H. Pang, P. E. Magnino and L. DeSantis (1998). "Activation of phospholipase C and guanylyl cyclase by endothelins in human trabecular meshwork cells." Curr Eye Res 17(12): 1110–1117.

Haque, M. S., T. Taniguchi, K. Sugiyama, K. Okada and Y. Kitazawa (1995). "The ocular hypotensive effect of the ETB receptor selective agonist, sarafotoxin S6c, in rabbits." Invest Ophthalmol Vis Sci 36(5): 804–808.

Harazny, J. M., M. Ritt, D. Baleanu, C. Ott, J. Heckmann, M. P. Schlaich, G. Michelson and R. E. Schmieder (2007). "Increased wall: lumen ratio of retinal arterioles in male patients with a history of a cerebrovascular event." Hypertension 50(4): 623–629.

He, Z., A. J. Vingrys, J. A. Armitage, C. T. Nguyen and B. V. Bui (2014). "Chronic hypertension increases susceptibility to acute IOP challenge in rats." Invest Ophthalmol Vis Sci 55(12): 7888–7895.

Holappa, M., H. Vapaatalo and A. Vaajanen (2017). "Many Faces of Renin-angiotensin System - Focus on Eye." Open Ophthalmol J 11: 122–142.

Hollo, G., P. Kothy, P. Lakatos and P. Vargha (2002). "Endothelin-A receptor antagonist BQ-485 protects against intraocular pressure spike induced by laser trabeculoplasty in the rabbit." Ophthalmologica 216(6): 459–462.

Hopps, E., R. Lo Presti and G. Caimi (2017). "Matrix Metalloproteases in Arterial Hypertension and their Trend after Antihypertensive Treatment." Kidney Blood Press Res 42(2): 347–357.

Howell, G. R., D. G. Macalinao, G. L. Sousa, M. Walden, I. Soto, S. C. Kneeland, J. M. Barbay, B. L. King, J. K. Marchant, M. Hibbs, B. Stevens, B. A. Barres, A. F. Clark, R. T. Libby and S. W. John (2011). "Molecular clustering identifies complement and endothelin induction as early events in a mouse model of glaucoma." J Clin Invest 121(4): 1429–1444.

Howell, G. R., I. Soto, X. Zhu, M. Ryan, D. G. Macalinao, G. L. Sousa, L. B. Caddle, K. H. MacNicoll, J. M. Barbay, V. Porciatti, M. G. Anderson, R. S. Smith, A. F. Clark, R. T. Libby and S. W. M. John (2012). "Radiation treatment inhibits monocyte entry into the optic nerve head and prevents neuronal damage in a mouse model of glaucoma." J Clin Invest 122(4): 1246–1261.

Hu, H., W. Lu, M. Zhang, X. Zhang, A. J. Argall, S. Patel, G. E. Lee, Y. C. Kim, K. A. Jacobson, A. M. Laties and C. H. Mitchell (2010). "Stimulation of the P2X7 receptor kills rat retinal ganglion cells in vivo." Exp Eye Res 91(3): 425–432.

Hyman, L., A. P. Schachat, Q. He and M. C. Leske (2000). "Hypertension, cardiovascular disease, and age-related macular degeneration. Age-Related Macular Degeneration Risk Factors Study Group." Arch Ophthalmol 118(3): 351–358.

Iannucci, V., P. Manni, L. Alisi, G. Mecarelli, A. Lambiase and A. Bruscolini (2023). "Bilateral Angle Recession and Chronic Post-Traumatic Glaucoma: A Review of the Literature and a Case Report." Life (Basel) 13(9).

Ikram, M. K., J. C. Witteman, J. R. Vingerling, M. M. Breteler, A. Hofman and P. T. de Jong (2006). "Retinal vessel diameters and risk of hypertension: the Rotterdam Study." Hypertension 47(2): 189–194.

Intengan, H. D. and E. L. Schiffrin (2000). "Structure and mechanical properties of resistance arteries in hypertension: role of adhesion molecules and extracellular matrix determinants." Hypertension 36(3): 312–318.

Iturriaga, R., J. Alcayaga, M. W. Chapleau and V. K. Somers (2021). "Carotid body chemoreceptors: physiology, pathology, and implications for health and disease." Physiol Rev 101(3): 1177–1235.

Iwabe, S., M. Lamas, C. G. Vasquez Pelaez and F. G. Carrasco (2010). "Aqueous humor endothelin-1 (Et-1), vascular endothelial growth factor (VEGF) and cyclooxygenase-2 (COX-2) levels in Mexican glaucomatous patients." Curr Eye Res 35(4): 287–294.

Jassim, A. H., D. M. Inman and C. H. Mitchell (2021). "Crosstalk Between Dysfunctional Mitochondria and Inflammation in Glaucomatous Neurodegeneration."

Front Pharmacol 12: 699623.

Jethva, J., P. Bhagat, K. Prajapati and G. Tank (2022). "Safety, efficacy, and patient selection of ripasudil in patients with uncontrolled glaucoma with maximum conventional medical therapy." Indian J Ophthalmol 70(6): 2020–2023.

Jin, S. W., H. R. Seo, S. S. Rho and S. H. Rho (2017). "The Effects of Nocturnal Dip and Blood Pressure Variability on Paracentral Scotoma in Early Open-Angle Glaucoma." Semin Ophthalmol 32(4): 504–510.

Johnson, T. V., N. D. Bull and K. R. Martin (2011). "Neurotrophic factor delivery as a protective treatment for glaucoma." Exp Eye Res 93(2): 196–203.

Jonas, J. B., A. M. Schmidt, J. A. Muller-Bergh, U. M. Schlotzer-Schrehardt and G. O. Naumann (1992). "Human optic nerve fiber count and optic disc size." Invest Ophthalmol Vis Sci 33(6): 2012–2018.

Ju, W. K., K. Y. Kim, J. D. Lindsey, M. Angert, K. X. Duong-Polk, R. T. Scott, J. J. Kim, I. Kukhmazov, M. H. Ellisman, G. A. Perkins and R. N. Weinreb (2008). "Intraocular pressure elevation induces mitochondrial fission and triggers OPA1 release in glaucomatous optic nerve." Invest Ophthalmol Vis Sci 49(11): 4903–4911.

Ju, W. K., Q. Liu, K. Y. Kim, J. G. Crowston, J. D. Lindsey, N. Agarwal, M. H. Ellisman, G. A. Perkins and R. N. Weinreb (2007). "Elevated hydrostatic pressure triggers mitochondrial fission and decreases cellular ATP in differentiated RGC-5 cells." Invest Ophthalmol Vis Sci 48(5): 2145–2151.

Kahler, J., S. Mendel, J. Weckmuller, H. D. Orzechowski, C. Mittmann, R. Koster, M. Paul, T. Meinertz and T. Munzel (2000). "Oxidative stress increases synthesis of big endothelin-1 by activation of the endothelin-1 promoter." J Mol Cell Cardiol 32(8): 1429–1437.

Kaiser, H. J., J. Flammer, T. Graf and D. Stumpfig (1993). "Systemic blood pressure in glaucoma patients." Graefes Arch Clin Exp Ophthalmol 231(12): 677–680.

Kamikawatoko, S., T. Tokoro, H. Azuma, H. Hamasaki and A. Ishida (1995). "The effects of endothelin-1 on isolated bovine ciliary muscles." Exp Eye Res 61(5): 559–564.

Kandzari, D. E., M. Bohm, F. Mahfoud, R. R. Townsend, M. A. Weber, S. Pocock, K. Tsioufis, D. Tousoulis, J. W. Choi, C. East, S. Brar, S. A. Cohen, M. Fahy, G. Pilcher, K. Kario and S. H.-O. M. T. Investigators (2018). "Effect of renal denervation on blood pressure in the presence of antihypertensive drugs: 6-month efficacy and safety results from the SPYRAL HTN-ON MED proof-of-concept randomised trial." Lancet 391(10137): 2346–2355.

Kapetanakis, V. V., M. P. Chan, P. J. Foster, D. G. Cook, C. G. Owen and A. R. Rudnicka (2016). "Global variations and time trends in the prevalence of primary open angle glaucoma (POAG): a systematic review and meta-analysis." Br J Ophthalmol 100(1): 86–93.

Kashiwagi, K., O. Hosaka, F. Kashiwagi, K. Taguchi, J. Mochizuki, H. Ishii, H. Ijiri, K. Tamura and S. Tsukahara (2001). "Systemic circulatory parameters. comparison between patients with normal tension glaucoma and normal subjects using ambulatory monitoring." Jpn J Ophthalmol 45(4): 388–396.

Kashyap, M. K., V. Yadav, B. S. Sherawat, S. Jain, S. Kumari, M. Khullar, P. C. Sharma and R. Nath (2005). "Different antioxidants status, total antioxidant power and free radicals in essential hypertension." Mol Cell Biochem 277(1-2): 89–99.

Kelly, D. J. and S. M. Farrell (2018). "Physiology and Role of Intraocular Pressure in Contemporary Anesthesia." Anesth Analg 126(5): 1551–1562.

Kels, B. D., A. Grzybowski and J. M. Grant-Kels (2015). "Human ocular anatomy." Clin Dermatol 33(2): 140–146.

Kermer, P., N. Klocker, M. Labes and M. Bahr (1998). "Inhibition of CPP32-like proteases rescues axotomized retinal ganglion cells from secondary cell death in vivo." J Neurosci 18(12): 4656–4662.

Kerrigan, L. A., D. J. Zack, H. A. Quigley, S. D. Smith and M. E. Pease (1997). "TUNEL-positive ganglion cells in human primary open-angle glaucoma." Arch Ophthalmol 115(8): 1031–1035.

Kiel, J. W., M. Hollingsworth, R. Rao, M. Chen and H. A. Reitsamer (2011). "Ciliary blood flow and aqueous humor production." Prog Retin Eye Res 30(1): 1–17.

Kim, J., D. Y. Park, H. Bae, D. Y. Park, D. Kim, C. K. Lee, S. Song, T. Y. Chung, D. H. Lim, Y. Kubota, Y. K. Hong, Y. He, H. G. Augustin, G. Oliver and G. Y. Koh (2017). "Impaired angiopoietin/Tie2 signaling compromises Schlemm's canal integrity and induces glaucoma." J Clin Invest 127(10): 3877–3896.

Kim, K. E., S. Oh, S. U. Baek, S. J. Ahn, K. H. Park and J. W. Jeoung (2020). "Ocular Perfusion Pressure and the Risk of Open-Angle Glaucoma: Systematic Review and Meta-analysis." Sci Rep 10(1): 10056.

Kinlay, S., M. A. Creager, M. Fukumoto, H. Hikita, J. C. Fang, A. P. Selwyn and P. Ganz (2001). "Endothelium-derived nitric oxide regulates arterial elasticity in human arteries in vivo." Hypertension 38(5): 1049–1053.

Kong, M., Y. Kwun, J. Sung, D. I. Ham and Y. M. Song (2015). "Association Between Systemic Hypertension and Macular Thickness Measured by Optical Coherence Tomography." Invest Ophthalmol Vis Sci 56(4): 2144–2150.

Korbmacher, C., H. Helbig, H. Haller, K. A. Erickson-Lamy and M. Wiederholt (1989). "Endothelin depolarizes membrane voltage and increases intracellular calcium concentration in human ciliary muscle cells." Biochem Biophys Res Commun 164(3): 1031–1039.

Kouassi Nzoughet, J., J. M. Chao de la Barca, K. Guehlouz, S. Leruez, L. Coulbault, S. Allouche, C. Bocca, J. Muller, P. Amati-Bonneau, P. Gohier, D. Bonneau, G. Simard, D. Milea, G. Lenaers, V. Procaccio and P. Reynier (2019). "Nicotinamide Deficiency in Primary Open-Angle Glaucoma." Invest Ophthalmol Vis Sci 60(7): 2509–2514.

Krupin, T., S. Orgül, G. A. Cioffi, D. R. Bacon and E. M. Van Buskirk (1996). "An Endothelin-1-Induced Model of Chronic Optic Nerve Ischemia in Rhesus Monkeys." J Glaucoma 5(2): 135–138.

Kuehn, M. H., C. Y. Kim, J. Ostojic, M. Bellin, W. L. Alward, E. M. Stone, D. S. Sakaguchi, S. D. Grozdanic and Y. H. Kwon (2006). "Retinal synthesis and deposition of complement components induced by ocular hypertension." Exp Eye Res 83(3): 620–628.

Kurihara, H., Y. Kurihara and Y. Yazaki (2001). Lessons from Gene Deletion of Endothelin Systems. Endothelin and Its Inhibitors. T. D. Warner. Berlin, Heidelberg, Springer Berlin Heidelberg: 141–154.

Kuroda, Y., A. Uji and N. Yoshimura (2016). "Factors associated with optic nerve head blood flow and color tone: a retrospective observational study." Graefes Arch Clin Exp Ophthalmol 254(5): 963–970.

Lakshmanan, Y., F. S. Y. Wong and H. H. Chan (2023). "Long-Term Effects on Retinal Structure and Function in a Mouse Endothelin-1 Model of Retinal Ganglion Cell Degeneration." Invest Ophthalmol Vis Sci 64(11): 15.

LaMarca, B. B., K. Cockrell, E. Sullivan, W. Bennett and J. P. Granger (2005). "Role of endothelin in mediating tumor necrosis factor-induced hypertension in pregnant rats." Hypertension 46(1): 82–86.

Lambert, W. S., B. J. Carlson, C. R. Formichella, R. M. Sappington, C. Ahlem and D. J. Calkins (2017). "Oral Delivery of a Synthetic Sterol Reduces Axonopathy and Inflammation in a Rodent Model of Glaucoma." Front Neurosci 11: 45.

Lee, D. L., L. C. Sturgis, H. Labazi, J. B. Osborne, Jr., C. Fleming, J. S. Pollock, M. Manhiani, J. D. Imig and M. W. Brands (2006). "Angiotensin II hypertension is attenuated in interleukin-6 knockout mice." Am J Physiol Heart Circ Physiol 290(3): H935–940.

Lee, J., J. Choi, D. Jeong, S. Kim and M. S. Kook (2015). "Relationship between daytime variability of blood pressure or ocular perfusion pressure and glaucomatous visual field progression." Am J Ophthalmol 160(3): 522–537 e521.

Lee, K., H. Yang, J. Y. Kim, G. J. Seong, C. Y. Kim and H. W. Bae (2020). "Risk Factors Associated with Structural Progression in Normal-Tension Glaucoma: Intraocular Pressure, Systemic Blood Pressure, and Myopia." Invest Ophthalmol Vis Sci 61(8): 35.

Lee, N. Y., Y. Jung, K. Han and C. K. Park (2017). "Fluctuation in systolic blood pressure is a major systemic risk factor for development of primary open-angle glaucoma." Sci Rep 7: 43734.

Lee, N. Y., H. Y. Park, C. K. Park and M. D. Ahn (2012). "Analysis of systemic endothelin-1, matrix metalloproteinase-9, macrophage chemoattractant protein-1, and high-sensitivity C-reactive protein in normal-tension glaucoma." Curr Eye Res 37(12): 1121–1126.

Lee, P. Y., D. Zhao, V. H. Y. Wong, V. Chrysostomou, J. G. Crowston and B. V. Bui (2022). "The Effect of Aging on Retinal Function and Retinal Ganglion Cell Morphology Following Intraocular Pressure Elevation." Front Aging Neurosci 14: 859265.

Lee, S., L. Sheck, J. G. Crowston, N. J. Van Bergen, E. C. O'Neill, F. O'Hare, Y. X. Kong, V. Chrysostomou, A. L. Vincent and I. A. Trounce (2012). "Impaired complex-I-linked respiration and ATP synthesis in primary open-angle glaucoma patient lymphoblasts." Invest Ophthalmol Vis Sci 53(4): 2431–2437.

Lepple-Wienhues, A., F. Stahl and M. Wiederholt (1991). "Differential smooth muscle-like contractile properties of trabecular meshwork and ciliary muscle." Exp Eye Res 53(1): 33–38.

Leske, M. C., S. Y. Wu, B. Nemesure and A. Hennis (2002). "Incident open-angle glaucoma and blood pressure." Arch Ophthalmol 120(7): 954–959.

Leskova, W., R. Warar and N. R. Harris (2020). "Altered Retinal Hemodynamics and Mean Circulation Time in Spontaneously Hypertensive Rats." Invest Ophthalmol Vis Sci 61(10): 12.

Levkovitch-Verbin, H. (2015). "Retinal ganglion cell apoptotic pathway in glaucoma: Initiating and downstream mechanisms." Prog Brain Res 220: 37–57.

Li, K. L., S. W. Shan, F. Y. Lin, C. Y. Ling, N. W. Wong, H. L. Li, W. Han, C. H. To and C. W. Do (2023). "Regulation of Aqueous Humor Secretion by Melatonin in Porcine Ciliary Epithelium." Int J Mol Sci 24(6).

Li, L., G. D. Fink, S. W. Watts, C. A. Northcott, J. J. Galligan, P. J. Pagano and A. F. Chen (2003). "Endothelin-1 increases vascular superoxide via endothelin(A)-NADPH oxidase pathway in low-renin hypertension." Circulation 107(7): 1053–1058.

Li, S., A. Zhang, W. Cao and X. Sun (2016). "Elevated Plasma Endothelin-1 Levels in

Normal Tension Glaucoma and Primary Open-Angle Glaucoma: A Meta-Analysis." J Ophthalmol 2016: 2678017.

Li, Y., Q. Wang, E. R. Muir, J. W. Kiel and T. Q. Duong (2020). "Retinal Vascular and Anatomical Features in the Spontaneously Hypertensive Rat." Curr Eye Res 45(11): 1422–1429.

Liddelow, S. A., K. A. Guttenplan, L. E. Clarke, F. C. Bennett, C. J. Bohlen, L. Schirmer, M. L. Bennett, A. E. Munch, W. S. Chung, T. C. Peterson, D. K. Wilton, A. Frouin, B. A. Napier, N. Panicker, M. Kumar, M. S. Buckwalter, D. H. Rowitch, V. L. Dawson, T. M. Dawson, B. Stevens and B. A. Barres (2017). "Neurotoxic reactive astrocytes are induced by activated microglia." Nature 541(7638): 481–487.

Liefeldt, L., B. Rylski, F. Walcher, J. Manhart, S. Kron, Y.-W. Rosenke, M. Paul, H.-H. Neumayer, K. Amann and H. Peters (2010). "Effects of transgenic endothelin-2 overexpression on diabetic cardiomyopathy in rats." Eur J Clin Invest 40(3): 203–210.

Lightman, S., E. Rechthand, C. Latker, A. Palestine and S. Rapoport (1987). "Assessment of the permeability of the blood-retinal barrier in hypertensive rats." Hypertension 10(4): 390–395.

Lim, H. B., M. W. Lee, J. H. Park, K. Kim, Y. J. Jo and J. Y. Kim (2019). "Changes in ganglion cell-Inner plexiform layer thickness and retinal microvasculature in hypertension: an optical coherence tomography angiography study." Am J Ophthalmol 199: 167–176.

Ling, L., J. J. Maguire and A. P. Davenport (2013). "Endothelin-2, the forgotten isoform: emerging role in the cardiovascular system, ovarian development, immunology and cancer." Br J Pharmacol 168(2): 283–295.

Luo, C., X. Yang, A. D. Kain, D. W. Powell, M. H. Kuehn and G. Tezel (2010). "Glaucomatous tissue stress and the regulation of immune response through glial Toll-like receptor signaling." Invest Ophthalmol Vis Sci 51(11): 5697–5707.

Luo, Z., M. Li, M. Ye, P. Ji, X. Lou, J. Huang, K. Yao, Y. Zhao and H. Zhang (2020). "Effect of electrical stimulation of cervical sympathetic ganglia on intraocular pressure regulation according to different circadian rhythms in rats." Invest

Ophthalmol Vis Sci 61(11): 40.

Lusthaus, J. and I. Goldberg (2019). "Current management of glaucoma." Med J Aust 210(4): 180–187.

Mac Nair, C. E., K. A. Fernandes, C. L. Schlamp, R. T. Libby and R. W. Nickells (2014). "Tumor necrosis factor alpha has an early protective effect on retinal ganglion cells after optic nerve crush." J Neuroinflammation 11: 194.

Maday, S., A. E. Twelvetrees, A. J. Moughamian and E. L. Holzbaur (2014). "Axonal transport: cargo-specific mechanisms of motility and regulation." Neuron 84(2): 292–309.

Maddineni, P., R. B. Kasetti, P. D. Patel, J. C. Millar, C. Kiehlbauch, A. F. Clark and G. S. Zode (2020). "CNS axonal degeneration and transport deficits at the optic nerve head precede structural and functional loss of retinal ganglion cells in a mouse model of glaucoma." Mol Neurodegener 15(1): 48.

Mahaling, B., S. W. Y. Low, M. Beck, D. Kumar, S. Ahmed, T. B. Connor, B. Ahmad and S. S. Chaurasia (2022). "Damage-Associated Molecular Patterns (DAMPs) in Retinal Disorders." Int J Mol Sci 23(5).

Mahmud, A. and J. Feely (2005). "Arterial stiffness is related to systemic inflammation in essential hypertension." Hypertension 46(5): 1118–1122.

Marola, O. J., G. R. Howell and R. T. Libby (2022). "Vascular derived endothelin receptor A controls endothelin-induced retinal ganglion cell death." Cell Death Discov 8(1): 207.

Matsuda, S., S. Umemoto, K. Yoshimura, S. Itoh, T. Murata, T. Fukai and M. Matsuzaki (2015). "Angiotensin II Activates MCP-1 and Induces Cardiac Hypertrophy and Dysfunction via Toll-like Receptor 4." J Atheroscler Thromb 22(8): 833–844.

Matsumoto, S., T. Yorio, P. E. Magnino, L. DeSantis and I. H. Pang (1996). "Endothelin-induced changes of second messengers in cultured human ciliary muscle cells." Invest Ophthalmol Vis Sci 37(6): 1058–1066.

McGrady, N. R., A. Z. Minton, D. L. Stankowska, S. He, H. B. Jefferies and R. R.

Krishnamoorthy (2017). "Upregulation of the endothelin A (ET(A)) receptor and its association with neurodegeneration in a rodent model of glaucoma." BMC Neurosci 18(1): 27.

Meyer, J. H., J. Brandi-Dohrn and J. Funk (1996). "Twenty four hour blood pressure monitoring in normal tension glaucoma." Br J Ophthalmol 80(10): 864–867.

Mi, X. S., X. Zhang, Q. Feng, A. C. Lo, S. K. Chung and K. F. So (2012). "Progressive retinal degeneration in transgenic mice with overexpression of endothelin-1 in vascular endothelial cells." Invest Ophthalmol Vis Sci 53(8): 4842–4851.

Mills, K. T., J. D. Bundy, T. N. Kelly, J. E. Reed, P. M. Kearney, K. Reynolds, J. Chen and J. He (2016). "Global Disparities of Hypertension Prevalence and Control: A Systematic Analysis of Population-Based Studies From 90 Countries." Circulation 134(6): 441–450.

Mills, K. T., A. Stefanescu and J. He (2020). "The global epidemiology of hypertension." Nat Rev Nephrol 16(4): 223–237.

Minton, A. Z., N. R. Phatak, D. L. Stankowska, S. He, H. Y. Ma, B. H. Mueller, M. Jiang, R. Luedtke, S. Yang, C. Brownlee and R. R. Krishnamoorthy (2012). "Endothelin B receptors contribute to retinal ganglion cell loss in a rat model of glaucoma." PLoS One 7(8): e43199.

Mirzaei, M., V. K. Gupta, N. Chitranshi, L. Deng, K. Pushpitha, M. Abbasi, J. M. Chick, R. Rajput, Y. Wu, M. J. McKay, G. H. Salekdeh, V. B. Gupta, P. A. Haynes and S. L. Graham (2020). "Retinal proteomics of experimental glaucoma model reveal intraocular pressure-induced mediators of neurodegenerative changes." J Cell Biochem 121(12): 4931–4944.

Mitchell, P., A. J. Lee, E. Rochtchina and J. J. Wang (2004). "Open-angle glaucoma and systemic hypertension: the blue mountains eye study." J Glaucoma 13(4): 319–326.

Mitchell, P., H. Leung, J. J. Wang, E. Rochtchina, A. J. Lee, T. Y. Wong and R. Klein (2005). "Retinal vessel diameter and open-angle glaucoma: the Blue Mountains Eye

Study." Ophthalmology 112(2): 245–250.

Miyazaki, M., K. Segawa and Y. Urakawa (1987). "Age-related changes in the trabecular meshwork of the normal human eye." Jpn J Ophthalmol 31(4): 558–569.

Momose, N., K. Fukuo, S. Morimoto and T. Ogihara (1993). "Captopril inhibits endothelin-1 secretion from endothelial cells through bradykinin." Hypertension 21(6 Pt 2): 921–924.

Moreau, P., L. V. d'Uscio, S. Shaw, H. Takase, M. Barton and T. F. Luscher (1997). "Angiotensin II increases tissue endothelin and induces vascular hypertrophy: reversal by ET(A)-receptor antagonist." Circulation 96(5): 1593–1597.

Muzyka, M., M. H. Nizankowska, M. Koziorowska and H. Zajac-Pytrus (1997). "[Occurrence of nocturnal arterial hypotension in patients with primary open-angle glaucoma and normal tension glaucoma]." Klin Oczna 99(2): 109–113.

Mylona, I., M. Dermenoudi, N. Ziakas and I. Tsinopoulos (2019). "Hypertension is the Prominent Risk Factor in Cataract Patients." Medicina (Kaunas) 55(8).

Nagano, H., P. Z. Wei, C. Q. Wen, T. Jomori, H. Oku, T. Ikeda, Y. Saito and Y. Tano (2007). "Effects of kallidinogenase on ischemic changes induced by repeated intravitreal injections of endothelin-1 in rabbit retina." Curr Eye Res 32(2): 113–122.

Nakas-Icindic, E., A. Zaciragic, A. Hadzovic and N. Avdagic (2004). "Endothelin in health and disease." Bosn J Basic Med Sci 4(3): 31–34.

Nemesure, B., R. Honkanen, A. Hennis, S. Y. Wu, M. C. Leske and G. Barbados Eye Studies (2007). "Incident open-angle glaucoma and intraocular pressure." Ophthalmology 114(10): 1810–1815.

Neufeld, A. H., M. R. Hernandez and M. Gonzalez (1997). "Nitric oxide synthase in the human glaucomatous optic nerve head." Arch Ophthalmol 115(4): 497–503.

Nixon, P. J., B. V. Bui, J. A. Armitage and A. J. Vingrys (2001). "The contribution of cone responses to rat electroretinograms." Clin Exp Ophthalmol 29(3): 193–196.

O'Brien, C. and Z. Butt (1999). "Blood flow velocity in the peripheral circulation of glaucoma patients." Ophthalmologica 213(3): 150–153.

Okamoto, K. (1974). "Establishment of the stroke-prone spontaneously hypertensive

rat (SHR)." Circ Res 34: " I–143"–" I–153".

Okamoto, K. and K. Aoki (1963). "Development of a strain of spontaneously hypertensive rats." Jpn Circ J 27: 282–293.

Oku, H., T. Sugiyama, S. Kojima, T. Watanabe and I. Azuma (1999). "Experimental optic cup enlargement caused by endothelin-1-induced chronic optic nerve head ischemia." Surv Ophthalmol 44 Suppl 1: S74–84.

Oku, H., T. Sugiyama, S. Kojima, T. Watanabe and T. Ikeda (2000). "Improving effects of topical administration of iganidipine, a new calcium channel blocker, on the impaired visual evoked potential after endothelin-1 injection into the vitreous body of rabbits." Curr Eye Res 20(2): 101–108.

Okumura, Y., K. Yuki and K. Tsubota (2012). "Low diastolic blood pressure is associated with the progression of normal-tension glaucoma." Ophthalmologica 228(1): 36–41.

Oliveira, M. B., J. P. C. Vasconcellos, V. P. Costa and M. B. Melo (2014). "Inflammatory Cytokines in Aqueous Humor and Plasma are associated with Primary Open angle Glaucoma in a Brazilian population." Invest Ophthalmol Vis Sci 55(13): 5711–5711.

Ong, K., A. Farinelli, F. Billson, M. Houang and M. Stern (1995). "Comparative study of brain magnetic resonance imaging findings in patients with low-tension glaucoma and control subjects." Ophthalmology 102(11): 1632–1638.

Orgül, S., G. A. Cioffi, D. J. Wilson, D. R. Bacon and E. M. Van Buskirk (1996). "An endothelin-1 induced model of optic nerve ischemia in the rabbit." Invest Ophthalmol Vis Sci 37(9): 1860–1869.

Orzalesi, N., L. Rossetti, S. Omboni, O. S. Group and Conproso (2007). "Vascular risk factors in glaucoma: the results of a national survey." Graefes Arch Clin Exp Ophthalmol 245(6): 795–802.

Pagano, L., J. W. Lee, M. Posarelli, G. Giannaccare, S. Kaye and A. Borgia (2023). "ROCK Inhibitors in Corneal Diseases and Glaucoma-A Comprehensive Review of These Emerging Drugs." J Clin Med 12(21).

Panza, J. A., P. R. Casino, C. M. Kilcoyne and A. A. Quyyumi (1993). "Role of endothelium-derived nitric oxide in the abnormal endothelium-dependent vascular relaxation of patients with essential hypertension." Circulation 87(5): 1468–1474.

Patel, R., J. D. Cardneau, S. M. Colles and L. M. Graham (2006). "Synthetic smooth muscle cell phenotype is associated with increased nicotinamide adenine dinucleotide phosphate oxidase activity: effect on collagen secretion." J Vasc Surg 43(2): 364–371.

Pease, M. E., S. J. McKinnon, H. A. Quigley, L. A. Kerrigan-Baumrind and D. J. Zack (2000). "Obstructed axonal transport of BDNF and its receptor TrkB in experimental glaucoma." Invest Ophthalmol Vis Sci 41(3): 764–774.

Pekny, M. and M. Nilsson (2005). "Astrocyte activation and reactive gliosis." Glia 50(4): 427–434.

Peräsalo, R. and C. Raitta (1990). "Low blood pressure—a risk factor for nerve fibre loss in institionalized geriatric glaucoma patients." Acta Ophthalmol 68(S195): 65–67.

Perkovic, V., R. Huxley, Y. Wu, D. Prabhakaran and S. MacMahon (2007). "The burden of blood pressure-related disease: a neglected priority for global health." Hypertension 50(6): 991–997.

Perret, R. S. and G. D. Sloop (2000). "Increased peak blood velocity in association with elevated blood pressure." Ultrasound Med Biol 26(9): 1387–1391.

Pillunat, L. E., R. Stodtmeister, R. Marquardt and A. Mattern (1989). "Ocular perfusion pressures in different types of glaucoma." Int Ophthalmol 13(1-2): 37–42.

Plange, N., M. Kaup, L. Daneljan, H. G. Predel, A. Remky and O. Arend (2006). "24-h blood pressure monitoring in normal tension glaucoma: night-time blood pressure variability." J Hum Hypertens 20(2): 137–142.

Prasanna, G., R. Krishnamoorthy, A. F. Clark, R. J. Wordinger and T. Yorio (2002). "Human optic nerve head astrocytes as a target for endothelin-1." Invest Ophthalmol Vis Sci 43(8): 2704–2713.

Quigley, H. A., R. W. Nickells, L. A. Kerrigan, M. E. Pease, D. J. Thibault and D. J. Zack (1995). "Retinal ganglion cell death in experimental glaucoma and after axotomy occurs by apoptosis." Invest Ophthalmol Vis Sci 36(5): 774–786.

Quintero, H., Y. Shiga, N. Belforte, L. Alarcon-Martinez, S. El Hajji, D. Villafranca-Baughman, F. Dotigny and A. Di Polo (2022). "Restoration of mitochondria axonal transport by adaptor Disc1 supplementation prevents neurodegeneration and rescues visual function." Cell Rep 40(11): 111324.

Ramdas, W. D., R. C. Wolfs, A. Hofman, P. T. de Jong, J. R. Vingerling and N. M. Jansonius (2011). "Ocular perfusion pressure and the incidence of glaucoma: real effect or artifact? The Rotterdam Study." Invest Ophthalmol Vis Sci 52(9): 6875–6881.

Razeghinejad, M. R., S. J. Fudemberg and G. L. Spaeth (2012). "The changing conceptual basis of trabeculectomy: a review of past and current surgical techniques." Surv Ophthalmol 57(1): 1–25.

Resch, H., G. Garhofer, G. Fuchsjager-Mayrl, A. Hommer and L. Schmetterer (2009). "Endothelial dysfunction in glaucoma." Acta Ophthalmol 87(1): 4–12.

Ribeiro, M. O., E. Antunes, G. de Nucci, S. M. Lovisolo and R. Zatz (1992). "Chronic inhibition of nitric oxide synthesis. A new model of arterial hypertension." Hypertension 20(3): 298–303.

Richler, M., E. B. Werner and D. Thomas (1982). "Risk factors for progression of visual field defects in medically treated patients with glaucoma." Can J Ophthalmol 17(6): 245–248.

Rojas, B., B. I. Gallego, A. I. Ramírez, J. J. Salazar, R. de Hoz, F. J. Valiente-Soriano, M. Avilés-Trigueros, M. P. Villegas-Perez, M. Vidal-Sanz and A. Triviño (2014). "Microglia in mouse retina contralateral to experimental glaucoma exhibit multiple signs of activation in all retinal layers." J Neuroinflammation 11: 1–24.

Rosello-Lleti, E., F. G. de Burgos, P. Morillas, R. Cortes, L. Martinez-Dolz, L. Almenar, L. Grigorian, P. Orosa, M. Portoles, V. Bertomeu and M. Rivera (2012). "Impact of cardiovascular risk factors and inflammatory status on urinary 8-OHdG in essential hypertension." Am J Hypertens 25(2): 236–242.

Sabbatini, M., P. Strocchi, L. Vitaioli and F. Amenta (2001). "Changes of retinal neurons and glial fibrillary acid protein immunoreactive astrocytes in spontaneously

hypertensive rats." J Hypertens 19(10): 1861–1869.

Sahin, O. Z., S. B. Sahin, T. Ayaz, Z. Karadag, K. Turkyilmaz, E. Aktas and M. Bostan (2015). "The impact of hypertension on retinal nerve fiber layer thickness and its association with carotid intima media thickness." Blood Press 24(3): 178–184.

Sappington, R. M., M. Chan and D. J. Calkins (2006). "Interleukin-6 protects retinal ganglion cells from pressure-induced death." Invest Ophthalmol Vis Sci 47(7): 2932–2942.

Sappington, R. M., T. Sidorova, D. J. Long and D. J. Calkins (2009). "TRPV1: contribution to retinal ganglion cell apoptosis and increased intracellular Ca2+ with exposure to hydrostatic pressure." Invest Ophthalmol Vis Sci 50(2): 717–728.

Schiffrin, E. L. (2005). "Vascular endothelin in hypertension." Vascul Pharmacol 43(1): 19–29.

Sedeek, M. H., M. T. Llinas, H. Drummond, L. Fortepiani, S. R. Abram, B. T. Alexander, J. F. Reckelhoff and J. P. Granger (2003). "Role of reactive oxygen species in endothelin-induced hypertension." Hypertension 42(4): 806–810.

Sharma, P., A. Hingorani, H. Jia, R. Hopper and M. J. Brown (1999). "Quantitative association between a newly identified molecular variant in the endothelin-2 gene and human essential hypertension." J Hypertens 17(9): 1281–1287.

Sheng, Z. H. and Q. Cai (2012). "Mitochondrial transport in neurons: impact on synaptic homeostasis and neurodegeneration." Nat Rev Neurosci 13(2): 77–93.

Shestopalov, V. I., M. Spurlock, O. W. Gramlich and M. H. Kuehn (2021). "Immune Responses in the Glaucomatous Retina: Regulation and Dynamics." Cells 10(8).

Shi, J. M. and S. B. Jia (2012). "Selective laser trabeculoplasty." Int J Ophthalmol 5(6): 742–749.

Shichiri, M., Y. Hirata, K. Ando, T. Emori, K. Ohta, S. Kimoto, M. Ogura, A. Inoue and F. Marumo (1990). "Plasma endothelin levels in hypertension and chronic renal failure." Hypertension 15(5): 493–496.

Shin, J. W., Y. H. Jo, M. K. Song, H. J. Won and M. S. Kook (2021). "Nocturnal blood pressure dip and parapapillary choroidal microvasculature dropout in normal-tension

glaucoma." Sci Rep 11(1): 206.

Sicard, P., N. Acar, S. Gregoire, B. Lauzier, A. M. Bron, C. Creuzot-Garcher, L. Bretillon, C. Vergely and L. Rochette (2007). "Influence of rosuvastatin on the NAD(P)H oxidase activity in the retina and electroretinographic response of spontaneously hypertensive rats." Br J Pharmacol 151(7): 979–986.

Sin, B. H., B. J. Song and S. P. Park (2013). "Aqueous vascular endothelial growth factor and endothelin-1 levels in branch retinal vein occlusion associated with normal tension glaucoma." J Glaucoma 22(2): 104–109.

Singh, K. and S. J. Gedde (2011). "Interpretation and misinterpretation of results from the tube versus trabeculectomy study." Int Ophthalmol Clin 51(3): 141–154.

Sinski, M., J. Lewandowski, J. Przybylski, P. Zalewski, B. Symonides, P. Abramczyk and Z. Gaciong (2014). "Deactivation of carotid body chemoreceptors by hyperoxia decreases blood pressure in hypertensive patients." Hypertens Res 37(9): 858–862.

Smeitink, J., L. van den Heuvel and S. DiMauro (2001). "The genetics and pathology of oxidative phosphorylation." Nat Rev Genet 2(5): 342–352.

Sommer, A. and J. M. Tielsch (1996). "Risk factors for open-angle glaucoma: the Barbados Eye Study." Arch Ophthalmol 114(2): 235.

Song, Y., Q. Song, L. Li, J. Xu and X. Liu (2018). "Effect of ranibizumab on levels of IL-6 and VEGF in peripheral blood and aqueous humor of glaucoma rat model and association of IL-6 and VEGF with optic nerve damage." Exp Ther Med 16(3): 2506–2510.

Soto, I. and G. R. Howell (2014). "The complex role of neuroinflammation in glaucoma." Cold Spring Harb Perspect Med 4(8).

Srivastava, B. K. and M. Rema (2005). "Does hypertension play a role in diabetic retinopathy?" J Assoc Physicians India 53: 803–808.

Stein, J. D., D. Ruiz, Jr., D. Belsky, P. P. Lee and F. A. Sloan (2008). "Longitudinal rates of postoperative adverse outcomes after glaucoma surgery among medicare beneficiaries 1994 to 2005." Ophthalmology 115(7): 1109–1116 e1107.

Stone, E. M., J. H. Fingert, W. L. Alward, T. D. Nguyen, J. R. Polansky, S. L. Sunden,

D. Nishimura, A. F. Clark, A. Nystuen, B. E. Nichols, D. A. Mackey, R. Ritch, J. W. Kalenak, E. R. Craven and V. C. Sheffield (1997). "Identification of a gene that causes primary open angle glaucoma." Science 275(5300): 668–670.

Stroman, G. A., W. C. Stewart, K. C. Golnik, J. K. Cure and R. E. Olinger (1995). "Magnetic resonance imaging in patients with low-tension glaucoma." Arch Ophthalmol 113(2): 168–172.

Sugiyama, T., S. Moriya, H. Oku and I. Azuma (1995). "Association of endothelin-1 with normal tension glaucoma: clinical and fundamental studies." Surv Ophthalmol 39 Suppl 1: S49–56.

Sun, Y. and L. E. H. Smith (2018). "Retinal Vasculature in Development and Diseases." Annu Rev Vis Sci 4: 101–122.

Sundaresan, P., D. A. Simpson, C. Sambare, S. Duffy, J. Lechner, A. Dastane, E. W. Dervan, N. Vallabh, V. Chelerkar, M. Deshpande, C. O'Brien, A. J. McKnight and C. E. Willoughby (2015). "Whole-mitochondrial genome sequencing in primary open-angle glaucoma using massively parallel sequencing identifies novel and known pathogenic variants." Genet Med 17(4): 279–284.

Sung, K. R., S. Lee, S. B. Park, J. Choi, S. T. Kim, S. C. Yun, S. Y. Kang, J. W. Cho and M. S. Kook (2009). "Twenty-four hour ocular perfusion pressure fluctuation and risk of normal-tension glaucoma progression." Invest Ophthalmol Vis Sci 50(11): 5266–5274.

Suzuki, H., A. Swei, B. W. Zweifach and G. W. Schmid-Schonbein (1995). "In vivo evidence for microvascular oxidative stress in spontaneously hypertensive rats. Hydroethidine microfluorography." Hypertension 25(5): 1083–1089.

Tan, Z. Y., Y. Lu, C. A. Whiteis, A. E. Simms, J. F. Paton, M. W. Chapleau and F. M. Abboud (2010). "Chemoreceptor hypersensitivity, sympathetic excitation, and overexpression of ASIC and TASK channels before the onset of hypertension in SHR." Circ Res 106(3): 536–545.

Tanase, D. M., E. M. Gosav, S. Radu, A. Ouatu, C. Rezus, M. Ciocoiu, C. F. Costea and M. Floria (2019). "Arterial Hypertension and Interleukins: Potential Therapeutic

Target or Future Diagnostic Marker?" Int J Hypertens 2019: 3159283.

Taniguchi, T., M. S. Haque, K. Sugiyama, K. Okada, Y. Nakai and Y. Kitazawa (1996). "Effects of endothelin A and B receptors on aqueous humor dynamics in the rabbit eye." J Ocul Pharmacol Ther 12(2): 123–130.

Tanito, M., S. Kaidzu, Y. Takai and A. Ohira (2015). "Correlation between Systemic Oxidative Stress and Intraocular Pressure Level." PLoS One 10(7): e0133582.

Telegina, D., O. Kozhevnikova and N. Kolosova (2018). "Changes in retinal glial cells with age and during development of age-related macular degeneration." Biochemistry (Moscow) 83(9): 1009–1017.

Tezel, G., M. A. Kass, A. E. Kolker, B. Becker and M. B. Wax (1997). "Plasma and aqueous humor endothelin levels in primary open-angle glaucoma." J Glaucoma 6(2): 83–89.

Tezel, G., L. Y. Li, R. V. Patil and M. B. Wax (2001). "TNF-alpha and TNF-alpha receptor-1 in the retina of normal and glaucomatous eyes." Invest Ophthalmol Vis Sci 42(8): 1787–1794.

Tezel, G. and M. B. Wax (2000). "Increased production of tumor necrosis factor-alpha by glial cells exposed to simulated ischemia or elevated hydrostatic pressure induces apoptosis in cocultured retinal ganglion cells." J Neurosci 20(23): 8693–8700.

Tezel, G., X. Yang, C. Luo, A. D. Kain, D. W. Powell, M. H. Kuehn and H. J. Kaplan (2010). "Oxidative stress and the regulation of complement activation in human glaucoma." Invest Ophthalmol Vis Sci 51(10): 5071–5082.

Tham, Y. C., X. Li, T. Y. Wong, H. A. Quigley, T. Aung and C. Y. Cheng (2014). "Global prevalence of glaucoma and projections of glaucoma burden through 2040: a systematic review and meta-analysis." Ophthalmology 121(11): 2081–2090.

Tham, Y. C., S. H. Lim, P. Gupta, T. Aung, T. Y. Wong and C. Y. Cheng (2018). "Inter-relationship between ocular perfusion pressure, blood pressure, intraocular pressure profiles and primary open-angle glaucoma: the Singapore Epidemiology of Eye Diseases study." Br J Ophthalmol 102(10): 1402–1406.

Tielsch, J. M., J. Katz, A. Sommer, H. A. Quigley and J. C. Javitt (1995).

"Hypertension, perfusion pressure, and primary open-angle glaucoma. A population-based assessment." Arch Ophthalmol 113(2): 216–221.

Topouzis, F., A. L. Coleman, A. Harris, C. Jonescu-Cuypers, F. Yu, L. Mavroudis, E. Anastasopoulos, T. Pappas, A. Koskosas and M. R. Wilson (2006). "Association of blood pressure status with the optic disk structure in non-glaucoma subjects: the Thessaloniki eye study." Am J Ophthalmol 142(1): 60–67.

Townsend, R. R., F. Mahfoud, D. E. Kandzari, K. Kario, S. Pocock, M. A. Weber, S. Ewen, K. Tsioufis, D. Tousoulis, A. S. P. Sharp, A. F. Watkinson, R. E. Schmieder, A. Schmid, J. W. Choi, C. East, A. Walton, I. Hopper, D. L. Cohen, R. Wilensky, D. P. Lee, A. Ma, C. M. Devireddy, J. P. Lea, P. C. Lurz, K. Fengler, J. Davies, N. Chapman, S. A. Cohen, V. DeBruin, M. Fahy, D. E. Jones, M. Rothman, M. Bohm and S. H.-O. M. t. investigators* (2017). "Catheter-based renal denervation in patients with uncontrolled hypertension in the absence of antihypertensive medications (SPYRAL HTN-OFF MED): a randomised, sham-controlled, proof-of-concept trial." Lancet 390(10108): 2160–2170.

Tribble, J. R., F. Hui, H. Quintero, S. El Hajji, K. Bell, A. Di Polo and P. A. Williams (2023). "Neuroprotection in glaucoma: Mechanisms beyond intraocular pressure lowering." Mol Aspects Med 92: 101193.

Tribble, J. R., A. Otmani, S. Sun, S. A. Ellis, G. Cimaglia, R. Vohra, M. Joe, E. Lardner, A. P. Venkataraman, A. Dominguez-Vicent, E. Kokkali, S. Rho, G. Johannesson, R. W. Burgess, P. G. Fuerst, R. Brautaset, M. Kolko, J. E. Morgan, J. G. Crowston, M. Votruba and P. A. Williams (2021). "Nicotinamide provides neuroprotection in glaucoma by protecting against mitochondrial and metabolic dysfunction." Redox Biol 43: 101988.

Tsao, C. W., A. W. Aday, Z. I. Almarzooq, C. A. M. Anderson, P. Arora, C. L. Avery, C. M. Baker-Smith, A. Z. Beaton, A. K. Boehme, A. E. Buxton, Y. Commodore-Mensah, M. S. V. Elkind, K. R. Evenson, C. Eze-Nliam, S. Fugar, G. Generoso, D. G. Heard, S. Hiremath, J. E. Ho, R. Kalani, D. S. Kazi, D. Ko, D. A. Levine, J. Liu, J. Ma, J. W. Magnani, E. D. Michos, M. E. Mussolino, S. D. Navaneethan, N. I. Parikh, R. Poudel,

M. Rezk-Hanna, G. A. Roth, N. S. Shah, M. P. St-Onge, E. L. Thacker, S. S. Virani, J. H. Voeks, N. Y. Wang, N. D. Wong, S. S. Wong, K. Yaffe, S. S. Martin, E. American Heart Association Council on, C. Prevention Statistics and S. Stroke Statistics (2023). "Heart Disease and Stroke Statistics-2023 Update: A Report From the American Heart Association." Circulation 147(8): e93–e621.

Vaajanen, A., E. Mervaala, O. Oksala and H. Vapaatalo (2008). "Is there a relationship between blood pressure and intraocular pressure? An experimental study in hypertensive rats." Curr Eye Res 33(4): 325–332.

Van Bergen, N. J., J. G. Crowston, J. E. Craig, K. P. Burdon, L. S. Kearns, S. Sharma, A. W. Hewitt, D. A. Mackey and I. A. Trounce (2015). "Measurement of Systemic Mitochondrial Function in Advanced Primary Open-Angle Glaucoma and Leber Hereditary Optic Neuropathy." PLoS One 10(10): e0140919.

Van Keer, K., J. B. Breda, L. A. Pinto, I. Stalmans and E. Vandewalle (2016). "Estimating Mean Ocular Perfusion Pressure Using Mean Arterial Pressure and Intraocular Pressure." Invest Ophthalmol Vis Sci 57(4): 2260.

van Koeverden, A. K., Z. He, C. T. O. Nguyen, A. J. Vingrys and B. V. Bui (2018). "Systemic hypertension is not protective against chronic intraocular pressure elevation in a rodent model." Sci Rep 8(1): 7107.

Vaziri, N. D., X. Q. Wang, F. Oveisi and B. Rad (2000). "Induction of oxidative stress by glutathione depletion causes severe hypertension in normal rats." Hypertension 36(1): 142–146.

Vernazza, S., S. Tirendi, A. M. Bassi, C. E. Traverso and S. C. Sacca (2020). "Neuroinflammation in Primary Open-Angle Glaucoma." J Clin Med 9(10).

Waki, M., T. Sugiyama, N. Watanabe, T. Ogawa, H. Shirahase and I. Azuma (2001). "Effect of Topically Applied Iganidipine Dihydrochloride, a Novel Ca(2+) Antagonist, on Optic Nerve Head Circulation in Rabbits." Jpn J Ophthalmol 45(1): 114.

Wang, H., X. Song, M. Li, X. Wang, Y. Tao, X. Xiya, H. Liu, Y. Zhao, D. Chang and Q. Sha (2020). "The role of TLR4/NF-kappaB signaling pathway in activated microglia of rats with chronic high intraocular pressure and vitro scratch

injury-induced microglia." Int Immunopharmacol 83: 106395.

Wang, J. J., P. Mitchell and W. Smith (1997). "Is there an association between migraine headache and open-angle glaucoma? Findings from the Blue Mountains Eye Study." Ophthalmology 104(10): 1714–1719.

Wang, J. W., Y. M. Liu, X. F. Zhao and H. Zhang (2017). "Gastrodin protects retinal ganglion cells through inhibiting microglial-mediated neuroinflammation in an acute ocular hypertension model." Int J Ophthalmol 10(10): 1483–1489.

Wang, L., G. A. Cioffi, G. Cull, J. Dong and B. Fortune (2002). "Immunohistologic evidence for retinal glial cell changes in human glaucoma." Invest Ophthalmol Vis Sci 43(4): 1088–1094.

Wang, L., B. Fortune, G. Cull, J. Dong and G. A. Cioffi (2006). "Endothelin B receptor in human glaucoma and experimentally induced optic nerve damage." Arch Ophthalmol 124(5): 717–724.

Wang, R. F., S. M. Podos, J. B. Serle and O. C. Baltatu (2011). "Effect of SPP 301, an endothelin antagonist, on intraocular pressure in glaucomatous monkey eyes." Curr Eye Res 36(1): 41–46.

Wang, X., T. L. LeVatte, M. L. Archibald and B. C. Chauhan (2009). "Increase in endothelin B receptor expression in optic nerve astrocytes in endothelin-1 induced chronic experimental optic neuropathy." Exp Eye Res 88(3): 378–385.

Weinand, F. S. and F. Althen (2006). "Long-term clinical results of selective laser trabeculoplasty in the treatment of primary open angle glaucoma." Eur J Ophthalmol 16(1): 100–104.

Whelton, P. K., R. M. Carey, W. S. Aronow, D. E. Casey, Jr., K. J. Collins, C. Dennison Himmelfarb, S. M. DePalma, S. Gidding, K. A. Jamerson, D. W. Jones, E. J. MacLaughlin, P. Muntner, B. Ovbiagele, S. C. Smith, Jr., C. C. Spencer, R. S. Stafford, S. J. Taler, R. J. Thomas, K. A. Williams, Sr., J. D. Williamson and J. T. Wright, Jr. (2018). "2017 ACC/AHA/AAPA/ABC/ACPM/AGS/APhA/ASH/ASPC/NMA/PCNA Guideline for the Prevention, Detection, Evaluation, and Management of High Blood Pressure in Adults: A Report of the American College of Cardiology/American Heart

Association Task Force on Clinical Practice Guidelines." J Am Coll Cardiol 71(19): e127–e248.

Widlansky, M. E., D. T. Price, N. Gokce, R. T. Eberhardt, S. J. Duffy, M. Holbrook, C. Maxwell, J. Palmisano, J. F. Keaney, Jr., J. D. Morrow and J. A. Vita (2003). "Short- and long-term COX-2 inhibition reverses endothelial dysfunction in patients with hypertension." Hypertension 42(3): 310–315.

Wiederholt, M., H. Thieme and F. Stumpff (2000). "The regulation of trabecular meshwork and ciliary muscle contractility." Prog Retin Eye Res 19(3): 271–295.

Wierzbowska, J., R. Wierzbowski, A. Stankiewicz, B. Siesky and A. Harris (2012). "Cardiac autonomic dysfunction in patients with normal tension glaucoma: 24-h heart rate and blood pressure variability analysis." Br J Ophthalmol 96(5): 624–628.

Williams, P. A., J. M. Harder, N. E. Foxworth, K. E. Cochran, V. M. Philip, V. Porciatti, O. Smithies and S. W. John (2017). "Vitamin B(3) modulates mitochondrial vulnerability and prevents glaucoma in aged mice." Science 355(6326): 756–760.

Williams, P. A., J. M. Harder and S. W. M. John (2017). "Glaucoma as a Metabolic Optic Neuropathy: Making the Case for Nicotinamide Treatment in Glaucoma." J Glaucoma 26(12): 1161–1168.

Williams, P. A., J. R. Tribble, K. W. Pepper, S. D. Cross, B. P. Morgan, J. E. Morgan, S. W. John and G. R. Howell (2016). "Inhibition of the classical pathway of the complement cascade prevents early dendritic and synaptic degeneration in glaucoma." Mol Neurodegener 11: 26.

Wu, S. Y., B. Nemesure, A. Hennis, M. C. Leske and G. Barbados Eye Studies (2006). "Nine-year changes in intraocular pressure: the Barbados Eye Studies." Arch Ophthalmol 124(11): 1631–1636.

Wustmann, K., J. P. Kucera, I. Scheffers, M. Mohaupt, A. A. Kroon, P. W. de Leeuw, J. Schmidli, Y. Allemann and E. Delacretaz (2009). "Effects of chronic baroreceptor stimulation on the autonomic cardiovascular regulation in patients with drug-resistant arterial hypertension." Hypertension 54(3): 530–536.

Wyss, J. M. (1993). "The role of the sympathetic nervous system in hypertension."

Curr Opin Nephrol Hypertens 2(2): 265–273.

Xu, L., H. Wang, Y. Wang and J. B. Jonas (2007). "Intraocular pressure correlated with arterial blood pressure: the beijing eye study." Am J Ophthalmol 144(3): 461–462.

Xu, L., J. Q. Zhou, S. Wang, Y. X. Wang, Q. S. You, H. Yang, Y. Q. Zhang, M. Y. Wu, Y. F. Lu, Y. Y. Fan and J. B. Jonas (2013). "Localized retinal nerve fiber layer defects and arterial hypertension." Am J Hypertens 26(4): 511–517.

Yamamoto, T. and Y. Kitazawa (1998). "Vascular pathogenesis of normal-tension glaucoma: a possible pathogenetic factor, other than intraocular pressure, of glaucomatous optic neuropathy." Prog Retin Eye Res 17(1): 127–143.

Yamori, Y. (2013). "Development of the spontaneously hypertensive rat (SHR) and of various spontaneous rat models, and their implications." Handbook of hypertension 4: 224–239.

Yang, X., G. Hondur and G. Tezel (2016). "Antioxidant Treatment Limits Neuroinflammation in Experimental Glaucoma." Invest Ophthalmol Vis Sci 57(4): 2344–2354.

Yang, X., C. Luo, J. Cai, D. W. Powell, D. Yu, M. H. Kuehn and G. Tezel (2011). "Neurodegenerative and inflammatory pathway components linked to TNF-alpha/TNFR1 signaling in the glaucomatous human retina." Invest Ophthalmol Vis Sci 52(11): 8442–8454.

Ye, M., J. Huang, Q. Mou, J. Luo, Y. Hu, X. Lou, K. Yao, B. Zhao, Q. Duan, X. Li, H. Zhang and Y. Zhao (2021). "CD82 protects against glaucomatous axonal transport deficits via mTORC1 activation in mice." Cell Death Dis 12(12): 1149.

Yu, D. Y., S. J. Cringle, C. Balaratnasingam, W. H. Morgan, P. K. Yu and E. N. Su (2013). "Retinal ganglion cells: Energetics, compartmentation, axonal transport, cytoskeletons and vulnerability." Prog Retin Eye Res 36: 217–246.

Zalba, G., G. San Jose, M. U. Moreno, M. A. Fortuno, A. Fortuno, F. J. Beaumont and J. Diez (2001). "Oxidative stress in arterial hypertension: role of NAD(P)H oxidase." Hypertension 38(6): 1395–1399.

Zeng, Z., M. You, C. Fan, R. Rong, H. Li and X. Xia (2023). "Pathologically high intraocular pressure induces mitochondrial dysfunction through Drp1 and leads to retinal ganglion cell PANoptosis in glaucoma." Redox Biol 62: 102687.

Zhang, S., H. Wang, Q. Lu, G. Qing, N. Wang, Y. Wang, S. Li, D. Yang and F. Yan (2009). "Detection of early neuron degeneration and accompanying glial responses in the visual pathway in a rat model of acute intraocular hypertension." Brain Res 1303: 131–143.

Zhang, Y., S. Huang, B. Xie and Y. Zhong (2024). "Aging, Cellular Senescence, and Glaucoma." Aging Dis 15(2): 546–564.

Zhang, Z. H., S. G. Wei, J. Francis and R. B. Felder (2003). "Cardiovascular and renal sympathetic activation by blood-borne TNF-alpha in rat: the role of central prostaglandins." Am J Physiol Regul Integr Comp Physiol 284(4): R916–927.

Zhao, D., J. Cho, M. H. Kim and E. Guallar (2014). "The association of blood pressure and primary open-angle glaucoma: a meta-analysis." Am J Ophthalmol 158(3): 615–627 e619.

Zhao, D., C. T. O. Nguyen, Z. He, V. H. Y. Wong, A. K. van Koeverden, A. J. Vingrys and B. V. Bui (2018). "Age-related changes in the response of retinal structure, function and blood flow to pressure modification in rats." Sci Rep 8(1): 2947.

Zhao, Z., H. Wang, Y. Wang, J. Li, Y. X LI, H. Xin, J. Liu and X. Guan (2018). "The mechanisms of Ang II-induced hypertensive vascular remodeling under suppression of CD68 in macrophages." Eur Rev Med Pharmacol Sci 22(18).

Zheng, Y., T. Y. Wong, P. Mitchell, D. S. Friedman, M. He and T. Aung (2010). "Distribution of ocular perfusion pressure and its relationship with open-angle glaucoma: the singapore malay eye study." Invest Ophthalmol Vis Sci 51(7): 3399–3404.